INFORMATION TO USERS

This manuscript has been reproduced from the microfilm master. UMI films the text directly from the original or copy submitted. Thus, some thesis and dissertation copies are in typewriter face, while others may be from any type of computer printer.

The quality of this reproduction is dependent upon the quality of the copy submitted. Broken or indistinct print, colored or poor quality illustrations and photographs, print bleedthrough, substandard margins, and improper alignment can adversely affect reproduction.

In the unlikely event that the author did not send UMI a complete manuscript and there are missing pages, these will be noted. Also, if unauthorized copyright material had to be removed, a note will indicate the deletion.

Oversize materials (e.g., maps, drawings, charts) are reproduced by sectioning the original, beginning at the upper left-hand corner and continuing from left to right in equal sections with small overlaps.

Photographs included in the original manuscript have been reproduced xerographically in this copy. Higher quality 6" x 9" black and white photographic prints are available for any photographs or illustrations appearing in this copy for an additional charge. Contact UMI directly to order.

Bell & Howell Information and Learning
300 North Zeeb Road, Ann Arbor, MI 48106-1346 USA

UMI®
800-521-0600

Molecular and Genetic Characterization of *shiva/slimb*, a gene which regulates pattern formation in the fruit fly *Drosophila melanogaster*

A Dissertation

Presented to the Faculty of the Graduate School

of

Yale University

in Candidacy for the Degree of

Doctor of Philosophy

by

Nicole Alexandra Theodosiou

Dissertation Director: Tian Xu, Ph.D.

December 1999

Abstract

Molecular and Genetic Characterization of *shiva/slimb*, a gene which regulates pattern formation in the fruit fly *Drosophila melanogaster*

Nicole Alexandra Theodosiou

1999

This thesis presents the characterization of the gene *shiva*, and provides evidence that *shiva* plays an essential role in regulating pattern formation during development in *Drosophila melanogaster*. Mutant *shiva* flies exhibit outgrowths and leg duplications similar to the phenotype caused by misexpression of Hedgehog (Hh). Mosaic analysis in mutants has shown that *shiva* modulates Hh-signaling to control the transcription of Hh-target genes. *shiva* represses Hh-target genes along both the anterior-posterior axis and dorsal-ventral axis. Based on these analyses, a model is proposed for the role of *shiva* in pattern formation, as related to the Hh-signaling pathway. The theory that the dorsal-ventral axis is specified during embryogenesis and retained in developing imaginal tissues is challenged; instead the dorsal-ventral axis is actively maintained during imaginal development. The data further support a model in which the dorsal-ventral and anterior-posterior signaling pathways are coordinated by *shiva* in the leg imaginal disc. Genetic and molecular characterization of the *shiva* locus led to the cloning of the *shiva* gene. The *shiva* product encodes a component of the ubiquitin-mediated proteolytic machinery. This gene was independently isolated by Jiang and Struhl [Nature (1998) 391:493] and named *slimb*.

Early genetic characterization of the gene *shiva* led to the identification of a weak pupal-lethal allele with bar eyes. Analysis of this allele in combination with clonal analysis in the eye disc reveals that *shiva* acts to regulate MF progression by impairing Hh-signaling. Overexpression studies of *hh* and *shiva* support a model in which *shiva* and *hh* coordinate MF progression.

ACKNOWLEDGEMENTS

Just as no gene acts alone, no graduate student conducts their thesis alone. I have many people to acknowledge for getting me through this time. Members of my thesis committee including Lynn Cooley and Xin-Yuan Fu were both supportive and encouraging as my project progressed and experienced the occasional curve ball. Before leaving Yale, Spyros Artavanis-Tsakonas sat on my committee always quick with a joke and a piece of advice. Two faculty not on my committee contributed to my growth in graduate school, and continue to look out for me: Gabriel Haddad and Michael Stern. Most importantly, I must thank my advisor Tian Xu. Tian and I started Yale at the same time, and I was there to see his lab grow and his career progress. These are very exciting and trying times in a new investigator's career, and I feel honored that I could not only experience his achievements with him, but also be a part of that first group of people to help him achieve his goals. Tian is not only a good scientist, he is a philosopher. Along with all the scientific advice and encouragement, I also received a lot of advice on my career as well as my personal growth.

Tian's lab is a remarkable collection of people. I feel privileged to have worked with such a supportive group who always made time to help one another. I am indebted to Huang He for input, assistance, and frank discussions of the *shiva* eye project. Without Huang the project would not have moved as smoothly, and he taught me the rewards of a healthy collaboration. Special thanks to the original crew of lab members: Maie St. John, Rod Stewart, Greg Turenchalk, Sheng Zhang, and Wei-Yi Wang. Special thanks to Wan Yu for everything, and to Reza for his tra-la-la's and

sane advice. Nothing in our lab happens without Kris Sepanek, and I thank her for keeping everything running smoothly.

I must also acknowledge several people outside of the lab. To the entire Yavari family: many thanks for housing a homeless graduate student and for the many late-night living room chats. Janet Lee and Henry Chang not only encouraged me in my career, but also shared constructive discussions about my research. Thanks also to Shani Peretz and David Boisvert for their friendships. This thesis would also not be possible with out the continuous assistance over the years by Betsy Jasiorkowski, who does a marvelous job of keeping a herd of frenzied graduate students in line.

My family and I are extremely close, and it is because of their help and support that I got to graduate school. My parents George and Niki, and my sister Noël are all my best friends. I also have my own new family now with Mark Napier. Mark, without you I would not have sustained a smile on my face these last two years. Thanks for being by my side and making me a stronger person.

Finally, I dedicate this dissertation to my grandfather Constantine N. Gherondache (fondly known as Papou). Although a successful scientist and physician himself, I make this dedication because throughout my years in graduate school he always reminded me that there were other, sometimes more important things in life.

TABLE OF CONTENTS

Chapter I. General Introduction 1

Chapter II. Genetic and molecular analysis of the *shiva* locus

Introduction 17

Results 18

A. P-lines 18

P-lines confirmed as *shiva* alleles 19

P(1)00295 and P(1)05415 excision lines generated and examined 19

B. Genomic Mapping

Isolation of *shiva* genomic DNA 20

Mapping *shiva* alleles 21

Discussion 21

Chapter III. The *shiva* gene and its products

Introduction 27

Results 27

A. *shiva* cDNAs

cDNA isolated and mapped to the *shiva* gene 27

The 3.5 kb transcript rescues the lethality of *shiva* mutations 30

shiva encodes a member of the Cdc4/Met30 family 30

Null *shiva* allele identified ($shiva^{e4\text{-}1}$) 31

H-*shiva* cloned 32

B. *shiva* expression

Northern analysis 32

SHIVA antibodies 33

in situ's 34

Discussion 36

Chapter IV. Analysis of the *shiva* phenotype

Introduction 52

Results

A. Leg: Patterning defects in *shiva* mosaic legs 53

shiva mutant clones alter pattern formation in legs of mosaic flies 53

shiva mutant clones misexpress *dpp* and *wg* in leg imaginal discs 54

Effects of *shiva* mutant clones on *hh* and *ptc* expression patterns 56

B. Wing: Patterning defects of wing in *shiva* mosaic flies

Mosaic analysis of *shiva* in wings 57

shiva mutant clones perturb *dpp* expression in the developing wing blade 58

Discussion 59

shiva has a non-cell autonomous effect in developing tissues to induce outgrowths 59

Expression of *dpp* and *wg* is regulated in both the A/P and D/V axes of the leg disc 60

Chapter V. Genetic Epistasis

Introduction 70

Results

A. *dpp, shiva* and *wg, shiva* double mutant clones 70

B. *hh, shiva* and *smo, shiva* double mutant clones 72

hh, shiva 72

smo, shiva 73

Discussion

dpp and *wg* are direct effectors of the *shiva* signal 74

dpp and *wg* are simultaneously required to transduce the *shiva* signal 74

shiva intersects Hh-signaling upstream of *smo* 76

Double mutant clone analysis differs between *shiva, smo* and *slimb, smo* 76

shiva integrates D/V and A/P signals to confer wild type *dpp* and *wg* expression patterns 77

Chapter VI. Role for *shiva* in eye development

Introduction 91

Results

A. $shiva^{e52}$ reveals that *shiva* plays a role during eye development 91

B. *shiva* regulates *dpp* expression in eye discs 93

e52 mutant 93

$shiva^{e4\text{-}1}$ mutant clones 93

C. *shiva* is required for MF progression 94

D. *hh* and $shiva^{e52}$ mutants 96

hh expression in $shiva^{e52}$ mutants 96

hh-1, $shiva^{e52}$ double mutants 97

E. *hh* and *shiva* overexpression restores neural differentiation in e52 discs 97

MF morphology 99

Discussion 99

Chapter VII. Experimental Procedures 115

Appendix A. Excision Lines 124

References 127

LIST OF ABBREVIATIONS

A	anterior
Ab	antibody
A/P	anterior-posterior
ATP	adenosine triphosphate
BrdU	5-bromo-2'deoxyuridine
D	dorsal
D/V	dorsal-ventral
DIG	digoxygenin
DMSO	dimethyl sulfoxide
DNA	deoxyribonucleic acid
dpp	decapentaplegic
EDTA	ethylenediamine-tetra-acetic acid
FLP	Flpase
GST	glutathione s-transferase
hh	hedgehog
kb	kilobase pairs
kDa	kilodaltons
kV	kilovolt
lacZ	β-galactocidase
µg	microgram
µl	microliter
MF	morphogenetic furrow
ml	milliliter
mM	milli-molar
NGS	normal goat serum

P	posterior
PBT	PBS + 0.1% Tween
P/D	proximo-distal (axis)
pka	protein kinase A
ptc	patched
RT	room temperature
Sb	Stubble
sc	scute
SDS	sodium dodecyl sulfate
SEM	scanning electron micrograph
slmb	slimb
smo	smoothened
SSC	sodium chloride-sodium citrate
Tb	Tubby
TE	10 mM Tris HCl pH 7.8, 1 mM EDTA
TNF	tumor necrosis factor
V	ventral
w	white
wg	wingless
UAS	upstream activation sequence
Ub	ubiquitin
UTR	untranslated region
y	yellow

LIST OF FIGURES

Figure 1	Schematic of the leg imaginal disc	11
Figure 2	Structure of the *Drosophila* eye	13
Figure 3	The developing fly eye	15
Figure 4	Mosaic phenotypes of original *shiva* allele	23
Figure 5	Map of the *shiva* genomic region containing several alleles of the *shiva* gene	25
Figure 6	Map of the *shiva* genomic region	40
Figure 7	*shiva* expression constructs	42
Figure 8	SHIVA protein and its homologs	44
Figure 9	Northern analysis reveals 3 developmentally regulated *shiva* transcripts in *Drosophila*	46
Figure 10	Northern analysis of human tissues reveals three developmentally regulated *shiva* transcripts	48
Figure 11	Expression of the *shiva* transcript demonstrated by *in situ* hybridization	50
Figure 12	Analysis of the *shiva* mosaic phenotype in adult legs	62
Figure 13	*shiva* clonal phenotype in leg imaginal discs	64
Figure 14	The *shiva* adult mosaic phenotype in wings	66
Figure 15	*shiva* mutant clones in wing imaginal discs	68
Figure 16	Generating double mutant clones using *shiva* rescue construct	79
Figure 17	Generating *shiva* mutant clones by using *shiva* rescue construct	81
Table 1	Double mutant clone analysis in legs	83
Table 2	Double mutant clone analysis in wings	85

Figure 18	Generating *hh, shiva* double mutant clones.....	87
Figure 19	A model for *shiva* function in the developing leg.....	89
Figure 20	The *shiva*^{e52} mutant has a bar eye phenotype.....	103
Figure 21	*dpp* expression and MF progression in *shiva*^{e52} mutants.....	105
Figure 22	*shiva* mosaic phenotype in the developing eye.....	107
Figure 23	*hh* and *shiva* overexpression restores differentiation in *shiva*^{e52} mutants.....	109
Table 3	*hh* and *shiva* overexpression studies in *shiva*^{e52} mutants.....	111
Figure 24	The "push-push" model controlling MF progression....	113

Chapter I. General Introduction

It goes back to the Greeks. Since Ancient Greece and Aristotle's first descriptions of the developing chicken, developmental biologists have been awed by the formation of the embryo, limbs, and organs in developing animals (Aristotle, 350 BC; Aristotle, 350 BC). The coordination of cell proliferation and pattern formation to create individual beings is truly amazing. However, it was not until this last century that the proper genetic and molecular tools were developed to address these basic questions. In the last twenty years alone, developmental biologist have evolved from acute observers to active manipulators. The biggest advances have been in the model system *Drosophila melanogaster*, which remains the most powerful genetic model organism. It was the "dead embryo" genetic screen of Nusslein-Volhard and Wieschaus, which began to unravel the mystery of pattern formation (Nusslein-Volhard and Wieschaus, 1980).

The screen for maternal effect genes during *Drosophila* embryogenesis exposed a large number of genes that are critical to patterning of the embryo. Despite the large number of genes isolated in the screen, mutations in these genes had only four basic phenotypes. The mutations in genes exhibiting segment polarity defects have since been shown to also play critical roles during pattern formation of the limbs. The segment polarity genes are highly conserved evolutionarily from flies to humans. Recent work has shown that this group of genes is involved not only in mammalian embryogenesis, but also in the development of limbs, organ systems and tissues, and cancer genetics.

In *Drosophila*, each adult appendage develops from an imaginal disc; a single layer of epithelial cells that are set aside during embryogenesis. Imaginal discs grow in size during first, second and early third instar larval stages. In late 3rd instar larval and pupal stages imaginal discs organize into patterns of adult structures. Each imaginal disc is divided into two unique compartments, anterior and posterior, whose boundaries are defined and maintained from early in development. For instance, the adult leg develops from the leg imaginal disc, such that the center-most cells become the distal tip, and the outermost cells develop proximal to the main body. Genetic studies have identified a number of signaling molecules responsible for orchestrating the precise patterning of the discs for the correct adult structures. It is the organizing activity of these signaling molecules which specifies anteroposterior (A/P), dorsoventral (D/V), and proximodistal (P/D) axes in the limbs of *Drosophila*. Although these signaling molecules are found in all developing discs, they play slightly varied roles in different discs. For this overview, the development of the leg and eye discs will be considered, as my research mainly focused on patterning in these structures.

Anteroposterior Axis Formation in Leg Imaginal Discs

Studies in recent years have led to a better understanding of the interactions between signaling molecules necessary to establish the A/P axis in imaginal discs. The activity of the *engrailed* (*en*) gene product in posterior cells is responsible not only for defining the A/P boundary and preventing their intermixing, but also in directing the posterior cells to form posterior structures

(Guillen et al., 1995; Lawrence and Morata, 1976; Tabata et al., 1995). *Engrailed* expressing cells in imaginal discs organize cell patterning by activating the *hedgehog* (*hh*) protein (Lee et al., 1992; Tabata et al., 1992). Hh, a posteriorly expressed secretory protein, in turn induces neighboring anterior compartment cells to secrete their own anterior determinants: the *Drosophila* TGFß homolog *decapentaplegic* (*dpp*), and the Wnt family member, *wingless* (Basler and Struhl, 1994; Capdevila and Guerrero, 1994; Tabata and Kornberg, 1994). *dpp* and *wg* are not expressed throughout the anterior compartment, but rather in triangular sections that directly abut the A/P boundary: *dpp* in the dorsal anterior is required for specification of dorsal strucutres, *wg* in the ventral anterior determines ventral structures (Ferguson and Anderson, 1992; Irish and Gelbart, 1987; Struhl and Basler, 1993). The establishment of these anterior quadrants results in a dynamic 'wall' separating anterior from posterior (Fig. 1).

The highly restricted domains of *dpp*- and *wg*- expressing cells are maintained by *patched* (*ptc*) and *protein kinase A* (*pka* or *DC0*) in the A/P axis. *ptc*, which encodes the *hh* receptor, (Chen and Struhl, 1996; Marigo et al., 1996; Stone et al., 1996) is expressed in low levels throughout the anterior, blocking expression of *dpp*, *wg* and *ptc* itself (Ingham et al., 1991; Li et al., 1995; Phillips et al., 1990). Hh blocks the *ptc* repressing activity, allowing the transmembrane protein Smoothened (Smo) to initiate expression of *dpp* and *wg* in their respective quadrants, and upregulate *ptc* at the A/P border (Capdevila et al., 1994; Heuvel and Ingham, 1996).

The fine orchestration of the Hh/Ptc & PKA pathways is involved solely in establishing and maintaining A/P patterning integrity. Inactivation or ectopic expression of components of these pathways deregulate *dpp* and *wg* expression

only in the A/P axis (Basler and Struhl, 1994; Capdevila and Guerrero, 1994; Felsenfeld and Kennison, 1995; Ingham et al., 1991; Li et al., 1995; Tabata and Kornberg, 1994). Mutant clones for *ptc* and *pka* or ectopic expression of *hh* induces ectopic *dpp* expression in the dorsal-anterior and ectopic *wg* expression in the ventral-anterior of the leg disc (Basler and Struhl, 1994; Capdevila and Guerrero, 1994; Ingham et al., 1991; Jiang and Struhl, 1995; Lepage et al., 1995; Pan and Rubin, 1995; Phillips et al., 1990). However, mutations in components of the A/P signaling pathway do not alter *wg* and *dpp* expression patterns in the D/V axis, *e.g.*, *dpp* is never found in the ventral. Thus, a different signaling pathway must regulate *dpp* and *wg* expression along the D/V axis. To date no evidence exists of a D/V signaling pathway. It is possible that the D/V axis defined during embryogenesis is retained in imaginal tissues.

One mechanism that prevents misexpression of *wg* in the dorsal-anterior and *dpp* in the ventral-anterior is the antagonistic relationship between *wg* and *dpp*. It has been shown that clones mutant for components of the *wg* or *dpp* signaling pathways ectopically express *dpp* or *wg* in the ventral and dorsal quadrants, respectively (Brook and Cohen, 1996; Jiang and Struhl, 1996; Penton and Hoffman, 1996; Theisen et al., 1996). These results suggest that *dpp* and *wg* mutually repress each other's expression, preventing their co-expression within the same disc compartment. Although this mechanism can prevent co-expression of *dpp* and *wg*, an unidentified mechanism is required for programming *dpp* expression in dorsal, and *wg* in ventral cells in response to Hh signaling (Basler and Struhl, 1994; Campbell and Tomlinson, 1995).

Proximodistal Axis Formation in Leg Discs

The formation of the proximodistal (P/D) axis in the legs of flies is dependent on initiating events from two extracellular signaling molecules: *dpp* and *wg*. Although *wg* and *dpp* are known to determine ventral and dorsal structures, respectively, it was nonetheless surprising when a reduction of *wg* activity during larval stages results in loss of ventral structures as well as a shortening of the leg along the P/D axis (Wilder and Perrimon, 1995). This suggested that *wg* also plays a role in P/D axis formation. *wg* acts by inactivating Shaggy/Zeste white 3 (Sgg/Zw3) protein kinase for specifying ventral cell fates in the leg (Diaz-Benjumea et al., 1994). Mutant clones for *sgg/zw3* outside of the endogenous range for *wg* expression reorganize the D/V axis similar to ectopic *wg*-expressing clones: both result in the bifurcation of legs when located in the dorsal region, and the ectopic structures are positioned with opposite polarity to the endogenous legs. However, ectopic limbs derived from *sgg/zw3* clones fail to develop distal structures (lacking claws), while *wg* expressing clones are able to develop bifurcated legs with distal claws. This suggests that *wg* signaling acts by independent pathways when specifying D/V versus P/D axes.

Present models suggest that *wg* and *dpp* are both required for formation of a distal organizing center, and that the organizing center is initiated at the point where *dpp* and *wg* expressing cells meet (Fig. 1) (Campbell and Tomlinson, 1995). Evidence supporting such a model for initiation of the proximodistal axis comes from ectopic protein experiments. Ectopic expression of both *dpp* and *wg* can induce secondary P/D axes only when they are in close proximity with the D/V border. Simply, clones of cells expressing *wg* may induce formation of an ectopic limb only when these clones are positioned near the D/V axis, and thus close to

dpp-expressing cells (Struhl and Basler, 1993). No supernumerary structures are formed, however, when *wg* clones are at a distance to the D/V axis and *dpp*-expressing cells. Likewise, ectopic *dpp* expressing clones are able to induce a secondary P/D axis only when positioned adjacent to *wg*-expressing cells.

The point at which *dpp* and *wg* expressing cells meet, two additional pattern determining molecules are expressed: *aristaless* (*al*) and *distaless* (*dll*). Mutants for *distaless* fail to develop distal-most leg structures, while *aristaless* mutants have reduced proximal-most leg structures (Campbell et al., 1993). As previously mentioned, supernumerary structures arise only when *wg* is ectopically expressed in the vicinity of endogenous *dpp*-expressing cells. The junction of *wg* and *dpp* expressing cells initiates the distal organizing center in a disc. If this is true, it is expected that supernumerary limbs arise as a result of induction of an ectopic distal organizing center which should include ectopic *al* and *dll* expression. Indeed, it has been shown that dorsally located *wg*-expressing cells can induce ectopic *dll* (Diaz-Benjumea et al., 1994). Likewise, ectopic *wg* expression also induces the expression of *al* (Campbell et al., 1993). It therefore follows that when *hh* is ubiquitously expressed, inducing *dpp* and *wg* expression throughout their respective dorsal and ventral anterior quadrants, *al* and *dll* are expressed in a line bordering the D/V axis. This results in oval-shaped leg discs, in which *dll* and *al* are expressed as a line along the *wg-dpp* boundary (Campbell et al., 1993; Diaz-Benjumea et al., 1994).

Development in the Eye Imaginal Disc

The *Drosophila* eye provides an excellent model for studying how positional information can lead to cell identity. The adult fly eye is composed of approximately 800 facets, or ommatidia. Each ommatidium has a stereotypical arrangement of eight photoreceptor cells and 12 accessory cells (Fig. 2). The precise arrangement of ommatidia in a two-dimensional lattice is crucial for proper vision in the fly. As with other structures in *Drosophila*, the adult eye is derived from a monolayer of epithelium in the developing larva called the imaginal disc. During late larval stages, a wave of differentiation proceeds across the eye imaginal disc from posterior to anterior. This wave is marked by an indentation in the epithelium, and thus is called the morphogenetic furrow (MF) (Fig. 3, upper panel). Ahead of or anterior to the MF, cells divide asynchronously and remain undifferentiated. Cells entering the MF arrest in G1. As cells exit posterior to the MF, they enter a synchronized S phase and begin to differentiate and form ommatidial preclusters. In this way, a MF moves one cell row at a time, leaving clusters of differentiating photoreceptor cells in its wake which will go on to form a two-dimensional lattice.

Many groups have addressed the mechanisms by which the MF progresses, and the coordination between MF movement and cell cycle synchronization. The major players in MF progression are all too familiar: *hedgehog* (*hh*), *decapentaplegic* (*dpp*), and *wingless* (*wg*) (Fig. 3, lower panel). These players have their positions: photoreceptor cells differentiating posterior to the MF secrete *hh*; *dpp* is expressed in a stripe within the MF; and *wg* is expressed at the lateral margins of the disc anterior to the MF. Hh drives the anterior progression of the MF, and activates *dpp* transcription in the MF (Heberlein et al., 1995; Ma et al., 1993). Experiments using a temperature-sensitive allele as well as

an eye-specific mutant for *hh* have shown that a decrease in *hh* activity leads to an absence of *dpp* expression and an arrest of the MF. *dpp* in the MF acts as a cell cycle block, arresting cells in G1 (Horsfield et al., 1998; Penton et al., 1997). While *hh* and *dpp* act in propelling the MF forwards, *dpp* 's antagonist, *wg*, acts as a brake for MF progression at the lateral margins (Treisman and Rubin, 1995). However, it has been proposed that another molecule(s) or mechanism must be in place in the center of the disc, anterior to the MF, which acts to regulate MF progression.

Several models have been proposed to explain progression of the MF. The "pulling" model assumes that cells of the eye disc contain all the necessary information required to develop an adult eye (Ready et al., 1976). An inhibitory molecule in the anterior decays as a gradient towards the posterior. At a low threshold for this inhibitory factor, competent cells enter the MF. As the factor decays, the MF is pulled forward. In contrast, the "pushing" model suggests that a process of accretion drives movement of the MF (Lebovitz and Ready, 1986). Cells posterior to the MF provide a local inductive signal to naive anterior cells, with each new column of differentiating ommatidia acting as a template for the next. Support of this model comes from evidence that *hh* acts to induce *dpp* expression in the MF, thus driving it forward (Heberlein et al., 1993; Ma et al., 1993). Ectopic activation of *hh*-signaling anterior to the MF leads to ectopic MF formation, further supporting this model (Heberlein et al., 1995; Ma and Moses, 1995; Pan and Rubin, 1995; Strutt et al., 1995). However, mutant clones for *hh* and its receptor *smoothened* (*smo*) have failed to arrest MF progression, suggesting that *hh* is necessary but not sufficient for progression (Strutt and Mlodzik, 1997).

In this thesis I present my work characterizing the gene *shiva*, and provide evidence that it plays an essential role in regulating pattern formation. I report my genetic and molecular characterization of the *shiva* locus, which led to my cloning of the *shiva* gene. I further report the *shiva* phenotype in both developing and adult tissues in *Drosophila*. My work has also included characterizing the effect of *shiva* on components of the Hh-signaling pathway, which regulates pattern formation. Based on these analyses, I propose a model for the role of *shiva* in pattern formation, as related to the Hh-signaling pathway. I challenge the theory that the D/V axis is specified during embryogenesis and retained in developing imaginal tissues, and suggest that the D/V axis is actively maintained during imaginal development as well. I also propose that the D/V and A/P signaling pathways are coordinated by *shiva* in the leg imaginal disc.

Success of this part of my dissertation was overshadowed by the publication of another group, which cloned and characterized the same gene. They called this gene *slimb* (Jiang and Struhl, 1998). For the purposes of this dissertation I will continue to call this gene *shiva*, as I have for 5 years. There are great discrepancies in my data compared to that of the other group's results. When relevant, I will discuss these differences and attempt to give explanations for the basis for these discrepancies.

Early genetic characterization of the gene *shiva* led to the identification of a weak pupal-lethal allele with bar eyes. Analysis of this allele ($shiva^{e52}$) in combination with clonal analysis in the eye disc supports a model in which *shiva* acts by impairing Hh-signaling anterior to the MF. Over-expression of *hh* in the $shiva^{e52}$ mutant background can partially rescue neural differentiation,

confirming that although *hh* is necessary it is not sufficient to drive MF movement. Finally, I show evidence supporting a model in which *shiva* and *hh* act coordinately to regulate MF progression.

Figure 1. Schematic of the leg imaginal disc. The disc is positioned such that anterior is to the left, and ventral is down. Hh (orange) is expressed in cells of the posterior compartment. Dpp (red) is expressed in a dorsally-located stripe in anterior cells, adjacent to Hh-expressing cells. Wg (blue) is expressed in a ventral-anterior stripe adjacent to Hh-expressing cells. In the center of the disc, Wg- and Dpp-expressing cells meet, forming the distal organising center (circle). This is the central point from which the developing leg telescopes towards during pupation.

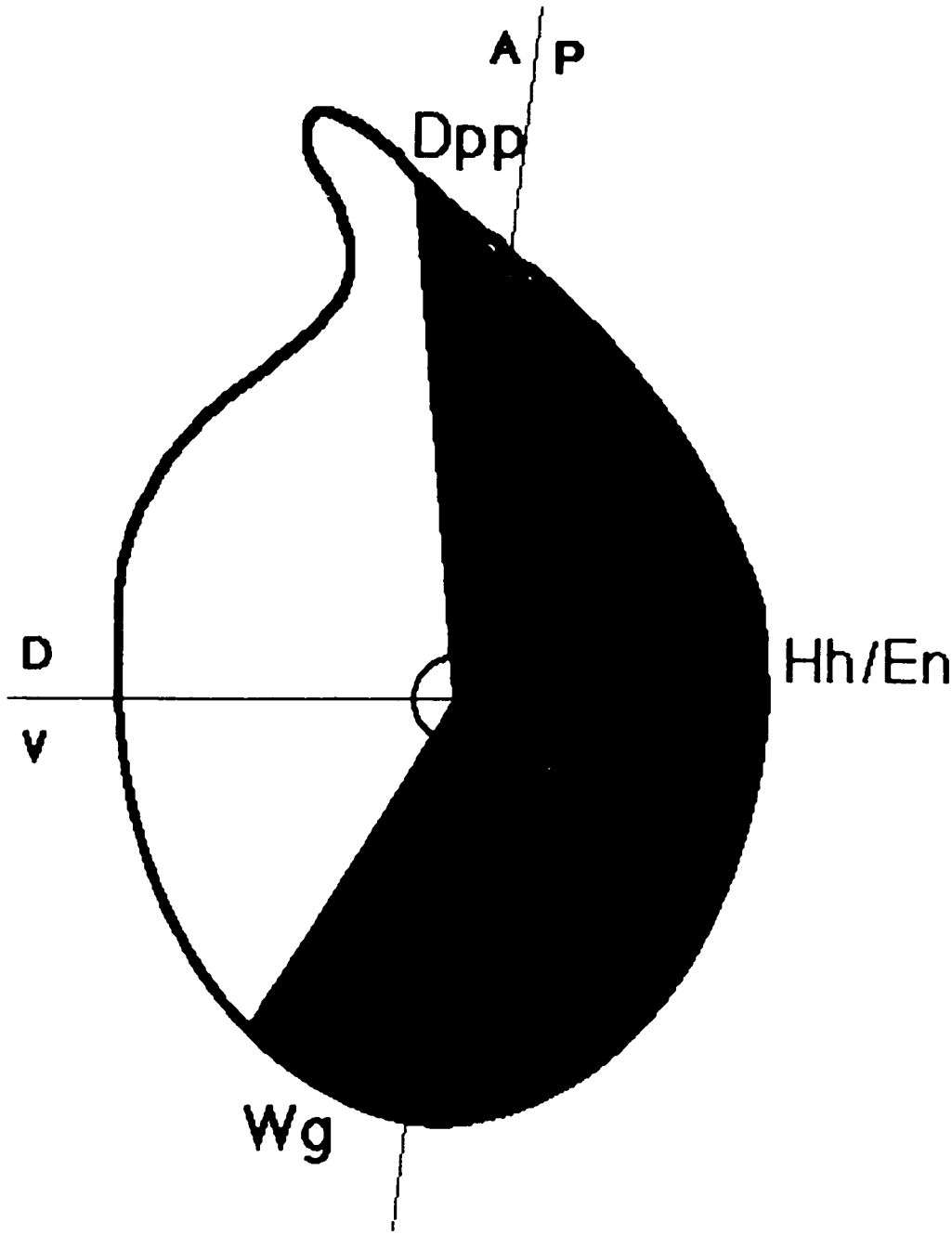
A
P
Dpp
D
V
Hh/En
Wg

Figure 2. Structure of the *Drosophila* eye. SEM of the adult eye illustrates the 800 individual eyes or ommatidia that comprise the fly compound eye (left panel). A section of a single ommatidia pictures the 8 photoreceptor cells (blue) and cone cells surrounded by pigment cells (upper right panel). A schematic of an ommatidium (lower left panel). The eighth photoreceptor cell is positioned in a plane below the seventh.

Drosophila eye structure

Figure 3. The developing fly eye. (upper panel) An eye imaginal disc stained for BrdU-incorporation (green) and propidium iodide (red). The indentation which identifies the MF is illustrated by the propidium iodide staining. Cells in the MF arrest in G1, and thus fail to incorporate BrdU. Cells exit the G1 arrest posterior to the MF in a synchronized S phase. Anterior to the MF cells divide asynchronously, while posterior they begin differentating. (lower panel) As with the leg disc, the Hh pathway relays positional information. Hh is expressed in posterior cells which have differentiated to become photoreceptor cells (orange). Hh induces *dpp* (red) expression in a stripe within the MF. At the lateral margins, *wg* is expressed (blue) and acts as a brake to MF movement.

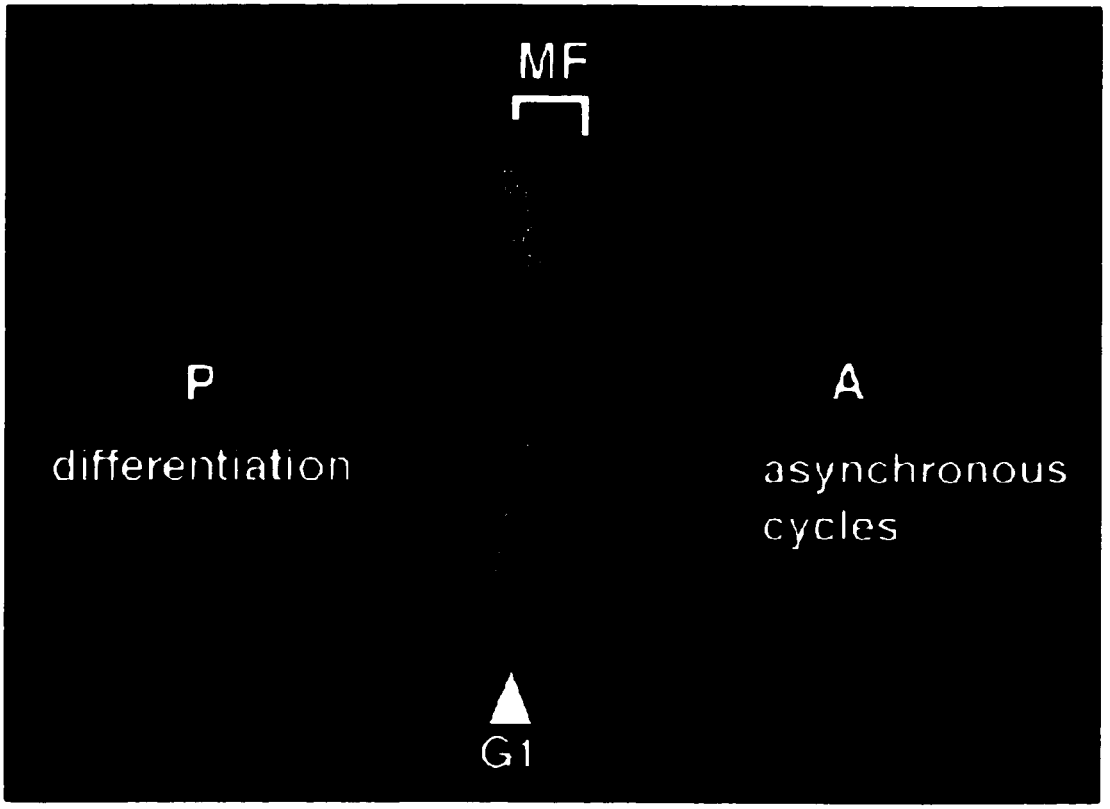
MF
P
differentiation
A
asynchronous
cycles
G1

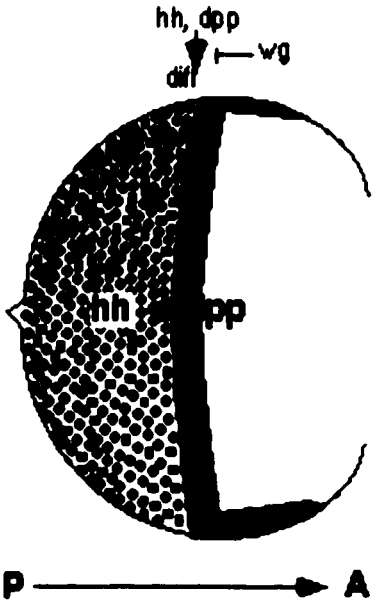
hh, dpp
wg
dif
hh
dpp
P
A

Chapter II. Genetic and Molecular analysis of the *shiva* locus

Introduction

Large-scale genetic screens were performed in *Drosophila* to isolate mutations in genes involved in pattern formation (Nusslein-Volhard and Wieschaus, 1980). Although these screens successfully identified a number of genes, they focused on the identification of embryonic mutants and were not sensitive enough to uncover all potential players. Introduction of the FLP/FRT system into flies enabled the generation of viable mosaic flies which contain homozygous mutant patches for known lethal mutations (Xu and Rubin, 1993; Xu et al., 1995). Using this system, Tian Xu undertook to isolate negative regulators of cell proliferation by screening for mosaic flies whose mutant patches had undergone over proliferation. In this screen a mosaic fly was identified whose outgrowth tissue and supernumerary limb phenotype suggested it played a role in pattern formation. This mutation was lethal in its homozygous state, and the ectopic limb phenotype associated with mosaic flies for the mutation was reproducible. I named the gene responsible for this phenotype *shiva* after the Hindu god who has extra arms.

The *shiva* gene was genetically mapped by Xu to a position on the right arm of chromosome III. A probe raised against the *white* gene in the P-element construct hybridized to location 93C on polytene chromosomes carrying the mutation for *shiva*. This original mutation for *shiva* was a P-element insertion designated $shiva^{P(l)00295}$. A second P-element insertion [P(l)05415] providing a

second mutation in the shiva gene, also mapped to 93C and failed to complement *shiva*$^{P(l)00295}$. In order to produce new alleles for *shiva*, Xu used the P(l)00295 and P(l)05415 P-insertions to generate excision lines that delete genomic DNA surrounding the *shiva* gene. Precise excision of the P-inserts reverted their lethality, demonstrating that the lethality of the P-alleles and the adult clonal phenotype of *shiva*$^{P(l)00295}$ were caused by mutations in the same gene.

To molecularly define the *shiva* gene, I isolated and restriction mapped over 40 kb of genomic DNA from the region. Using Southern analysis and DNA sequencing, I mapped the alleles *shiva*$^{P(l)00295}$ and *shiva*$^{P(l)05415}$. With the help of Wei-Yi Wang, 9 excision lines from the P-element insertions were mapped including a null allele for *shiva*, *shiva*$^{e4-1}$.

Results

A. P-lines

Mosaic flies with clones for *shiva*$^{P(l)00295}$ displayed tissue outgrowths that included patterned structures (Figure 4). The outgrowths were found throughout the bodies of mosaic animals, and even took on the form of ectopic supernumerary structures. This striking phenotype suggested that *shiva* may play important roles in both cell proliferation and pattern formation. As the original *shiva* mutation was a P-element insertion, it was important to generate and characterize possible mutations from the *shiva* region.

(1) P-lines confirmed as *shiva* alleles

An independent non-complementing P-element line was received from the Bloomington Stock Center: P(l)05415. P(l)05415 is lethal in its homozygous state. P(l)05415 is an allele of *shiva* as it failed to complement the original $shiva^{P(l)00295}$ mutation. Flies trans-heterozygous for P(l)05415 and $shiva^{P(l)00295}$ are lethal.

Precise excision of each P-element reverted the lethality associated with that allele, and restored its ability to complement the $shiva^{P(l)00295}$ allele. This indicated that the P-lines disrupted the *shiva* gene.

(2) P(l)00295 and P(l)05415 excision lines generated and examined

In order to facilitate in analyzing the structure and function of the *shiva* gene it was important to generate a number of alleles with a variety of lesions in the same region as the P-insertions. To do this, Tian Xu generated a collection of excision alleles created by causing the P(l)00295 and P(l)05415 inserts to transpose out of their genomic insertion sites. These events are often imprecise and can lead to deletions in DNA surrounding the P-elements, or to fragments of the P-element DNA being left behind. The hope is that the imprecise excision events create deletions of genomic DNA in the *shiva* region, giving rise to a new arsenal of *shiva* alleles.

56 independent excision lines were generated and characterized (Appendix A, pg.124). Examination of homozygotes revealed that 13 lines were viable, 38 lines were early lethal (lethal in embryonic or first instar stage) and 5 late pupal

lethal lines. Pupal cases from the five pupal lethal lines were dissected and found to have slightly varying phenotypes. For example, in line e5-1 the homozygous animals were pharate adult lethal and had extra bristles. In contrast, the pharate adults in line e28 displayed brown spots on their abdomens, and failed to develop the posterior tails of their bodies. Line e52 proved very interesting. Homozygotes from this line had very small eyes (half bar), small legs and wings, and fork-like bristles. This line was later used to study the role of *shiva* during eye development (see Chapter VI).

A table of all the excision lines and their phenotypes is given in Appendix A. More than 20 flies were examined for each line.

B. Genomic Mapping

(1) Isolation of *shiva* genomic DNA

Using a 3.3 kb HindIII fragment from the P(l)00295 plasmid rescue, I screened a genomic cosmid library and isolated two overlapping cosmids, #3 and 17. As cosmid #17 was slightly larger in size (close to 40 kb) it was used for extensive restriction enzyme analysis and Southern hybridization analysis. Fragments of the cosmid were subcloned into plasmid pBS(KS-) (Stratagene) and sequenced. A fraction of the cosmid is illustrated with relevant restriction sites (Fig. 5).

The location of the two P-insertions was determined by DNA sequencing. I sequenced the rescued DNA from P(l)00295 and P(l)05415 to determine their exact insertion points (Fig. 5). I also obtained DNA sequence from subcloned

genomic fragments. Comparison of sequence between the rescued DNA fragments and the genomic subclones allowed me to determine the precise location of the P-elements.

(2) Mapping *shiva* alleles

Genomic DNA was extracted from each excision line, digested with *Bgl*II and *Hind*III, and analyzed by Southern Blot to identify possible deletions. With the help of Wei-Yi Wang, Southern Blots were probed with a 1.6 kb *Bgl*II genomic fragment enabling me to approximate the size and position of deletions in 9 of the excision lines. The largest deletion of approximately 3 kb was in the line e4-1, which posed as a possible null allele (see Chapter III). Excision lines and their deletions are illustrated in Fig. 5.

Discussion

The isolation of a new gene mutation whose characterization could lead to a better understanding of the pathways involved in pattern formation set the stage for an exciting thesis project.

Genetic and molecular analysis of the *shiva* genomic region enabled me to lay a foundation for future efforts in understanding the *shiva* gene. As the original mutation for *shiva* was a P-insertion, it was very straight forward to determine that the P-element associated with lethality through precise excision was responsible for the adult mosaic outgrowth phenotype. An additional P-insertion was found that failed to complement P(l)00295. By generating excision

lines from these two P-insertions, I was able to later provide evidence needed in identifying a cDNA group corresponding to the *shiva* gene. These excision lines not only identified a possible null allele, but also several alleles with interesting phenotypes that later led to an understanding of development in different tissues.

Figure 4. Mosaic phenotypes of original *shiva* allele. Illustrated are samples of outgrowths observed in flies mosaic for the *shiva* P insertion allele, P(l)00295. Outgrowths were observed throughout the body of the fly including the eye (A) and leg (B-D). (A) A protrusion from the eye is composed of differentiated ommatidia (arrow). (B) A small leg outgrowth contains bristles. (C) Duplication of strucutres is often observed in mosaic flies, including small regions such as the male sex comb bristles (arrow). (D) A more dramatic example of structural duplication includes a bifurcated leg, the ectopic leg indicated by an arrow.

A
B
C
D

Figure 5. Map of the *shiva* genomic region containing several alleles of the *shiva* gene. The size scale for 1 kilobase is indicated above the map. *shiva*^{00295} is the original *shiva* allele caused by an insertion of over 10 kb in the 1.3 kb *Bgl*II-*Hind*III genomic segment. The P insertion P(l)05415 fails to complement *shiva*^{00295}, and thus must also be an allele for *shiva*. Of the excision lines generated from P(l)00295 and P(l)05415, 9 had discernable deletions. *shiva*$^{e4\text{-}1}$ had the largest deletion of approximately 3 kb, posing as a possible null allele. Lines *shiva*$^{e5\text{-}1}$, *shiva*^{e28}, *shiva*^{e31}, *shiva*^{e52}, and *shiva*$^{e5\text{-}1\text{-}2}$ are pupal lethal and had deletions of approximately 1 kb. Restriction sites are abbreviated as follows: B=*Bam*HI, G=*Bgl*II, H=*Hind*III, K=*Kpn*I, RI=*Eco*RI and X=*Xba*I.

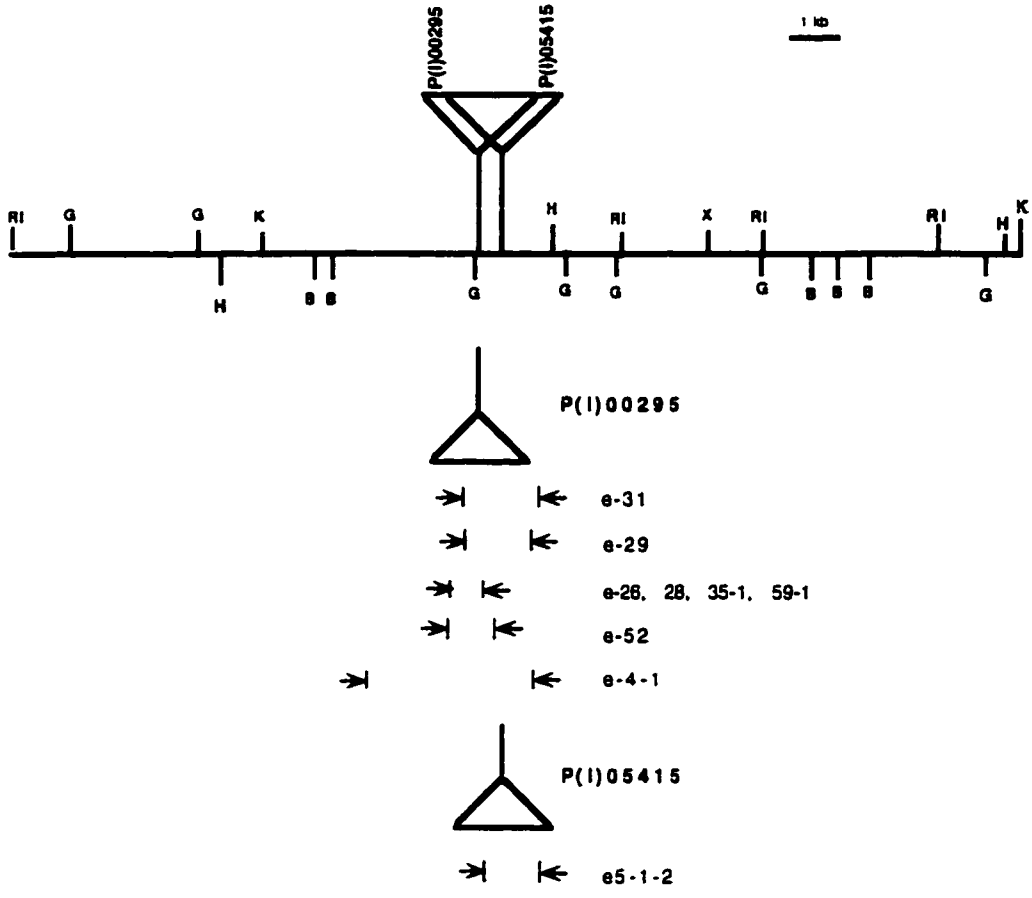
P(I)00295
P(I)05415
1 kb
RI
G
G
K
H
H
RI
X
RI
RI
H
K
H
B B
G
G
G
G
B B B
G
P(I)00295
e-31
e-29
e-28, 28, 35-1, 59-1
e-52
e-4-1
P(I)05415
e5-1-2

Chapter III. The *shiva* gene and its products

Introduction

From my preliminary characterization of the *shiva* phenotype it was clear that *shiva* played an important role in pattern formation. To better understand a role for *shiva* during development, I undertook to clone the *shiva* gene. I performed several rounds of cDNA screening, uncovering two groups of cDNA's. I demonstrated that one of these groups was the *shiva* gene, and that this transcript could rescue the lethality of homozygous mutant animals. The *shiva* transcript encodes a member for the Cdc4/Met30 family of proteins, demonstrated to be a component of the ubiquitin-mediated proteolytic machinery. Using the fly cDNA as a probe, I also identified the human *shiva* gene (H-*shiva*).

To learn about the expression of the *shiva* products during development, I used three approaches. Northern analysis confirmed the existence of multiple *shiva* transcripts during development. Monoclonal antibodies were also raised to the SHIVA protein in the hope that they would be valuable in determining *shiva* expression and function. Finally, I used the full-length *shiva* transcript as a probe in *in situ* experiments to determine the *shiva* expression pattern in imaginal discs.

Results

A. *shiva* cDNAs

(1) cDNA group isolated and mapped to the *shiva* gene

Several pieces of evidence indicated to me that the *shiva* gene lay near the P(l)00295 P-element. First, excision lines generated from P(l)00295 failed to compliment P(l)00295 itself. Second, precise excision of P(l)00295 reverted the homozygous lethal phenotype of P(l)00295 to wild type, or viable adults. I decided to use two genomic fragments to screen a *Drosophila* total imaginal disc cDNA library (supplied by A. Cowman); a 12.5 kb *Eco*RI fragment flanked the left side of P(l)00295, while a 9.8 kb *Bam*HI fragment flanked to the right (Fig. 6). As the two probes overlapped in the region of the P-element, I rationalized that plaques positive for both probes would contain the appropriate transcript for *shiva*.

Approximately 2×10^6 plaque-forming units were screened in the primary phase with the 12.5 kb *Eco*RI probe; thirty-five positive plaques were picked from the primary screen, and eighteen persisted as positive through the tertiary screen. Concurrently, the library was screened with the 9.8 kb *Bam*HI probe. Eighteen positive plaques were recovered in the primary screen with the *Bam*HI probe; nine were in common with the *Eco*RI probe, while nine were novel positives. Six of the nine novel positives recovered from the *Bam*HI probe persisted through a secondary screen. In summary, both the *Eco*RI and *Bam*HI probes uncovered nine positive plaques; an additional nine positives were unique to the *Eco*RI probe, while six were unique to the *Bam*HI probe.

Problems arose, however, while trying to group the different cDNAs isolated from the library screens. After reviewing the cosmid restriction map, I

discovered that the 12.5 kb *Eco*RI fragment used as a probe during the library screen was in fact a doublet. The doublet consisted of the predicted fragment spanning the P-element and an additional vector fragment with cDNA ends of .61 kb and 2.25 kb on either side. To elucidate which isolated cDNAs in fact mapped to the P-element insertion site two smaller fragments were chosen as probes (Fig. 6). A *Hind*III/*Kpn*I 6.0 kb fragment hybridized to cDNA clone numbers 6, 11A, 20, 29 and 19D. A *Hind*III/*Bam*HI 5.1 kb fragment hybridized with cDNAs 6 and 11A. Thus, the two smaller probes were able to classify the cDNA's into two groups: the first consisting of cDNA's 6 and 11A mapped to the right of P(l)00295 (Group 1), and the second (Group 2) consisting of cDNA's 19D, 20 and 29 which mapped to the left of P(l)00295 (Fig. 6).

I determined that Group 1 represented the transcript of the *shiva* gene. First, Southern hybridization of the cDNAs to the genomic DNA showed that the first group of cDNA's was proximal to the P(l)00295, while the second group mapped 3.6 kb to the left of P(l)00295. Second, the sequence of DNA rescued from P(l)00295 overlapped with sequence from cDNA 6, demonstrating that the P-element inserts into DNA transcribed in the cDNA clones. Finally, the null allele $shiva^{e4\text{-}1}$ carries a 3 kb deletion in a region which overlaps only with the cDNA group 6/11A (Fig. 6). All together, the evidence supports that the cDNA 6/11A group belongs to the *shiva* gene.

As cDNA 6 was slightly larger than cDNA 11A, I subcloned cDNA 6 into the Bluescript KS- vector (Stratagene) and sequenced the entire 3.5 kb insert (Fig. 7A). I used the MacVector program to produce theoretical translations in all reading frames on both strands of the cDNA. An open reading frame was found

and was submitted for a BlastP search for possible homologs. The sequence of *shiva* and its homologs are discussed below.

(2) The 3.5 kb cDNA rescues the lethality of *shiva* mutations

To verify that the 3.5 kb cDNA was encoded by the *shiva* gene, the cDNA was introduced into flies. A construct was made containing the full length 3.5 kb transcript in the pCaSpeR-hs expression vector (Fig. 7B) and Sheng Zhang introduced the construct into flies by germ line transformation. A single transformant line was recovered which mapped to the third chromosome. As the *shiva* gene also maps to chromosome III, Sheng jumped the insert to 2L for rescuing experiments. The lethal phenotype of flies homozygous for $shiva^{P(l)00295}$ was rescued by expressing the *shiva* transcript *P[hs-shiva31-1]* through daily heat shocks until hatching. This provided the final evidence that a disruption in the gene represented by cDNA 6was responsible for the *shiva* mutant phenotypes, including embryonic lethality caused by strong *shiva* alleles, $shiva^{P(l)00295}$.

(3) *shiva* encodes a member of the Cdc4/Met30 family

Sequence of the full-length *shiva* cDNA revealed an open reading frame encoding a putative 507 amino acid protein of the Cdc4/Met30 family (Fig. 8A). Proteins of this family are classified by two highly conserved motifs. An F-box motif exists in the N-terminal half of the predicted product. The C-terminal half consists of seven WD-40 (ß-transducin) repeats in tandem. Members of this

family of proteins have been linked to a large range of processes including cell division, immune responses, cell trafficking and now pattern formation (Laney and Hochstrasser, 1999; Maniatis, 1999; Neer et al., 1994).

An initial BlastP search revealed additional homologs in *C. elegans* and *Xenopus* (Fig. 8B). ß-TrCP from *Xenopus* shares 72% amino acid identity with D-SHIVA, with 91% identity in the C-terminus alone. ß-TrCP was identified as a suppressor of a temperature sensitive defect in an allele for cdc15, which is required for nuclear division in *S. cerevisiae* (Spevak et al., 1993). A second homolog identified by the Blast search was from *C. elegans*, designated K10B2.1 in Genbank. The *C. elegans* homolog contains 64% identity to SHIVA over all homologous regions, and 89% amino acid identity to SHIVA in its WD-40 repeat region. The existence of highly conserved SHIVA homologs in other species suggests that the protein could play similar roles in animal development.

(4) Null allele for *shiva* identified (*shiva*$^{e4\text{-}1}$)

Once the transcript for *shiva* was identified, I went back to the excision lines to identify a possible null allele for *shiva*. Mapping of cDNAs 6 and 11A provided molecular evidence for a null allele. The excision line e4-1 contained approximately a 3 kb deletion spanning from the *Bam*HI site left of P(l)00295 up to the *Hind*III site (Fig. 6). This deletion removes the 5' promoter region, the transcription initiation site, and coding sequences. Thus I conclude that no transcript can be produced in this mutant.

The *shiva* alleles *shiva*$^{e4\text{-}1}$ and *shiva*$^{P(l)00295}$ were the strongest *shiva* alleles both by genetic and molecular criteria. Both alleles were first instar lethal, and although I used them interchangeably, I have been careful to note their specific usage's.

(5) H-*shiva* cloned

To isolate the human homologue, the 1.5 kb coding sequence of the *Drosophila shiva* transcript was used as a probe to screen a human fetal brain cDNA library. The library was screened under low stringency conditions and 18 positives plaques were recovered in the primary phase. Secondary screening of the 18 positives plaques retrieved 4 positive plaques. A 2.2 kb transcript was assembled from cDNA extracted from the 4 positive plaques and it consists of a 1.5 kb coding region that shares 75% identity with the fly homologue (91% identity in the C-terminal region) (Fig. 8A, B). The human transcript, however, contains no upstream in frame stop codon. The same library was re-probed with the entire H-*shiva* transcript by Wei-Yi Wang. Re-probing the library failed to recover further 5' transcript, and no further attempts were made.

B. *shiva* expression

(1) Northern analysis

(a) *Drosophila*

To analyze the expression of *shiva*, I probed developmental and adult Northern blots generously provided by the laboratory of S. Artavanis-Tsakonas. These blots were probed with the full length 3.5 kb *shiva* cDNA. Northern analyses revealed that there were three transcripts (2.8 kb, 3.5 kb, and 4.1 kb) from the *shiva* gene during various developmental stages. 0-24 hour embryos expressed a single 3.5 kb transcript (Fig. 9(E)). At L1 larval stage, a second transcript of 2.8 kb became concurrently expressed (data not shown). Both the 2.8 and 3.5 kb transcripts were expressed until L3. In adult animals, males expressed two transcripts: a 4.1 kb and 2.8 kb; while females expressed 3 transcripts: 4.1 kb, 3.5 kb and 2.8 kb (Fig. 9(M and F)). As the 3.5 kb transcript was expressed only in adult females and early embryos, it is likely that the 3.5 kb transcript is maternal. Note that the maternal 3.5 kb transcript corresponds to the cloned cDNA that was used to fully rescue *shiva* mutant animals.

(b) human

Human northern blots (Stratagene) were probed with the full length human cDNA. Three transcripts for *shiva* were found in both human adult and developing tissues; a 6.0 kb, a 3.4 kb and a 2.4 kb transcript (Fig. 10A, B). The 6.0 kb transcript predominates in quantity in all tissues assayed with the exception of the adult testes, where the 2.4kb transcript was expressed at even higher levels. Increased expression of the 2.4 kb transcript was also observed in fetal liver tissue.

(2) SHIVA antibodies

SHIVA antibodies were raised to both the fly and human gene products. As the C-terminus of *shiva* shares high identity to other WD-40 repeat-containing proteins, the N-terminal region was chosen as the antigen. The N-terminus was fused to GST and resulting fusion proteins were expressed. Fusion proteins from the two constructs were prepared by inclusion body preps, as expression of these proteins proved to be insoluble. Proteins were injected into rats by Tie Qiang Ding. Many polyclonal and monoclonal antibody lines were produced for each fusion protein. Ding tested the different antibodies on Western blots to identify lines that detected SHIVA products of the correct sizes.

I extensively tested two of the antibodies (B14313 and M1407) against the *Drosophila* antigen by staining imaginal discs. Despite using and modifying a variety of staining protocols, I could not observe any staining which appeared to be *shiva*-specific. I eventually abandoned this endeavor. In contrast, Dr. Reza Yavari had wonderful success in staining human tissues, and found strong shiva expression in developing breast tissue, cartilage and hair follicles.

(3) *shiva in situ*'s

Determining the expression pattern of a gene during development is essential in understanding its function. As antibodies against SHIVA failed to be useful, I opted to ascertain the *shiva* expression pattern by *in situ* hybridization. A digoxigenin-labeled DNA probe of the entire *shiva*-coding region was generated and used to label Canton-S (wild type) discs.

a. wing discs

Expression of the *shiva* transcript in wing discs appeared to be very specific (Fig. 11A). In the wing blade, *shiva* is expressed along the wing margin in a region that corresponds to the area of the sensory organ precursor cells (arrow) (Campuzano and Modolell, 1992). This region also corresponds to the area of *scute* staining during wing development (see Chapter IV, Discussion). A second region of *shiva* expression is in the notum (arrowhead). Again, this defined region in the notum corresponds to sensory organ precursor cells and *scute* expression.

b. leg discs

shiva expression appeared to be both more ubiquitous and more ambiguous in the leg disc (Fig. 11B). Ten discs were closely examined, and the transcript appeared to be slightly more abundant in the anterior half of the disc. Expression of *shiva* was consistently observed at the dorsal tip of the disc (arrow).

c. eye discs

shiva expression followed a specific pattern in the eye disc (Fig. 11C). Expression was concentrated anterior to the MF, with very little *shiva* transcript observed in the posterior (Fig. 11C, D). While *shiva* expression in the anterior appeared to be ubiquitous, expression at the MF was very specific. Two thin bands of *shiva* expression lined the anterior and posterior margins of the MF (Fig. 11D). The significance of this pattern of expression and *shiva*'s role during eye development will be considered later (Chapter VI).

A reproducible expression pattern for *shiva* was also observed in the antennal disc. The *shiva* transcript was expressed in the center of the disc as well as the dorsal margin, suggesting a role for *shiva* in antennal development (Fig. 11C, arrows).

Discussion

Cloning of the gene *shiva* in *Drosophila* is a clear example of how a well-defined genetic organism can combine genetic and molecular tools for the easy identification of a gene locus. Once my original P-insertion ($shiva^{P(l)00295}$) was mapped to a specific genomic region, I was able to identify transcripts in this region. Genetics enabled me to discern the correct transcript for *shiva*. First, excision of the P-element lead to deletions in the *shiva* transcript. Second, several non-complimenting P-elements inserted within the transcript. Finally, introduction of the transcript back into flies by germline transformation was able to fully rescue the lethal phenotype of the original P-insertion. I also cloned the human homolog which shares a high degree of homology to the fly product, suggesting that *shiva*'s function may be evolutionarily conserved. In addition, I demonstrated that both the fly and human transcripts appear to be developmentally regulated.

SHIVA belongs to the Cdc4 family of proteins which is classified by two conserved domains: an N-terminal F-box and a C-terminal WD-40 repeat domain (Skowyra et al., 1997). Although when initially cloned *shiva* and its homologs had no known function, the archetype of this family, Cdc4 from *S. cerevisiae*, had

been shown to act as part of a multi-protein complex required to target substrates for ubiquitin-mediated degradation. Cdc4 is required for S phase entry into the cell cycle (Goebl et al., 1988; Willems et al., 1996; Yochem and Byers, 1987). Cdc4 mutants accumulate levels of the cyclin kinase inhibitor Sic1, and thus it was thought that Cdc4 targeted Sic1 for degradation, enabling cells to enter S phase. Several groups have demonstrated that Cdc4 acts by binding through its F-box to SKP1, an adaptor protein linking Cdc4 to the E2-conjugating enzyme Cdc53 (Bai et al., 1996; Feldman et al., 1997). The WD-40 (or ß-transducin) repeats in Cdc4's C-terminus identify and bind to the phosphorylated Sic1 substrate (Skowyra et al., 1997). Ubiquitination ensues after formation of this complex, and the Sic1 substrate is targeted for degradation. Recent biochemical data reveals that Cdc4 has properties of a ubiquitin (Ub) protein ligase. A sequence motif has been identified which contains a cysteine residue required for thioester bond formation between ubiquitin and its substrate (P. Zhou and P. Howley, personal communications). This motif and its catalytic cysteine are conserved in Cdc4 and SHIVA (Fig. 8C). Thus, it is likely that *shiva* encodes a putative Ub-ligase.

In the last year, βTrCP, the vertebrate homologue of *shiva* has been demonstrated to act in the ubiquitination of β-catenin and IκBα (Spencer et al., 1999; Winston et al., 1999; Yaron et al., 1998). IκBα sequesters the transcription factor NF-κB in the cytoplasm of quiescent cells. In response to stimuli such as TNFα, IκBα is phosphorylated and targeted for degradation, allowing NF-κB to enter the nucleus and bind its target genes. Groups have shown that in the presence of Ub-activating and –conjugating enzymes βTrCP ubiquinates

phosphorylated IκBα. This complex specifically recognizes a 19-amino acid destruction motif in IκBα (Winston et al., 1999). βTrCP also recognizes a destruction motif in β-catenin, whose levels are similarly regulated in a phosphorylation-dependent manner. β-catenin is a component of the TCF/Lef transcription factor complex that functions downstream of Wingless/Wnt signaling. βTrCP binds to both substrates through its WD40 repeats, and associates with the remainder of the Ub-proteolytic machinery through its F-box. A dominant-negative deletion mutant has also been identified for βTrCP, which lacks the N-terminal F-box. The dominant-negative deletion mutants tightly bind the phosphorylated substrates IκB and β-catenin but fail to support their ubiquitination, resulting in failure of activation of NF-kB and activating signaling dependent on the transcription factor Tcf, respectively (Winston et al., 1999; Yaron et al., 1998). Thus it appears that *shiva* and its homologs act in diverse signaling pathways, and that specificity of *shiva* targets may lie in their phosphorylated destruction motifs.

Three years after the cloning of *shiva*, the identical cDNA was identified and reported by Jiang and Struhl (Jiang and Struhl, 1998). This cDNA was published under the name of *slimb*. Data from the *slimb* paper differ significantly to my analysis of *shiva* and its function. When relevant, I will discuss in my dissertation the similarities and differences in our data.

In order to begin conducting functional studies for *shiva*, antibodies were raised against the N-terminal regions of both the fly and human protein products. Although the monoclonal antibodies generated appeared specific on Western blots, no specific staining in imaginal discs was ever attained despite

numerous attempts. I then proceeded to elucidate *shiva* expression patterns by *in situ* hybridization. The expression pattern for *shiva* in imaginal tissues turned out to be surprisingly specific. In particular, the coordination between *shiva* transcript expression and *scute* expression in the wing disc suggests that *shiva* may be linked to Notch signaling (Campuzano and Modolell, 1992). This may account for ectopic bristles observed in *shiva* mosaic wings (see Chapter IV). Additionally, the expression of *shiva* appears to be tightly regulated in the developing eye. The combination of *shiva*'s high degree of conservation to E3-ligases, its developmental regulation, and its specificity in expression patterns has proven to make *shiva* an exciting gene to study, and may link its function to a variety of signaling pathways.

Figure 6. Map of the *shiva* genomic region. The region illustrated depicts 20 kb of restriction-mapped genomic DNA isolated from a cosmid library. The size scale for 1 kilobase appears above the map. Hatched boxes indicate the probes used to isolate two groups of cDNAs. The cDNA transcripts are illustrated on the genomic restriction map. Group 2 corresponds to cDNA 19D, 20 and 29. Group 1 consists of cDNA6 and 11A. An arrow indicates the initiation codon and direction of transcription for Group 1. The *shiva*P-alleles (*shiva*^{00295} and *shiva*^{05415}) have P-elements in the first exon, and the excision line *shiva*$^{e4\text{-}1}$ deletes the *shiva* promoter and transcript regions. Restrictions sites: G=*Bgl*II, H=*Hind*III, X=*Xba*I, R=*Eco*RI, K=*Kpn*I.

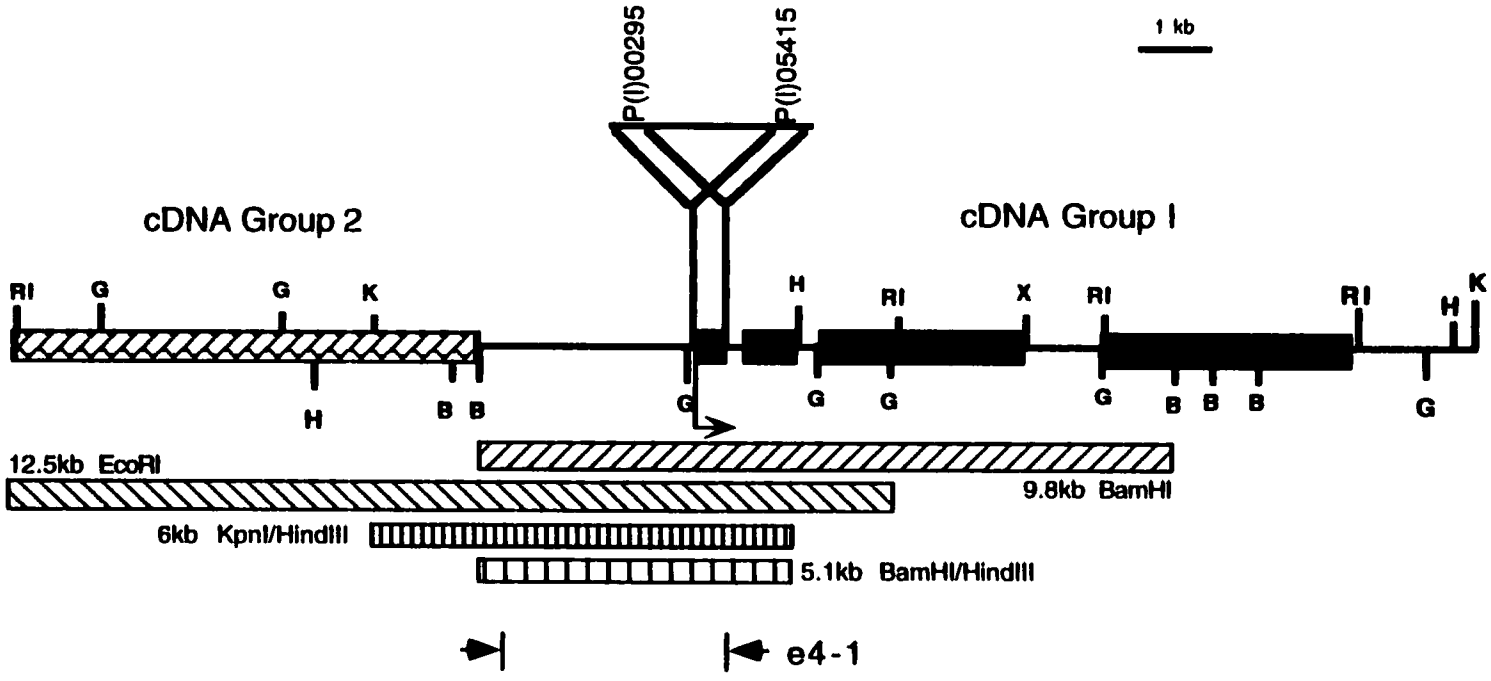
P(l)00295
P(l)05415
1 kb
cDNA Group 2
cDNA Group I
RI G G K H B B G H RI X RI RI H K G G G G B B B G
12.5kb EcoRI
9.8kb BamHI
6kb KpnI/HindIII
5.1kb BamHI/HindIII
e4-1

Figure 7. *shiva* expression constructs. (A) The 3.5 kb *shiva* transcript was initially cloned into the pBS(KS-) vector by partially digesting phage DNA with *Eco*RI and directly cloning into the vector *Eco*RI site. (B) pCaSpeR-hs-shiva was constructed by cloning a *Not*I-*Eco*RV fragment from BS-shiva3.5 into the *Not*I-*Stu*I sites of the plasmid pCaSpeR-hs. (C) pUAST-*shiva* was constructed by cloning a *Xba*I fragment from pBS-shiva3.5 directly into the *Xba*I site of the pUAST plasmid. The *Xba*I fragment includes the entire 5' untranslated and coding sequences, but lacks the 3' untranslated region.

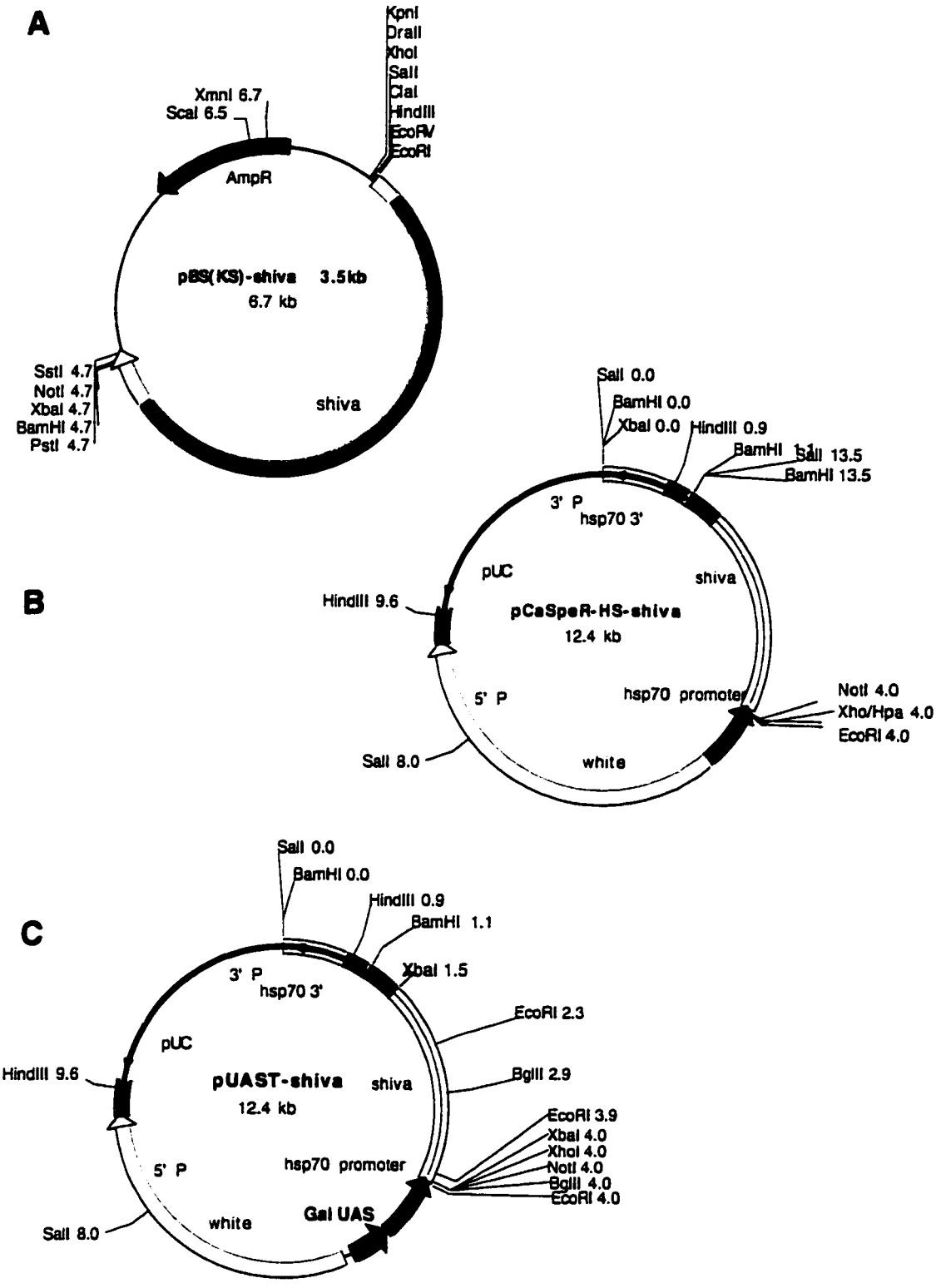
A
KpnI
DraII
XhoI
SalI
ClaI
HindIII
EcoRV
EcoRI
XmnI 6.7
ScaI 6.5
AmpR
pBS(KS)-shiva 3.5kb
6.7 kb
shiva
SstI 4.7
NotI 4.7
XbaI 4.7
BamHI 4.7
PstI 4.7
B
SalI 0.0
BamHI 0.0
XbaI 0.0
HindIII 0.9
BamHI 1.1
SalI 13.5
BamHI 13.5
3' P
hsp70 3'
pUC
shiva
HindIII 9.6
pCaSpeR-HS-shiva
12.4 kb
5' P
hsp70 promoter
NotI 4.0
Xho/Hpa 4.0
EcoRI 4.0
SalI 8.0
white
C
SalI 0.0
BamHI 0.0
HindIII 0.9
BamHI 1.1
XbaI 1.5
3' P
hsp70 3'
EcoRI 2.3
pUC
HindIII 9.6
pUAST-shiva
shiva
12.4 kb
BglII 2.9
EcoRI 3.9
XbaI 4.0
XhoI 4.0
NotI 4.0
BglII 4.0
EcoRI 4.0
5' P
hsp70 promoter
white
Gal UAS
SalI 8.0

Figure 8. SHIVA protein and its homologs

(A) Alignment of *Drosophila* and human *shiva* protein products illustrates two distinct regions. The N-terminal contains a cyclin F-box (dashed bar), while the C-terminal region contains seven WD-40 repeats (solid bars).). Identical residues are boxed, and dots denote gaps in the alignment. (B) Diagram of the SHIVA homologs. Percent identity over the homologous regions in the N-terminal and C-terminal regions compared to the *Drosophila* sequence. Included are the homologs, ß-TrCP from *Xenopus*(Spevak et al., 1993) and K10B2.1 from *C. elegans* (GI860695). Also included are the archetypes of this family, Met30 and CDC4 from *S. cerevisiae*. (C) Alignment of the CUTE box motif from human, fly, *Xenopus* and *C. elegans* sequences. The highly conserved cysteine is depicted in bold type.

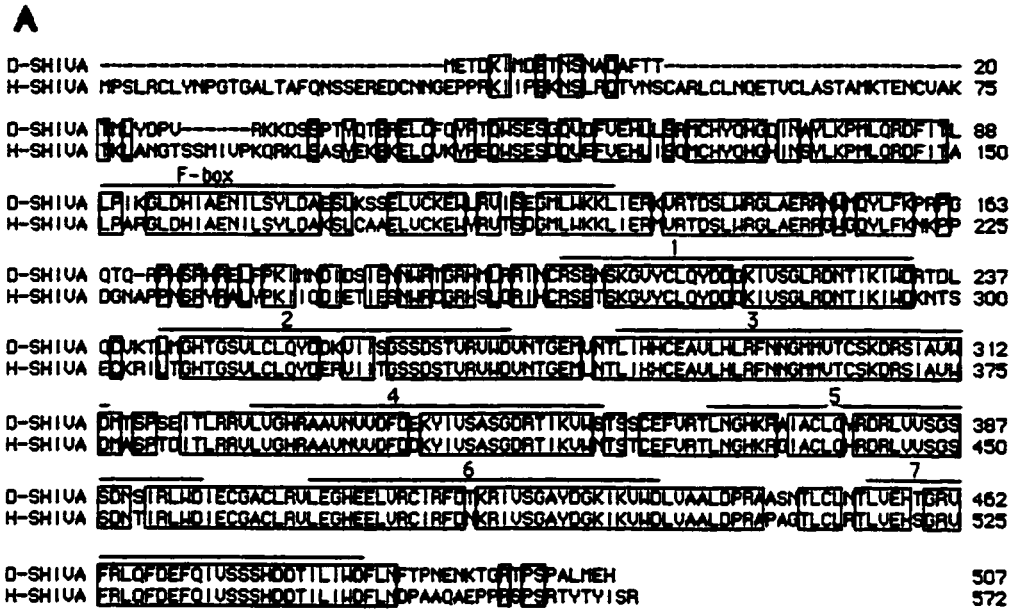
A
D-SHIVA
H-SHIVA
F-box
1
2
3
4
5
6
7
B
F-box
WD-40 repeats
SHIVA
D. melanogaster
80%
90%
H-SHIVA
H. sapiens
82%
91%
β-TRCP
Xenopus
40%
89%
K10B2.1
C. elegans
33%
31%
MET30
S. cerevisiae
36%
25%
CDC4
S. cerevisiae
C
consensus:
WD#-TG-C#+T#-GH
H-SHIVA
SHIVA
β-Trcp
K10B2.1
WDIECGACLRVLEGH
WDIECGACLRVLEGH
WDIECGACLRVLEGH
WDIHSGYCLRVLEGH
= hydrophobic residue

Figure 9. Northern analysis reveals 3 developmentally regulated *shiva* transcripts in *Drosophila*. Northern blots were generously provided by the Artavanis-Tsakonas lab. Lanes on the Northern blots are labeled as follows: E, 0-24 hour embryos; M, male adult flies; F, female adult flies. The 3.5 kb transcript observed in embryos is also in adult female flies. In addition, both adult males and females contain 4.1 and 2.8 kb *shiva* transcripts.

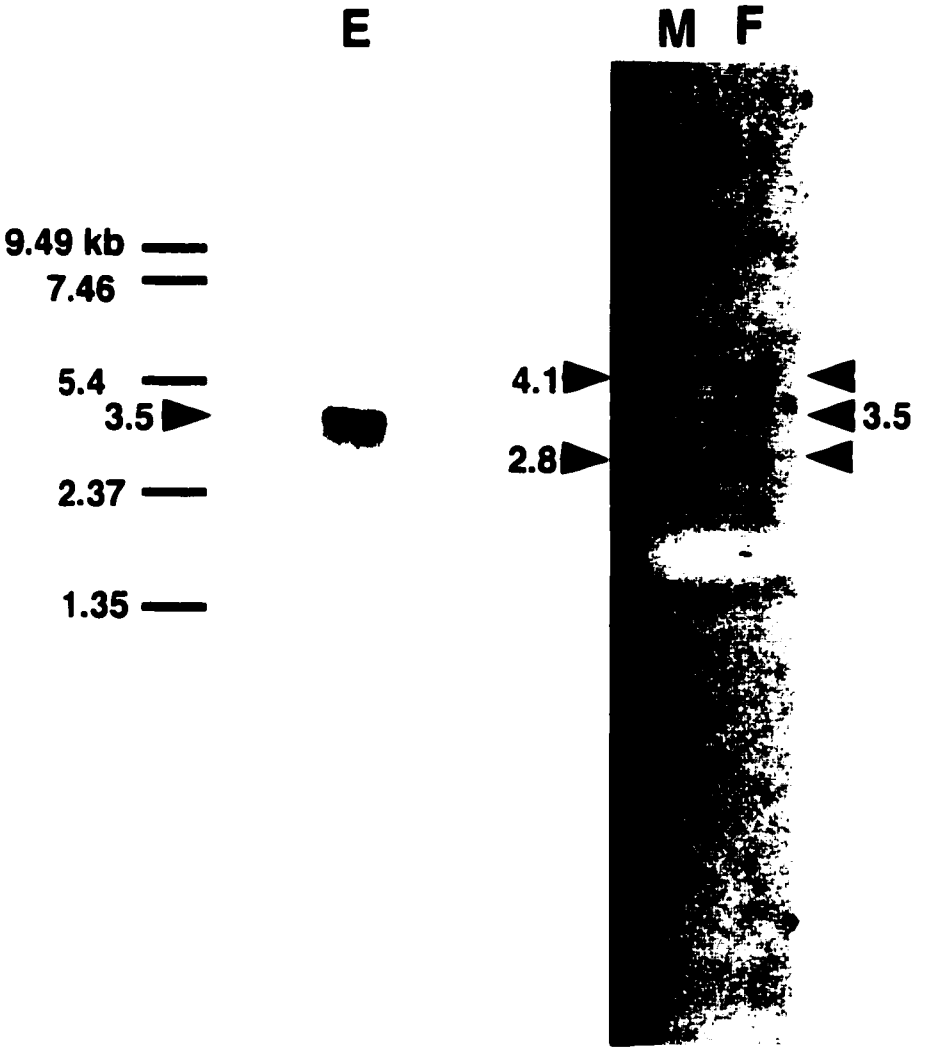
E
M
F
9.49 kb
7.46
5.4
3.5
2.37
1.35
4.1
2.8
3.5

Figure 10. Northern analysis of human tissues reveals 3 developmentally regulated *shiva* transcripts. (A) A Northern blot of adult human tissues (Stratagene) was hybridized against the full length human *shiva* transcript. Three *shiva* transcripts are expressed in all tissues tested: 6.0 kb, 3.4 kb, and 2.4 kb. Note that the testes expresses higher levels of transcripts than the other tissues, with the predominant being the 2.4 kb transcript. (B) A Northern blot of fetal human tissues displays the same-sized transcripts as in the adult tissues. Among the fetal tissues, the fetal liver appears to contain highest levels of *shiva* transcript.

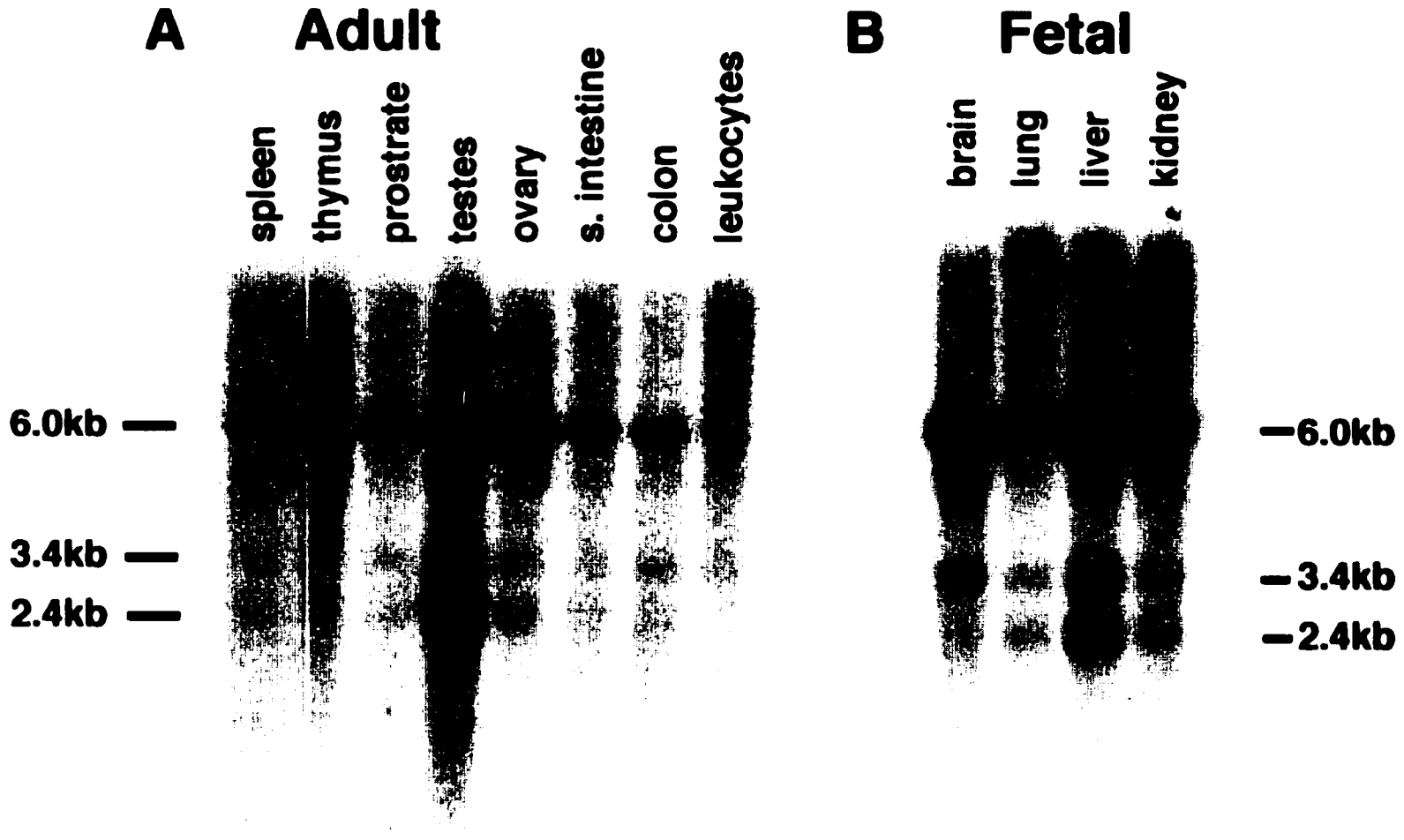
A
Adult
spleen
thymus
prostrate
testes
ovary
s. intestine
colon
leukocytes
6.0kb
3.4kb
2.4kb
B
Fetal
brain
lung
liver
kidney
6.0kb
3.4kb
2.4kb

Figure 11. Expression of the *shiva* transcript demonstrated by *in situ* hybridization. *In situ* of wild type imaginal discs using a DIG-labeled DNA probe containing the full-length *shiva* transcript. (A and B) Wing and leg discs are positioned anterior left and ventral down. (A) A wing disc with a region of *shiva* expression at the wing margin (arrow) and notum (arrowhead) (magnification at 16X). (B) A leg disc with low levels of ubiquitous expression, with a slight increase in levels of *shiva* transcript in the anterior. Increased *shiva* expression at the dorsal tip (arrow). (C and D) Eye discs positioned posterior left. Note that the *shiva* transcript is expressed anterior not posterior to the MF (magnification at 25X). (D) High magnification of the region boxed in (C) (magnification at 80X). *shiva* is expressed in two stripes (arrows) marking the anterior and posterior margins of the MF (bar).

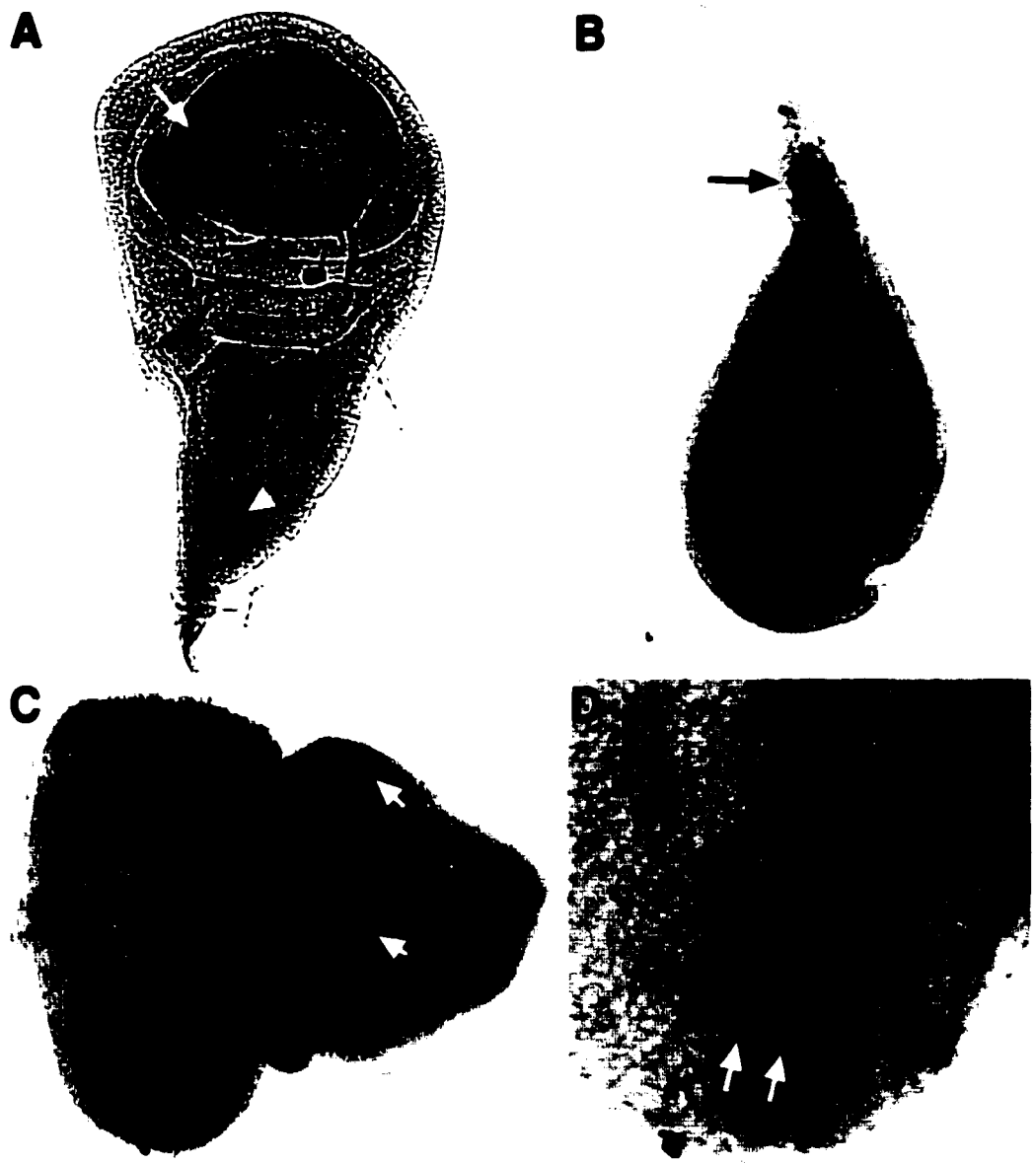
A
B
C
D

Chapter IV. Analysis of the *shiva* phenotype

Introduction

Although cloning a gene is an essential part of understanding its function, it is also necessary to define gene function through analysis of its mutant phenotypes. To fully understand *shiva*'s role during development, I characterized the *shiva* mutant phenotypes in a variety of tissues and developmental stages. Since mutations in the *shiva* locus were lethal to animals, I used the FLP/FRT system to generate marked mutant clones in both developing tissues and adult cuticle (Xu and Rubin, 1993). Clones can be induced at different developmental stages, thus tracking the function of a gene at a developmentally specific time in viable animals. In addition, this system can elucidate cell interaction mechanisms by defining the requirement of gene's function in neighboring cells.

The FLP/FRT system enabled me not only to better define *shiva*'s mutant phenotype in the adult fly, but also begin to define its function during development. From analysis of adult mosaic flies, I determined that *shiva* has a non-cell autonomous effect on surrounding wild type cells, inducing them to over proliferate. Occasionally, the resulting ectopic structures in *shiva* mosaic flies are supernumerary limbs suggesting *shiva* plays a role in pattern formation. By marking clones in developing tissues I also ascertained the effect of *shiva* on the expression patterns of other molecules involved in development. Thus, this system proved to be pivotal in characterizing *shiva*'s mutant phenotype and gene function.

Results

A. Leg: Patterning defects in *shiva* mosaic legs

(1) *shiva* mutant clones alter pattern formation in legs of mosaic flies

My preliminary phenotypic analyses suggested that *shiva* was involved in pattern formation during limb development. Mutant clones for *shiva* produced two phenotypes in mosaic legs: tissue outgrowths and bifurcated legs (Fig. 1). To analyze the *shiva* mosaic phenotype, the *yellow*$^-$ (y^-) and *Stubble*$^+$ (Sb^+) cuticle markers were used to label cells carrying a mutation for the null allele of *shiva* (*shiva*$^{e4-1}$) (Xu and Rubin, 1993). In mosaic legs, tissue outgrowths were the predominant observed phenotype, and were composed of *shiva*$^+$ cells (y^+ and *Sb*) (Fig. 12A). Similarly, supernumerary legs were derived from *shiva*$^+$ cells (Fig. 12C and E). While wild type legs are normally composed of dorsal, ventral and posterior structures (defined by bristle types) the supernumerary leg was composed solely of dorsal structures (compare Fig. 12C and E to D and F). On rare occasion a single y^- bristle was observed associated with an outgrowth. Although it appeared that *shiva*$^-$ cells were able to induce both patterning and proliferation changes in a developing leg, the *shiva*$^-$ cells themselves were not viable to adulthood. This suggested that the outgrowth was induced by a *shiva* clone originating from dorsally fated cells. It appears that the fate of these cells

was not altered by the absence of *shiva*, but rather the pattern of these cells was re-organized to create a new P/D axis. Thus, *shiva* appears to play roles in both cell proliferation and pattern formation.

(2) *shiva* mutant clones misexpress *dpp* and *wg* in leg imaginal discs

shiva-induced outgrowths are reminiscent of the phenotypes caused by misexpression of *dpp* and *wg* through perturbation of the Hh-signaling pathway (Basler and Struhl, 1994; Struhl and Basler, 1993; Wilder and Perrimon, 1995). Thus, we examined *dpp* and *wg* expression in *shiva* mosaic leg discs using *wg-lacZ* and *H1-1dpp-lacZ* reporter genes (Blackman et al., 1991; Kassis et al., 1992). Although *lacZ* reporter genes may not always reflect protein expression, these reporters have been shown to be faithful indicators of *wg* and *dpp* gene expression in the leg disc (Brook and Cohen, 1996; Jiang and Struhl, 1996; Jiang and Struhl, 1995; Lecuit and Cohen, 1997; Penton and Hoffman, 1996). $shiva^{e4\text{-}1}$ and $shiva^{P(l)00295}$ mutant clones were generated and identified by an absence of the cell marker π-Myc.

shiva mutant clones ectopically expressed *wg* and *dpp* in a cell-autonomous fashion, i.e., only mutant cells for *shiva* expressed ectopic *wg* and *dpp* (Fig. 13). Ectopic *wg* expression was observed in both ventral and dorsal regions of the leg disc (Fig. 13A-C, J). This was intriguing as activation of Hh-signaling leads to misexpression of *wg* only in the ventral domain of discs. To determine if the expression of *wg* in *shiva* clones followed a specific pattern in the leg disc, I mapped over 100 clones and catalogued their ability to express *wg*. Curiously, I

was able to subdivide the leg disc into 5 regions according to their ability to misexpress *wg* in *shiva*⁻ cells (Fig. 13J). Three of the five defined regions express *wg*. Clones in the native expression domain for *wg* (Region IV) and in the native expression domain for *dpp* (Region I) misexpressed *wg*. Interesting to note, Region I corresponds to the region of *shiva* expression observed in *in situ* experiments. Region III at the D/V midline also contained *shiva* clones that misexpress *wg*. In this case, not all the mutant cells of the clone misexpressed *wg* (compare to regions I and IV). This may be the result of antagonism by *dpp* expressed in the same clones (see below).

shiva null clones also expressed ectopic *dpp*. Similar to the results with *wg*, *dpp* was misexpressed both in its native domain of expression (the dorsal region), and outside of this region (Fig. 13D-I). At the D/V midline, *dpp* was expressed in only a subset of *shiva*⁻ cells in clones (Fig. 13G). However unlike with *wg*, I could not determine a distinct misexpression pattern for *dpp* despite evaluating 98 *shiva* clones. It is possible that *shiva* regulates *dpp* and *wg* expression differently.

In *shiva* mutant clones situated within or near the endogenous *dpp* expression zone, *dpp* was expressed in the mutant cells but down-regulated in adjacent wild-type cells (Fig. 13G-I). Previously it had been shown that *wg* and *dpp* signaling mutually antagonize each other's expression, which prevents expression of the two molecules in the same cells (Brook and Cohen, 1996; Jiang and Struhl, 1996; Penton and Hoffman, 1996; Theisen et al., 1996). Note that *wg* was also observed to be expressed in dorsally located clones (Fig. 13A). Ectopic expression of both *wg* and *dpp* in *shiva*⁻ clones in the dorsal-anterior of the leg disc indicates a disruption of this mutual antagonism.

(3) Effects of *shiva* mutant clones on *hh* and *ptc* expression

As it was clear that *shiva*'s role during leg development is to suppress *dpp* and *wg* expression, I asked if *shiva* was also effecting other components of Hh-signaling. To do this I examined the effects of *shiva* mutant clones on *P30,hh-lacZ* expression and also on *ptc-lacZ* expression. *hh* expression patterns and levels were unaffected in mosaic discs containing $shiva^{00295}$ clones (Fig. 13K and L). This suggested that *shiva* is acting to regulate *dpp* and *wg* expression downstream of Hh.

In contrast to the effect on *hh* expression, *shiva* mutant clones had an effect on *ptc-lacZ* expression patterns. *ptc* is normally expressed in a stripe along the A/P axis, and at lower levels throughout the anterior of the leg disc. *shiva* mutant clones had varying effects on *ptc* expression depending on their position in relation to the A/P border (Fig. 13M). Cells of clones which intersect the A/P border where *ptc* is normally expressed at high levels were absent of *ptc* expression (Fig. 13N). In contrast, *shiva* mutant clones adjacent to either side of the A/P border up-regulated *ptc* expression. Finally, clones removed from the border have no effect on *ptc* expression (Fig. 13M, asterisks). How could this be? It appears that *shiva* $^{-}$ clones only have an effect on *ptc* expression when associated with the A/P border and with endogenous Hh. *ptc* expression is normally regulated by Hh-signaling; in the presence of Hh, *ptc* expression is up-regulated (Chen and Struhl, 1996; Ingham et al., 1991; Phillips et al., 1990). If *shiva* mutations activate *dpp* and *wg* expression, then one would expect *ptc* to be

up-regulated. Since *shiva* has the opposite effect than would be predicted one could speculate that *shiva* interferes with Hh-signaling such that the feedback to regulate *ptc* expression is blocked. The point where *shiva* intersects Hh-signaling may be between *ptc* and *smo*, the transmembrane protein which transduces the Hh signal (see Chapter V).

B. Wing: Patterning defects of wing in *shiva* mosaic flies

(1) Mosaic analysis of *shiva* in wings

Similar to the leg, *shiva* mosaic wings displayed both tissue outgrowths and duplicated structures (Fig. 14). All outgrowths in the wing consisted of wild type cells. The outgrowths extended from both the ventral and dorsal surfaces of the blade and occurred in both the anterior and posterior halves of the wing (Fig. 14A). Occasionally, a few *shiva*$^-$ cells (*y*$^-$) were identified in the center of outgrowths (Fig. 14C); more often, the outgrowths contained small numbers of morphologically abnormal cells in similar positions (Fig. 14D).

Examination of these outgrowths revealed that they were organized into wing blade-like structures with wing margin bristles on the outer edge of each outgrowth. High magnification views of the *shiva* mosaic wings revealed that regardless of their position along the A/P axis, all outgrowths followed a very specific pattern. The bristles on the outer edge of each outgrowth directly reflected the bristle type located at the wing margin in the corresponding A/P position. For example, outgrowths between the first and second wing veins are

composed of third row bristles (Fig. 14B), while those spanning the third wing vein have second row bristles at their apex (Fig. 14C), etc. Thus, the *shiva*$^-$ cells in the wing appear to induce the proliferation of adjacent cells to form outgrowths.

Although the appearance of bristles on the edges of these outgrowths indicated that they have similar A/P values according to their original positions in the wing, these outgrowths were too small to reveal if they underwent any A/P axis reorganization. Infrequently, supernumerary wings developed from the wing hinge (Fig. 14E, F). Such wings were symmetric duplications of anterior-most structures, suggesting a reorganization of the A/P axis in *shiva*-induced outgrowths.

(2) *shiva* mutant clones perturb *dpp* expression in the developing wing blade

As *shiva*$^-$ cells can alter the expression patterns of *wg* and *dpp* in the leg imaginal disc, I tested whether clones for *shiva* could also alter the expression patterns of these molecules in the wing disc. *shiva* mutant clones induced ectopic *dpp* expression throughout the anterior wing blade (Fig. 15A-C). In contrast, mutant clones ectopically induced *wg-lacZ* expression only in those clones located in the region of the disc that gives rise to the notum (Fig. 15D-F). Thus, it appears that *shiva*'s role during wing development is primarily to regulate *dpp* expression in the wing blade.

In contrast to the leg disc, we did not observe any modification of *ptc* expression in *shiva* mosaic wing discs (Fig. 15G-J). Hh expression was also examined in *shiva*$^-$ clones, and no obvious change was detected (Fig. 15K, L).

Discussion

Characterization of the *shiva* phenotype using mosaic analysis is a perfect demonstration of the power of *Drosophila* genetics. From this rather simple set of experiments, the *shiva* mutant phenotype was discerned from developing to adult stages of development. I further gained insight into the genes regulated by *shiva* (*dpp* and *wg*), and the discrepancy in how *shiva* regulates these molecules in different tissues (leg versus wing). Finally, understanding was gained in how *shiva* mutant cells possibly interact with surrounding wild type cells.

shiva has a non-cell autonomous effect in developing tissues to induce outgrowths

A striking feature from the *shiva* clonal analysis is that although *shiva* has a cell-autonomous effect in the imaginal discs (i.e., the misexpression of *dpp* and *wg* in *shiva* mutant cells), the ultimate adult phenotype is one that is non-cell autonomous (i.e., adult structures are composed of wild type cells). How can this be? *shiva*$^-$ cells in imaginal tissues express the growth factors *dpp* and *wg*. It is possible that these growth factors induce surrounding wild type cells to proliferate. This is evidenced in both the wing and leg discs, where wild type cells (*myc*$^+$) surrounding *shiva* mutant clones greatly overproliferate (Fig. 15K, L). This observation is consistent with the results from the adult mosaic analyses, in which the ectopic structures consist of wild type cells. Where do the *shiva*$^-$ cells

go? Every outgrowth in *shiva* mosaic flies is associated with some scarring, as is depicted in Fig. 14D. The association of scaring and the rare occurrence of *shiva*$^-$ cells associated with outgrowths, suggests that *shiva*$^-$ cells are not viable, and the scaring observed is possibly a remnant of the mutant cells.

Expression of *dpp* and *wg* is regulated in both the A/P and D/V axes in the leg disc

shiva-induced outgrowths are reminiscent of the phenotypes caused by misexpression of *dpp* and *wg* (Basler and Struhl, 1994; Struhl and Basler, 1993; Wilder and Perrimon, 1995). Thus, we examined *dpp* and *wg* expression in *shiva* mosaic legs. Both *dpp* and *wg* were misexpressed in *shiva* mutant clones located in the dorsal and ventral leg compartments, as well as in some domains of the posterior compartment (Fig. 13).

The *shiva* phenotype differs from that of previously studied genes, in that it is the first gene found to deregulate both *wg* and *dpp* expression in the D/V axis. Disrupting components of the Hh signaling pathway deregulates *wg* and *dpp* only along the A/P axis. For example, ectopic activation of *hh* or removal of *ptc* and *pka* results in misexpression of *dpp* and *wg* in anterior cells that normally do not express these genes (Basler and Struhl, 1994; Jiang and Struhl, 1995; Li et al., 1995; Pan and Rubin, 1995). However, *wg* misexpression is always restricted to the ventral cells, while *dpp* misexpression is restricted to dorsal cells. Thus, the control of *wg* and *dpp* expression in the D/V axis is not disrupted. The mechanism restricting *wg* and *dpp* in the D/V axis is not known. It was believed

that the ability of dorsal cells to express *dpp* and of ventral cells to express *wg* is an inherent property of the D/V identity established during embryogenesis. The mutant phenotype of *shiva*$^-$ clones in discs provides the first evidence indicating that *wg* and *dpp* expression in the D/V axis is actively regulated during imaginal disc development, and is not solely defined during embryonic development.

The *shiva* phenotype described here was not observed in the previous study which used weak *slimb* alleles and revealed only A/P defects (Jiang and Struhl, 1998). The phenotypic differences probably reflect the fact that we have used a null allele instead of hypomorphic alleles for *shiva* in all our studies.

Figure 12. Analysis of the *shiva* mosaic phenotype in adult legs.

(A) SEM shows a leg outgrowth with *Sb*, y^+ bristles of *shiva*$^+$ cells. (B) A bifurcated leg from a *shiva*$^{e4\text{-}1}$ mosaic fly. (B-F) A wild type third leg (B, right) contains posterior transverse bristles (D, bar) and the signature ventral bristles (F, arrow). The ectopic leg (B, left) has dorsal bristles on both its sides (C, E). Both the wild type leg and the supernumerary leg are composed of wild type or *shiva*$^+$ y^+ bristles.

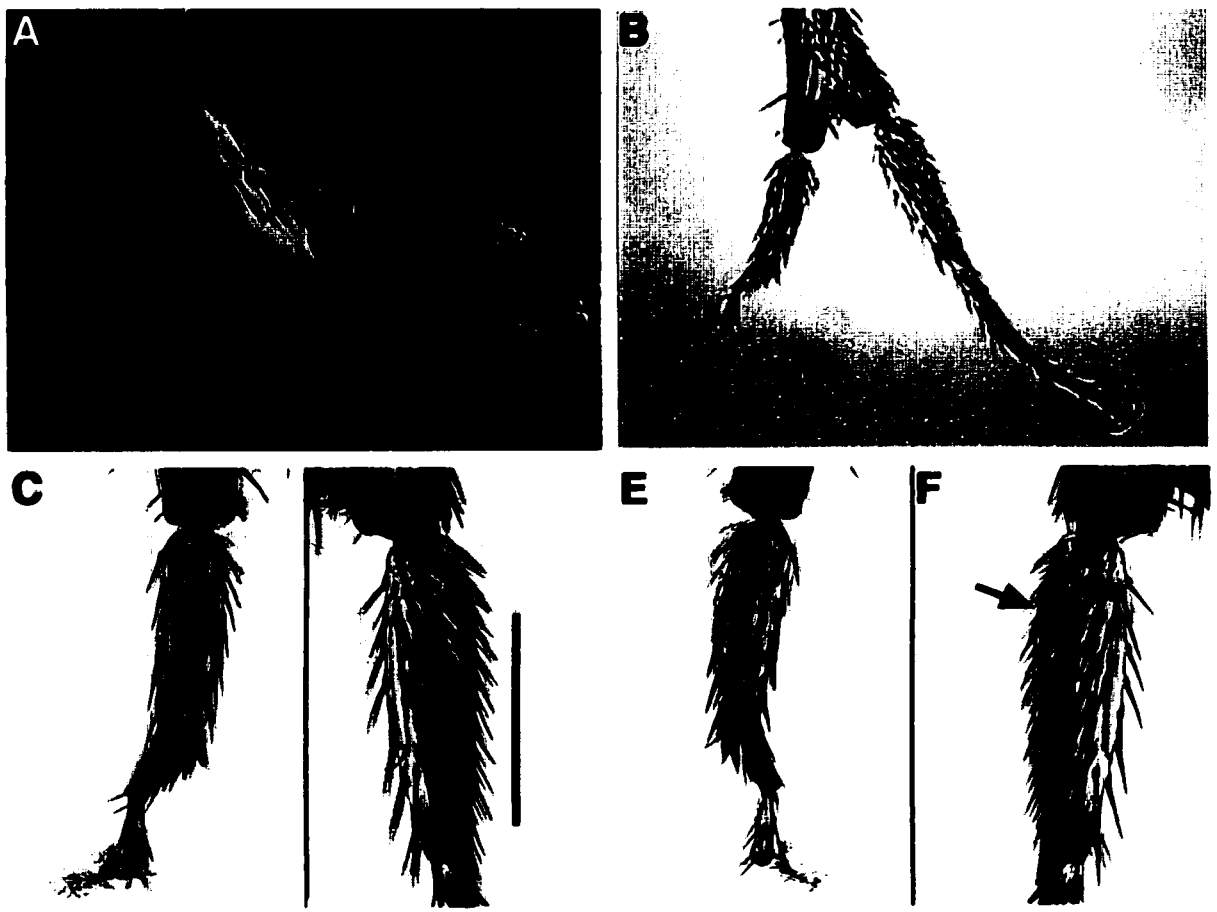
A
B
C
E
F

Figure 13. *shiva* clonal phenotype in leg imaginal discs.

In all panels, third instar leg discs are positioned with anterior to the left and ventral down. *shiva*$^-$ clones are marked by an absence of anti-Myc staining (green). *wg-lacZ, H1-1,dpp-lacZ, ptc-lacZ and P30,hh-lacZ* expression patterns are visualized with anti-ß-gal antibody (red). (A) Leg disc bearing *shiva*^{P00295} clones in the dorsal region associated with ectopic *wg-lacZ* expression. Close-up images of the clone in (A) illustrate *shiva*$^-$ clone (lacking green) (B) with ectopic *wg* expression (red) (C). (D) *shiva*$^{e4\text{-}1}$ clones also express ectopic *dpp*. Close-up images of the clone in (D) illustrate a *shiva*$^-$ clone (E) with ectopic *dpp* expression (red) (F). (G) *shiva*$^{e4\text{-}1}$ clones in the endogenous domain for *dpp* expression (arrow). Close-up images of the clone in (G, arrow) illustrate a *shiva*$^-$ clone (H) in which *dpp* is expressed in the *shiva*$^-$ cells, but is suppressed in nearby wild-type cells (I, arrow). (J) A composite view of *wg* expression in 103 analyzed *shiva*$^-$ clones, illustrating five subregions. At the dorsal tip (I) and ventral-anterior (IV) regions, *wg* is ectopically expressed in all *shiva*$^-$ cells of a clone. Region III, however, which spans the D/V border is unique in that only a fraction of the mutant cells express *wg*. No ectopic *wg* expression is observed in regions II and V. In contrast to their effects on *wg* and *dpp* expression, *shiva*^{P00295} clones do not alter *hh* expression (K). A close-up image of the clone in (K) illustrating the anterior *shiva*$^-$ clone (asterisk) does not express *hh* (L). (M) *shiva*^{P00295} clones located far anterior from the A/P border do not perturb *ptc* expression (asterisk). (N) In contrast, those clones that intersect the A/P border lack *ptc* expression (arrow), while those adjacent to the A/P border have elevated *ptc* expression.

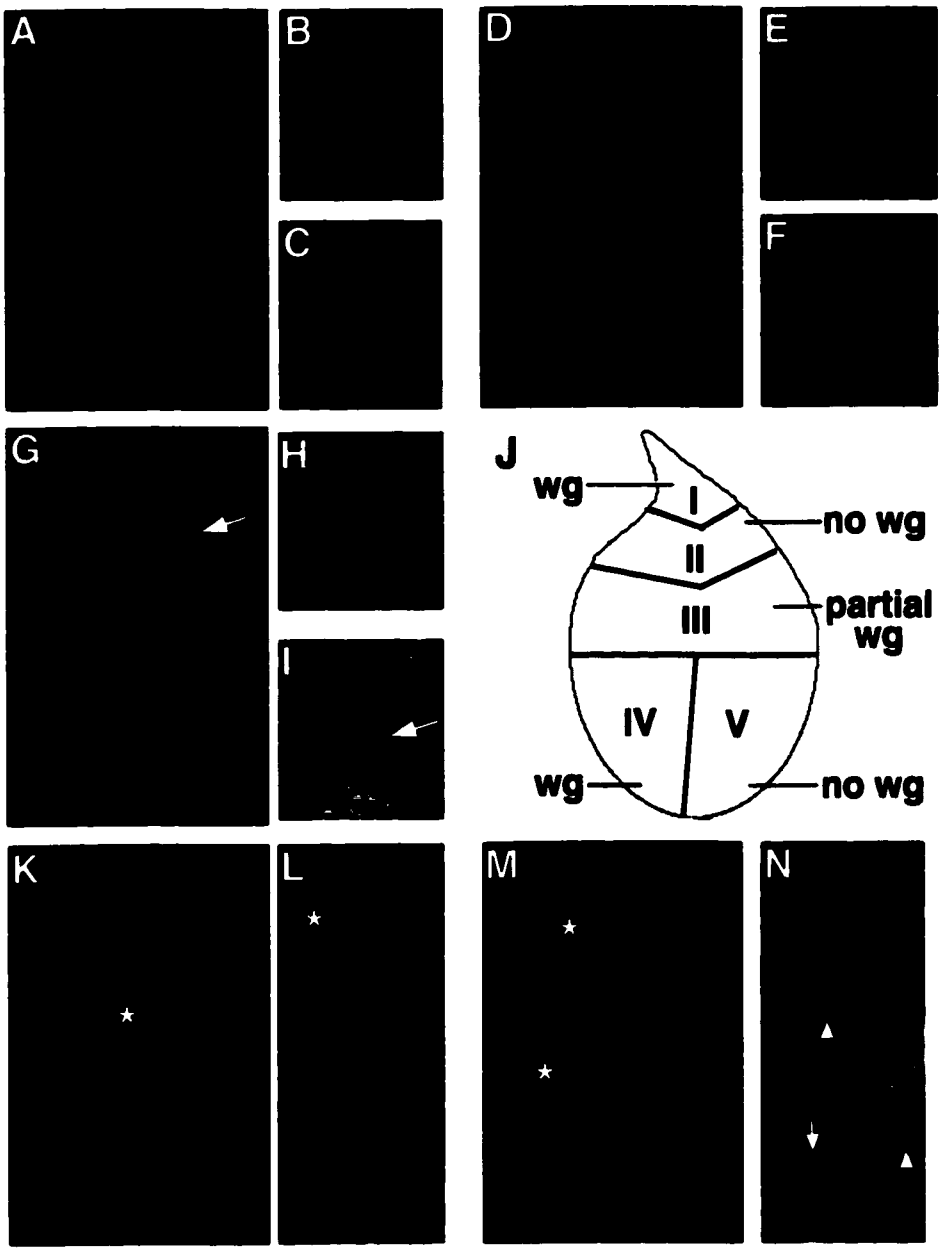
A
B
C
D
E
F
G
H
I
J
wg
I
no wg
II
III
partial
wg
IV
V
wg
no wg
K
L
M
N

Figure 14. The *shiva* adult mosaic phenotype in wings.

(A) A *shiva*$^{c4-1}$ mosaic wing blade with multiple outgrowths. Outgrowths extend from both dorsal and ventral surfaces of the wing blade, and are found in both anterior and posterior regions. (B) Close-up of a dorsally extending outgrowth in (A, arrow). Triple-row bristles are associated with this outgrowth. (C) Magnification of an outgrowth indicated by the yellow box in (A). The outgrowth spans both sides of the third wing vein, and contains second row bristles at its apex. Two y^-, Sb^+ bristles (*shiva*$^-$) are associated with this outgrowth (C, arrow) (D) Morphologically abnormal cells are seen at the center of an outgrowth (arrow). (E, arrow) The supernumerary wing contains near-mirror images of anterior-most structures (F).

A
B
C
D

Figure 15. *shiva*$^{-}$ clones in wing imaginal discs.

Third instar wing discs are positioned anterior down. *shiva*$^{e4\text{-}1}$ and *shiva*^{00295} clones are marked by the absence of π-Myc staining in green, all reporter genes are stained red.

(A-C) Ectopic *H1-1,dpp-lacZ* expression is associated with *shiva*$^{-}$ clones in both the A and P regions of the wing blade (A, arrowheads). (B, C) Close up of an anterior clone showing only the *shiva* cells express *dpp-lacZ*. The unstained area in the central-anterior region in (A) is not a clone.

(D-F) A disc mosaic for *shiva*^{00295} is stained with the *wg-lacZ* reporter gene (red). Clones for *shiva* induce ectopic *wg* expression only in the scutellum region of the notum. (E and F) Higher magnification clearly illustrates that only the *shiva*$^{-}$ cells are ectopically expressing *wg-lacZ*.

(G-J) *ptc-lacZ* expression is along the A/P stripe in the wing disc. (G) *shiva* mutant clones in the notum and the A/P stripe do not alter *ptc* expression patterns (asterisks). (H) Close up of the A/P border *shiva*$^{-}$ clone in G (asterisk) defined by π-Myc staining, does not perturb *ptc-lacZ* expression (I). (J) Merged image of (H) and (I).

(K and L) *shiva*$^{-}$ clones do not perturb endogenous *P30,hh-lacZ* expression. (L) High magnification of outgrowths on the disc edge, illustrating that overproliferating wild type cells surround *shiva*$^{-}$ clones (arrows).

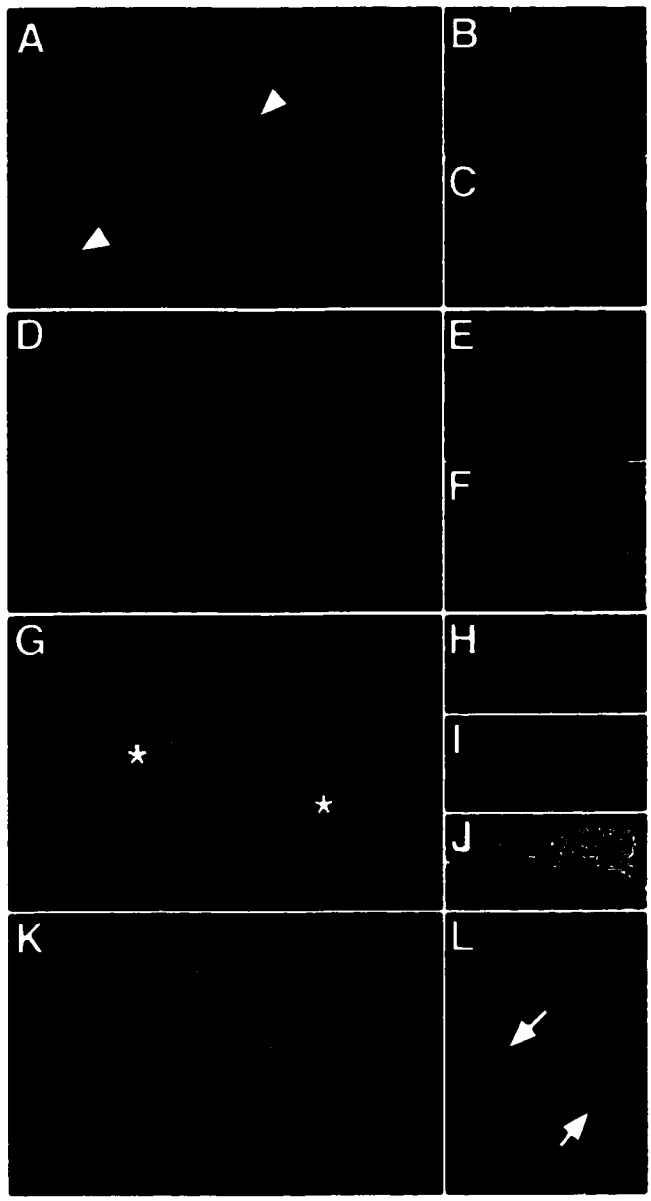
A
B
C
D
E
F
G
H
I
J
K
L

Chapter V. Genetic Epistasis

Introduction

The previous chapters have described the characterization of the various *shiva* phenotypes. No gene product however acts alone. It is important to understand the context or pathways within which a gene acts. This chapter is devoted to elucidating the genetic context for *shiva* during patterning of the leg and wing imaginal tissues.

As *shiva* mutant clones deregulate the expression of *dpp* and *wg*, it was first necessary to ask: are *dpp* and *wg* the direct effectors of the *shiva* signal? In other words, is the misexpression of *dpp* and *wg* in *shiva* mutant clones responsible for the outgrowth phenotype observed in adult *shiva* mosaic animals? Once *dpp* and *wg* were established as direct effectors of *shiva*, it was then necessary to determine at which point in the Hh-signaling pathway *shiva* influenced the expression of these molecules. This work is described below, as well as a model for a genetic role of *shiva* during limb development.

Results

A. *dpp, shiva* and *wg, shiva* double mutant clones

To test whether *dpp* and *wg* are direct effectors of the *shiva* signal, double mutant clones were built between *shiva* and *dpp*, and *shiva* and *wg*. Genetically this was tricky as *shiva* is positioned on 3R while *dpp* and *wg* are both on 2L. The

strategy I used took advantage of the *shiva* rescuing transformant line (Fig. 16). Clones were induced in flies homozygous for the *shiva* null allele on the third chromosome (*shiva*$^{P(l)00295}$ or *shiva*$^{e4-1}$), and trans-heterozygous for the *dpp*^{12}(or *wg*^{CX4}) null allele and the rescuing construct (*hs-shiva31*) on the left arm of chromosome 2. Both copies of the 2L chromosome also contained FRT sites at position 40A. Thus, heat shock enabled simultaneous rescue of the *shiva* homozygotes through expression of *hs-shiva31*, as well as the induction of clones on 2L through the induction of *hs-FLP*. To insure the full rescue of *shiva*$^{-}$ flies, eggs were collected every 24 hours, cultured at 25°C, and consequently heat-shocked every 24 hour interval until hatching.

As a control, I generated *shiva*$^{-}$ clones by FLPing the *hs-shiva31* rescuing construct on 2L in a homozygous *shiva* background (Fig. 17). The frequency of recombination for different FRT elements varies according to their chromosomal position. This control enabled a more exact comparison of clone frequencies by using identical FRT sites for generating the single and double mutant clones (compare Fig. 16 and 17). Induction of clones on 2L requires the simultaneous rescue of homozygous *shiva* mutant animals, which could also lead to a reduced clone frequency. Thus, by generating *shiva*$^{-}$ clones with the *hs-shiva31* rescuing construct I was best able to control for any irregularities in clone frequencies for comparison between double and single mutant clones. *shiva*$^{-}$ clones were induced using the *hs-shiva 31 P[FRT]40A* chromosome at a frequency of 65% of discs (Table 1 and 2).

The results of the double-mutant clone analysis showed that removal of *dpp* or *wg* from *shiva* clones abolished the *shiva* adult mosaic phenotype. Flies

mosaic for *dpp, shiva* double mutant clones exhibited a 96% reduction in leg outgrowths when compared to *shiva* mosaic flies (Table 1). Likewise, *wg, shiva* mosaic flies had a 99% reduction in leg outgrowths. A 97% reduction of wing outgrowths was seen in mosaic flies carrying *dpp, shiva* double mutant clones and flies carrying *wg, shiva* double mutant clones when compared to *shiva* mosaic flies (Table 2).

B. *hh, shiva* and *smo, shiva* double mutant clones

So far I have demonstrated that *shiva* restricts both *dpp* and *wg* expression, and that misexpression of these molecules in *shiva*$^-$ clones is responsible for the *shiva* adult mosaic phenotype. However, it was not clear whether *shiva* independently regulates both *dpp* and *wg*, or whether *shiva* controls *wg* and *dpp* expression from a common point upstream in the Hh signaling pathway. To further investigate *shiva*'s possible role in Hh-signaling, double mutant clones were constructed between *shiva* and other known Hh-signaling components.

(1) *hh, shiva*

As *shiva* mutant clones do not alter *hh-lacZ* expression patterns in imaginal discs, I predicted that *hh, shiva* double mutant clones would not alter the *shiva* adult mosaic phenotype. The null hh^{rJ413} allele was recombined onto the *FRT82-*$shiva^{P(l)00295}$ chromosome. The cross to generate double mutant clones is depicted in Figure 18, and clones were induced by heat shock at 24-hour

intervals until hatching. Although heat shock was not necessary in this case to rescue the flies, heat shock was performed at 24-hour intervals to induce clones at a frequency comparable to that of *shiva, dpp* and *shiva, wg* double mutant clones. No reduction of outgrowths was observed in flies mosaic for *hh, shiva* double mutant clones when compared to mosaic flies for *shiva* (Tables 1 and 2).

(2) *smo, shiva*

What was surprising was *shiva*'s relationship to *smo*. For my analysis I used the smo^{D16} mutation, which is caused by a DNA rearrangement and produces the most severe embryonic phenotype (Alcedo et al., 1996). The smo^{D16} allele is associated with a 38 base pair insertion after codon 124 that introduces two stop codons, one within and the other just downstream of the insertion (Chen and Struhl, 1998). Analysis by RT-PCR has demonstrated a several-fold reduction in the level of *smo* transcript, perhaps reflecting a destabilization due to premature translational termination (Chen and Struhl, 1998). smo^{D16} was recombined onto a chromosome arm containing FRT40, and *smo, shiva* clones were induced as previously described for *wg/dpp, shiva* clones (Figure 16). As was seen for *wg/dpp, shiva* clones, *smo, shiva* clones exhibited a reduction of 96% of leg outgrowths and wing outgrowths in mosaic flies (Tables 1 and 2). These results indicate that *shiva* acts upstream of *smo* to regulate *dpp* and *wg* expression. To verify this, I recombined *wg-lacZ* and *dpp-lacZ* onto smo^{D16} *FRT40* chromosome arms. Discs carrying *smo, shiva* double mutant clones were stained

and found to no longer ectopically express *wg-lacZ* or *dpp-lacZ* (results not shown). Thus, *shiva* indeed regulates *wg* and *dpp* expression upstream of *smo*.

Discussion

dpp and *wg* are direct effectors of the *shiva* signal

Previously in Chapter IV I reported that cells of *shiva* mutant clones misexpress *dpp* and *wg* in imaginal tissues. To address whether the outgrowth phenotype observed in *shiva* mosaic flies was the result of misexpression of *dpp* and *wg* in imaginal tissues, I built double mutant clones between *shiva* and *dpp*, and *shiva* and *wg*. Removal of *dpp* or *wg* gene expression from *shiva* mutant clones abolished nearly all outgrowths in adult mosaic animals. Reductions of 96% and 99% of outgrowths were observed in legs of *shiva, dpp* and *shiva, wg* mosaic flies, respectively. Likewise, reductions of 97% of outgrowths were observed in wings of *shiva, dpp* and *shiva, wg* mosaic flies. As removal of *dpp* and *wg* from *shiva* clones eliminated the *shiva* adult mosaic phenotype, ectopic expression of *dpp* and *wg* in *shiva*$^-$ clones is responsible for the *shiva* phenotype. Thus, *dpp* and *wg* are direct effectors of the *shiva* signal.

dpp and *wg* are simultaneously required to transduce the *shiva* signal

There are two curious elements to the double-mutant clone analysis of *dpp* and *wg* with *shiva*. First, double mutant clones for both *dpp, shiva* and *wg, shiva*

eliminated nearly all outgrowths in mosaic flies. This was surprising, as neither *dpp* nor *wg* is misexpressed in all *shiva* mutant clones distributed throughout the disc. It appears that both molecules are simultaneously required to generate the outgrowths in *shiva* mosaic animals.

Second, flies mosaic for *wg, shiva* double-mutant clones have a 97% reduction in wing outgrowths compared to flies mosaic for *shiva*$^-$ clones alone. However in wing discs, *shiva* clones do not express ectopic *wg*. Several possibilities exist as to why this may be so. First, the *wg-lacZ* reporter gene has been found by several groups to not be a true reporter of Wg protein expression in the wing disc (N. Russe, personal communication). Thus, it is possible that Wg protein expression is being up-regulated in *shiva* clones of the wing disc, and that an antibody to Wg protein would be a more reliable detector of *wg* misexpression. Another possibility is that *wg* is up-regulated in *shiva* clones of the wing disc at later stages of development (i.e., early pupae).

Wg signal transduction is associated with the accumulation of Armadillo (Arm) protein and the induction of the proneural gene Scute (Sc). Jiang et al., used antibodies to Arm and Sc to demonstrate that these molecules accumulate in *slmb* clones in wing discs (Jiang and Struhl, 1998). Jiang proposed that eliminating *slmb* in wing disc clones activates *wg* signaling, and that Wg protein is not required for Wg-signaling. However, my double-mutant clone analysis that *shiva, wg* clones fail to produce outgrowths in the wings of adult flies contradicts this, demonstrating that Wg is indeed required for transducing the *shiva* signal in the wing.

shiva intersects Hh-signaling upstream of _smo_

So far, my genetic epistasis data has determined that *shiva* acts normally to repress the expression of *dpp* and *wg*; the misexpression of *dpp* and *wg* in mutant clones for *shiva* results in the outgrowth phenotype in *shiva* mosaic adults. Dpp and Wg are the downstream products of the Hh-signaling pathway. To distinguish whether *shiva* is itself a component of the Hh-signaling pathway, or whether *shiva* acts independently of Hh-signaling to regulate *dpp* and *wg* expression, double mutant clones were again built, this time between *shiva* and *hh* and *shiva* and *smo*.

hh, shiva clones resulted in no reduction of outgrowths in mosaic flies, when compared to singly-mutant *shiva* mosaic flies (Table 1 and 2). Thus, *shiva* acts downstream or independent of Hh. Interestingly, *smo, shiva* double mutant clones resulted in a 99% reduction of outgrowths in mosaic flies. As I already knew that *dpp* and *wg* were the effectors of the *shiva* signal, I wanted to ascertain that the expression of *dpp* and *wg* were not deregulated in *smo, shiva* double mutants. I did this by recombining *dpp-lacZH1-1* and *wg-lacZ* reporter genes onto the smo^{D16} chromosome arm. No ectopic *dpp-lacZ* or *wg-lacZ* was found in *smo, shiva* mosaic discs, suggesting that *shiva* regulates the expression of *dpp* and *wg* upstream of *smo*.

Double mutant clone analysis differs between _shiva, smo_ and _slimb, smo_

As discussed, my results indicated that *shiva* lies upstream of *smo* in Hh-signaling. However, work by Jiang et al. suggested that *slmb* acts downstream of *smo*. This difference may be explained by the use of different alleles for *smo* and *slmb*. First, the group used two EMS-induced mutations for *slimb* ($slmb^1$ and $slmb^2$) which are pupae lethal in trans (Jiang and Struhl, 1998). This contrasts with the strong *shiva* allele used in our study ($shiva^{P(l)00295}$) which is homozygous lethal as early first instar larvae (Theodosiou et al., 1998). In addition, the smo^3 mutation used was a weaker *smo* allele than smo^{D16}. The smo^{D16} used in our analysis is associated with two nonsense mutations close to the 5' end of the coding sequence, and is considered a likely null allele (Chen and Struhl, 1998). Although the smo^3 allele has also been associated with a nonsense mutation, this mutation is after the third transmembrane domain of the protein. It is possible that the product of the smo^3 mutation is still able to reach the cell surface and transduce the Hh signal. The combination of weak alleles for both *slimb* and *smo* likely accounts for the discrepancy in our findings.

shiva integrates D/V and A/P signals to confer wild type _dpp_ and _wg_ expression patterns

Several pieces of evidence aided in generating a model for *shiva*'s role during leg development. First, *shiva* acts to restrict *dpp* and *wg* expression. In the absence of *shiva*, the expression of *dpp* and *wg* are deregulated. Through double mutant clone analysis, I demonstrated that *dpp* and *wg* are direct effectors of the *shiva* signal and responsible for the *shiva* adult mutant phenotypes. Unlike

components of the Hh-signaling pathway, *shiva* deregulates *dpp* and *wg* expression outside of their native dorsal and ventral compartments, respectively. Since the Hh pathway regulates *wg* and *dpp* expression in the A/P axis, our results suggest that a pathway different from Hh may operate in imaginal discs to restrict their expression in the D/V axis. This pathway can not be either the *wg* or *dpp*-signaling pathway since inactivation of *wg* or *dpp* signaling affects either *dpp* or *wg* expression, but not both (Brook and Cohen, 1996; Jiang and Struhl, 1996; Penton et al., 1997; Theisen et al., 1996). *shiva* is the first identified molecule that regulates both *wg* and *dpp* expression in the A/P as well as D/V axes. The fact that mutations in *shiva* affect patterning in both axes suggests that the A/P and D/V signals are coordinated to specify *wg* and *dpp* expression patterns, and that *shiva* plays an essential role in integrating these signals. Thus, in building a model I had to consider that *shiva* acts to restrict *dpp* and *wg* in a pathway that is independent of Hh-signaling. Lastly, my epistasis placed *shiva*'s control of *dpp* and *wg* expression upstream of *smo*.

In my model, I place *shiva* at a point of coordinating A/P and D/V signaling (Fig. 19). The A/P and D/V signals are coordinated to insure the restriction of *dpp* and *wg* expression to their dorsal and ventral domains, respectively. The A/P axis is determined by Hh-signaling. I have shown that *shiva* intersects Hh-signaling upstream of *smo*, and consequently have placed *shiva* intersecting A/P signaling at the point of *smo*. To date, there is no defined pathway to determine D/V signaling in the leg imaginal disc.

Figure 16. Generating double mutant clones using *shiva* rescue construct. Depicted is a cross to generate *dpp, shiva* double mutant clones. As *wg* and *smo* are also located on 2L, the same approach was used for generating *wg, shiva* and *smo, shiva* clones. The *shiva* rescue construct (*hs-shv31*) on an *FRT40A* chromosome was crossed to dpp^{12} on a *FRT40A* arm in a $shiva^{P(l)00295}$ background. Eggs were collected by transferring crosses to fresh vials at every 24-hour interval. After aging for one day at 25°C, a series of heat-shocks were begun at every 24-hour interval until hatching. Heat shocks at 38°C had the effect of fully rescuing homozygous flies for *shiva*, and simultaneously generating clones by inducing FLPase expression. The genotype of clones was homozygous for dpp^{12} and homozygous for $shiva^{P(l)00295}$. Twin spots contained two copies of the hs-shv31 rescue construct in the $shiva^{P(l)00295}$ background. Flies homozygous for *shiva* (non-*Tb*) were examined for outgrowths on their legs and wings.

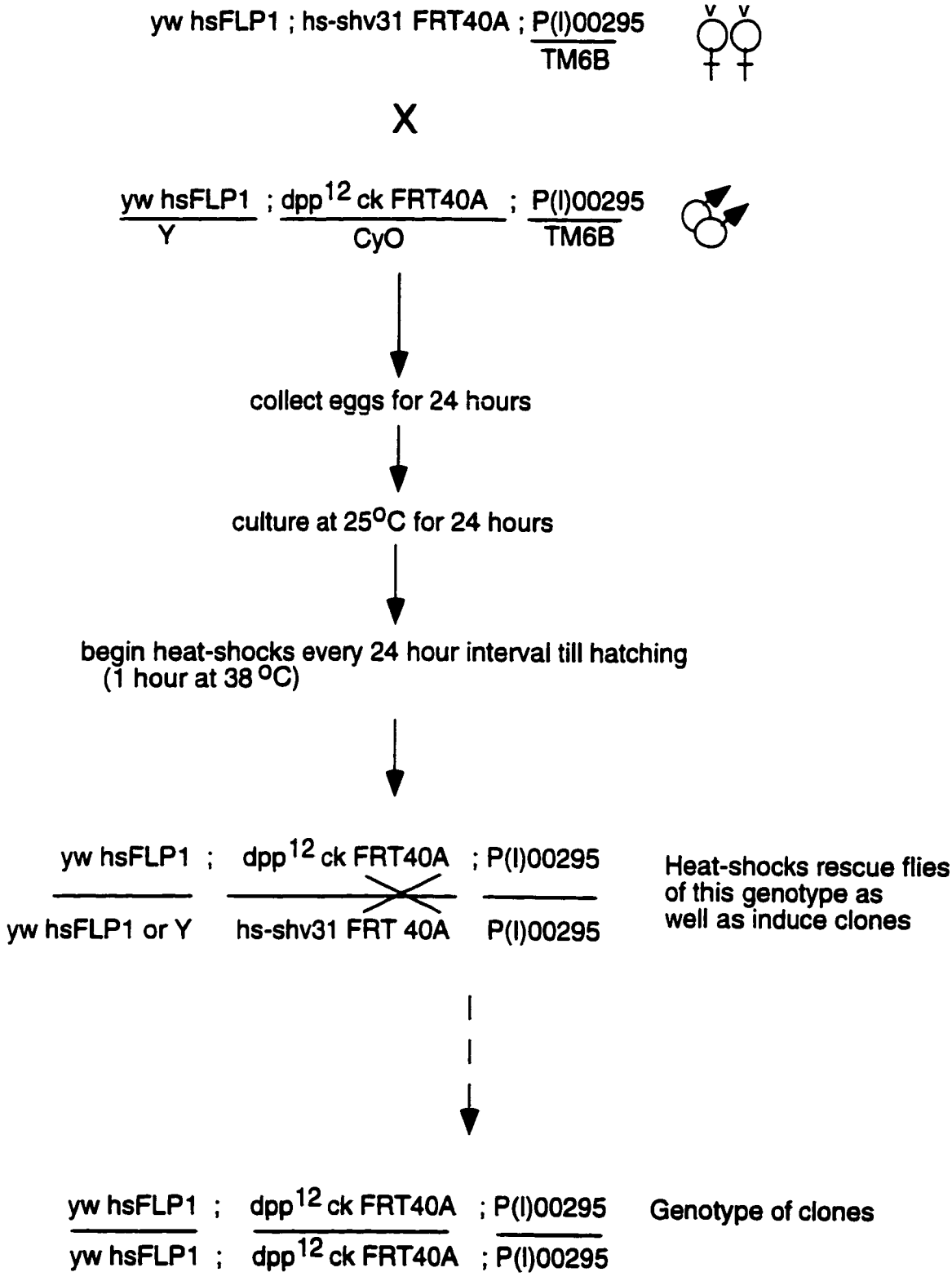
yw hsFLP1 ; hs-shv31 FRT40A ; P(l)00295 / TM6B
X
yw hsFLP1 / Y ; dpp12 ck FRT40A / CyO ; P(l)00295 / TM6B
collect eggs for 24 hours
culture at 25°C for 24 hours
begin heat-shocks every 24 hour interval till hatching
(1 hour at 38 °C)
yw hsFLP1 / yw hsFLP1 or Y ; dpp12 ck FRT40A / hs-shv31 FRT 40A ; P(l)00295 / P(l)00295
Heat-shocks rescue flies of this genotype as well as induce clones
yw hsFLP1 / yw hsFLP1 ; dpp12 ck FRT40A / dpp12 ck FRT40A ; P(l)00295 / P(l)00295
Genotype of clones

Figure 17. Generating *shiva* mutant clones by using *shiva* rescue construct. Similar strategy was used as with generating double mutant clones for *dpp, shiva*. In this instance, the *hs-shv31 FRT40A* chromosome was crossed to a chromosome containing the *FRT40A* site alone in a $shiva^{P(1)00295}$ mutant background. Daily heat shocks had the effect of simultaneously rescuing *shiva* homozygous mutant, and inducing $shiva^{-}$ clones. *shiva* mutant clones were induced under these conditions at a frequency of 65% of discs.

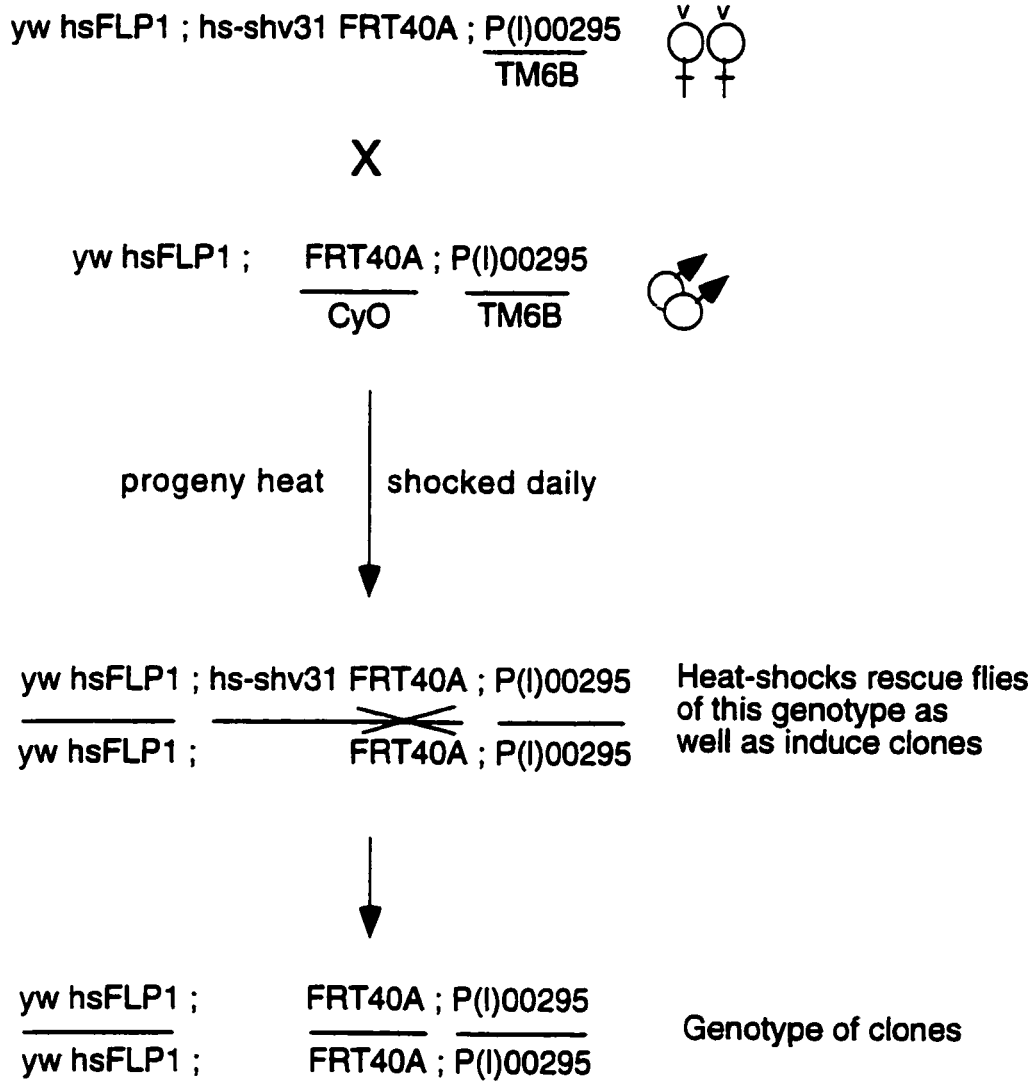
yw hsFLP1 ; hs-shv31 FRT40A ; P(l)00295
TM6B
X
yw hsFLP1 ; FRT40A ; P(l)00295
CyO TM6B
progeny heat shocked daily
yw hsFLP1 ; hs-shv31 FRT40A ; P(l)00295
yw hsFLP1 ; FRT40A ; P(l)00295
Heat-shocks rescue flies of this genotype as well as induce clones
yw hsFLP1 ; FRT40A ; P(l)00295
yw hsFLP1 ; FRT40A ; P(l)00295
Genotype of clones

Table 1. Double mutant clone analysis in legs. The legs of mosaic flies were scored for any abnormalities, including outgrowths, scaring or missing bristles. Single mutant clones for *shiva* were generated using the *shiva* rescue construct in a homozygous *shiva* mutant background (see Fig. 17) to better control for rates of recombination between experiments.

clonal genotype	number of flies with leg outgrowths
shiva	65/96
wg, shiva	1/150
dpp, shiva	3/118
smo, shiva	3/114
hh, shiva	97/126

Table 2. Double mutant clone analysis in wings. The wings of mosaic flies were scored for any abnormalities, including outgrowths, scaring or missing bristles. Single mutant clones for shiva were generated using the *shiva* rescue construct in a homozygous *shiva* mutant background (see Fig. 17) to better control for rates of recombination between experiments.

clonal genotype	number of flies with wing outgrowths
shiva	96/96
wg, *shiva*	4/150
dpp, *shiva*	3/118
smo, *shiva*	2/114
hh, *shiva*	126/126

Figure 18. Generating *hh, shiva* double mutant clones. As *shiva* and *hh* are both located on 3R, the *hh* null allele (*rJ413*) was recombined onto chromosome *FRT82B P(l)00295*. Flies carrying *FRT82B P(l)00295 rJ413* chromosomes were crossed to *FRT82B πM Sb* y^+. Eggs were collected at 24 hour intervals, and progeny were heat shocked daily at 38°C until hatching. In this experiment, heat shock induced clones carrying cells double mutant for *shiva* and *hh*. Clones were identified by the y^- and Sb^+ cuticle markers.

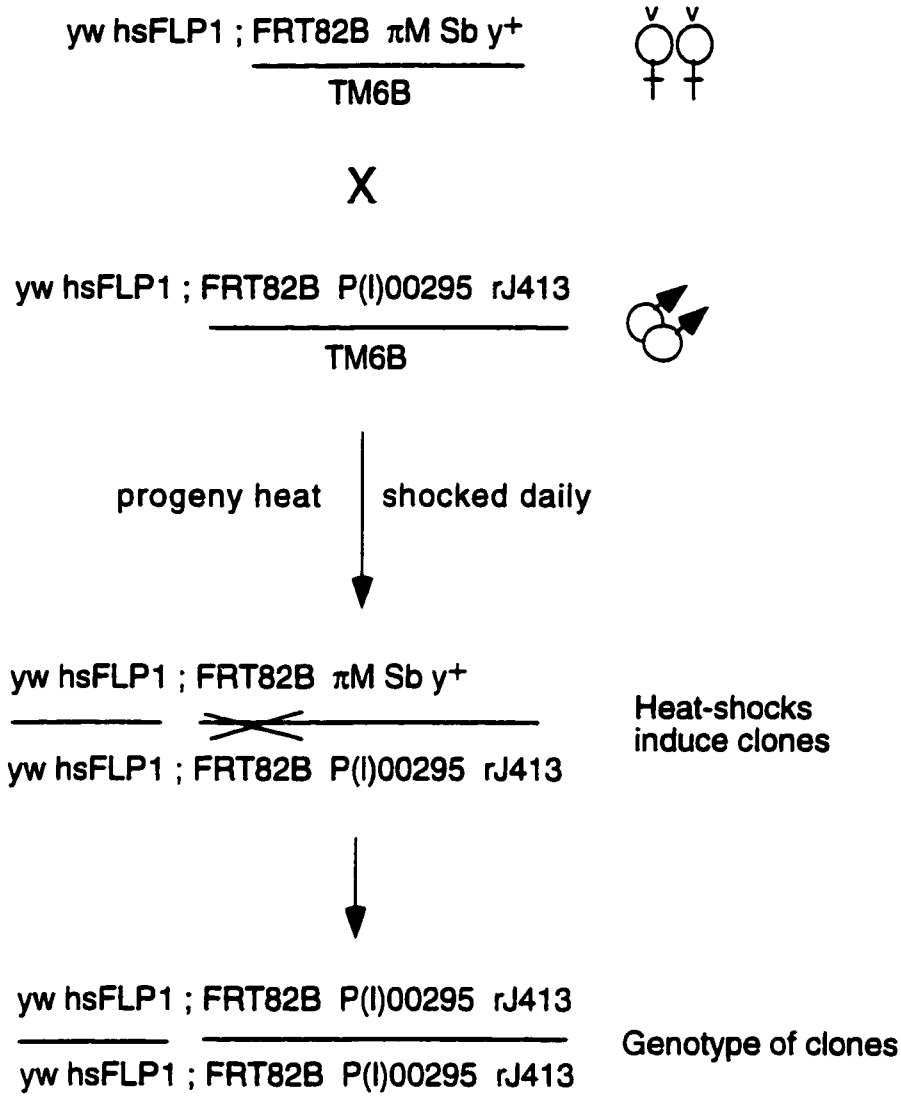
yw hsFLP1 ; FRT82B πM Sb y+
TM6B
X
yw hsFLP1 ; FRT82B P(l)00295 rJ413
TM6B
progeny heat shocked daily
yw hsFLP1 ; FRT82B πM Sb y+
yw hsFLP1 ; FRT82B P(l)00295 rJ413
Heat-shocks induce clones
yw hsFLP1 ; FRT82B P(l)00295 rJ413
yw hsFLP1 ; FRT82B P(l)00295 rJ413
Genotype of clones

Figure 19. A model for *shiva* function. *shiva* acts upstream of *smo* in A/P signaling which induces *wg* and *dpp* expression, and also participates in an unknown D/V signaling pathway (X) which restricts *wg* and *dpp* expression. Inactivation of *shiva* deregulates *wg* and *dpp* expression in both A/P and D/V axes.

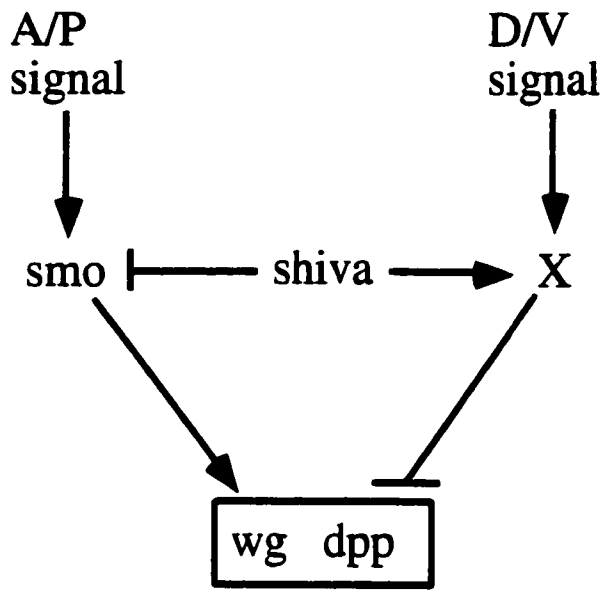
A/P
signal
D/V
signal
smo
shiva
X
wg
dpp

Chapter VI. Role for *shiva* in eye development

Introduction

The first five chapters of my dissertation covered the main body of my work in isolating and characterizing the original *shiva* phenotypes. This chapter on the role of *shiva* during eye development was a project I pursued in my last year in Xu's lab. The first hint I had that *shiva* played a role in eye development came from earlier experiments where I rescued the original *shiva* allele with the *shiva* transcript driven by the heat-shock promotor. The heat-shock promoter was leaky at 25°C; flies cultured at 25°C were rescued to pupal stage. Dissection of pupal cases revealed that the dead pupae contained bar eyes. Looking back to my notes on the excision lines generated from P(l)00295, I found a line which was also pupal lethal, and whose pupae contained bar eyes (e52) (Appendix A). The identification of an allele for *shiva* with an eye phenotype (Fig. 20G, H), coupled with the distinct expression pattern of *shiva* in eye discs encouraged me to pursue a possible role for *shiva* in eye development.

Results

A. *shiva*^{e52} reveals that *shiva* plays a role during eye development

Excision of P(l)00295 generated an allele for *shiva*, *shiva*^{e52}, containing approximately a 300bp deletion in the promoter region for *shiva* (Fig. 5). Animals

homozygous for *shiva*^{e52} died as pupae and contain bar eyes (Fig. 20B; Appendix A). Bar eyes lack ommatidia and are predominantly composed of bristles and pigment cells. To ascertain whether the bar eye phenotype was due to a developmental defect as opposed to a later massive cell death event, eye imaginal discs were stained with the photoreceptor cell-specific marker, Elav. In comparison to wild type eye discs, the *shiva*^{e52} mutant discs were significantly smaller in size and distorted from abnormal folding, making them difficult to handle. While wild type third instar discs contain many rows of photoreceptor cell clusters, the *shiva*^{e52} mutants contained on average 21 Elav-positive cells per disc (see legend Fig. 20D). This suggested that the bar eye phenotype observed in *shiva*^{e52} pupae was due to a failure in neural differentiation. However, the small size of the *shiva*^{e52} discs was curious.

To determine if the reduced disc size in *shiva*^{e52} mutants was the result of cell death, TUNEL labeling was performed. In contrast to wild type eye discs, which have little to no TUNEL labeling, third instar *shiva*^{e52} discs exhibited cell death throughout. Increased concentrations of DNA fragmentation were consistently observed at the dorsal lateral and posterior margins, as well as in the center of the disc (Fig. 20E and F). In contrast, younger *shiva*^{e52} discs (second instar) contain very few TUNEL-staining cells (data not shown). Thus it appears that the small disc and bar eye phenotype of *shiva*^{e52} mutants was due to a failure of neural differentiation, and the failure of cells to differentiate leads to programmed cell death. Due to the intriguing phenotype of the *shiva*^{e52} mutants and the specific expression pattern of *shiva* in the eye, I was very curious to elucidate a role for *shiva* during eye development.

B. *shiva* regulates *dpp* expression in eye discs

(1) e52 mutant

The *shiva*^{e52} mutant is reminiscent of other bar-eye mutants including the *hh* allele, *hh-1*. Flies homozygous for *hh-1* have bar-eyes with roughly eight rows of ommatidia. Failure of the MF to progress is attributed to the lack of *dpp* expression in furrows of *hh-1* mutants. To understand the nature of the *shiva*^{e52} bar eye, discs were analyzed for their expression of *dpp*. Like the *hh-1* mutants, the *shiva*^{e52} mutants did not express *dpp* in the MF (compare Fig. 21A and B). Thus, failure of the MF to progress across the disc was due in part to a loss of *dpp* function.

(2) *shiva*$^{e4\text{-}1}$ mutant clones

To further characterize the effect of *shiva* on *dpp* expression, clones containing the null mutation for *shiva* (e4-1) were generated and examined for their effect on *dpp-lacZ* expression. *shiva*$^{e4\text{-}1}$ mutant cells located inside or adjacent to the anterior edge of the MF misexpressed *dpp*. However, no ectopic *dpp* expression was observed in clones located posterior to or far anterior from the MF (Fig. 22A-C). Thus, it appeared that only those cells directly anterior to the MF (in proximity to Hh-expressing cells) were competent to express *dpp* in the absence of *shiva*.

The effects of *shiva*$^{e4\text{-}1}$ clones on *dpp* expression are unique. Other groups have demonstrated that *dpp* misexpression anterior to the MF can lead to ectopic furrow formation and ectopic neural differentiation (Pan and Rubin, 1995; Pignoni and Zipursky, 1997; Strutt et al., 1995). Our clonal analysis has revealed no evidence for ectopic furrow formation. Therefore, we speculated that *shiva* may be involved in MF progression.

Several clues led us to consider that *shiva* may play a role in MF progression. First, although neural differentiation was initiated in *shiva*^{e52} eye discs, it soon was aborted as evidenced by the scarcity of photoreceptor cells in the mutants (Fig. 20B and D). The expression of *dpp* in eye discs has been used by many groups as the standard marker for the MF. In *shiva*^{e52} discs, the lack of *dpp* expression suggests an aberration in the MF (Fig. 21B). Using *dpp* as a marker for the MF, we further observed MF progression defects in discs containing *shiva*$^{-}$ clones. When *shiva*$^{-}$ clones are positioned at the anterior edge of the MF, the MF no longer moves as a straight line (Fig. 22B and C, compare to Fig. 21A). Rather, the MF contained anterior bulges through the clones, suggesting that the MF progressed through *shiva*$^{-}$ cells more quickly than their surrounding wild type cells. With this evidence I pursued the possibility that *shiva* may play a role in MF progression.

C. *shiva* is required for MF progression

As the MF progresses across the disc, rows of differentiating photoreceptor cells are laid out one at a time. Thus, the various developmental

stages of the retina are displayed spatially. Any aberration in MF movement can be detected in the arrangement of photoreceptor cells. If *shiva*$^-$ cells indeed enter the MF earlier than wild type cells, I expected to find evidence of premature neuronal differentiation to be associated with *shiva*$^-$ clones. Detection of the Elav protein was used as a marker for photoreceptor cells in discs mosaic for *shiva*. Clusters of differentiating photoreceptor cells anterior to *shiva* mutant clones were more advanced developmentally than other clusters within the same row (Fig. 22D-F). This suggested that the MF moved more quickly through *shiva*$^-$ cells, allowing wild type cells anterior to the clone to begin differentiating earlier than neighboring cells within the same row. Since the absence of *shiva* in cells led to an acceleration of the MF through clones, I proceeded to investigate any aberrations in MF progression in the *shiva*^{e52} mutants.

As *shiva*^{e52} mutants fail to express *dpp*, it was important to ask whether or not a MF existed in these mutants; and if *shiva*^{e52} mutants contained any MF progression defects. Second and third instar eye discs were stained for BrdU incorporation and cells were marked with propidium iodide. In wild type discs, cells in the MF are identified by their arrest in G1 (an absence of BrdU incorporation) and an indentation in their nuclei (visualized by propidium iodide) (Fig. 21C, bracket). As cells leave the MF and enter S phase, BrdU is incoporated along a stripe following the posterior margin of the MF. Although both second and third instar discs exhibited a stripe of G1 cells lacking BrdU incorporation, the MF of *shiva*^{e52} discs were clearly abnormal (Fig. 21D and E). Wild type discs contain 8-9 rows of cells in their MF. In contrast, the furrows of *shiva*^{e52} mutants range from 6 rows of cells in second instar (Fig. 21D, right) to 19

rows of cells in third instar (Fig. 21E, right) (see legend to Fig. 21C-E). At the same time, the position of the posterior margin of the MF appears to remain constant. While the anterior edge of the MF moves forward in the absence of *shiva*, the posterior edge remains constant, expanding the stripe of G1 arrested cells in *shiva*^{e52} mutants. This suggests that *shiva* acts in coupling the movement of both margins of the MF across the disc.

D. *hh* and *shiva*^{e52} mutants

The *shiva*^{e52} mutants were phenotypically puzzling. Although lacking *dpp* expression, the mutant discs did contain a MF which continued to progress at its anterior margin, but was arrested at the posterior margin. The failure of neural differentiation to proceed in *shiva*^{e52} appeared to be due the arrest of the posterior edge of the MF. Since *hh* was demonstrated to push movement of the MF, I investigated the relationship between *hh* and *shiva* during eye development (Heberlein et al., 1995; Ma et al., 1993).

(1) *hh* expression in *shiva*^{e52} mutants

As *hh* is known to push the MF and induce *dpp* expression in the MF, I wanted to learn if the lack of neural differentiation in *shiva*^{e52} mutants was related to abnormalities in *hh* activity. Therefore, I examined the expression of *hh* in *shiva*^{e52} mutants. The *P30,hh-lacZ* reporter gene was recombined onto the *shiva*^{e52} chromosome arm, and homozygous discs were stained for *ß-galactosidase*

activity. Unlike wild type discs in which *hh* is expressed in photoreceptor cells posterior to the MF, the *shiva*^{e52} discs were deficient in *hh* (Fig. 23A, B). The lack of *hh* expression in *shiva*^{e52} mutants may explain the lack of *dpp* in these discs, as well as the absence of neural differentiation.

(2) *hh-1, shiva*^{e52} double mutants

To further evaluate the relationship between *shiva* and *hh* during eye development, I built double mutants between the eye-specific allele of *hh, hh-1,* and *shiva*^{e52}. The *hh-1* mutant is viable and contains 8 rows of photoreceptor cell clusters (Fig. 23C). *hh-1,shiva*^{e52} double mutant eye discs contain on average 12 Elav-positive cells compared to the average of 21 Elav-positive cells in *shiva*^{e52} mutants (Fig. 23D). Thus it appears that *shiva* and *hh* interact synergistically during eye development.

E. *hh* and *shiva* overexpression restores neural differentiation in e52 discs

As previously noted, the eye discs of *shiva*^{e52} mutants lack *dpp* expression as well as neural differentiation. In addition, mutant discs contain an MF which fails to proceed from the posterior margin. These phenotypes may be explained by the absence of *hh* expression in *shiva*^{e52} mutants. To test if neural differentitation could be rescued by *hh,* I expressed *hh* posterior to the furrow (*pGMR-GAL4,UAS-hh-1*). Indeed, expression of *hh* did restore photoreceptor cells differentiation, albeit only partially (Figure 23E, Table 3). This suggests and

supports previous evidence that *hh* is necessary but not sufficient to push the MF (Strutt and Mlodzik, 1997).

Since *hh* could only partially restore neural differentiation in *shiva*^{e52} mutants I was curious if the replacement of *shiva* expression back into this background would further restore differentiation. For the expression studies, a *UAS-shiva* construct was introduced into flies (Fig. 7). This work was done in collaboration with He Huang.

Over-expression of *shiva* posterior to the MF (*pGMR-GAL4,UAS-shiva*) partially rescued neural differentiation. This suggests that along with being required anterior to the MF, *shiva* is also required posterior to the MF for MF progression. However, *shiva* over-expression anterior to the MF (*ey-GAL4,UAS-shiva*) failed to rescue neural differentiation in *shiva*^{e52} mutants. This may appear to contradict the findings from clonal analysis that *shiva* is required anterior to the MF. Neither the *ey-* nor *GMR-GAL4* promoters is expressed in the entire disc. If *shiva* is required both anterior and posterior to the MF continuously during eye development, then expression in a limited domain of the eye would not be sufficient to fully rescue neural differentiation in *shiva*^{e52} mutants. The data also implies that the activity of *shiva* anterior to the MF is dependent upon a posterior signal, most likely *hh*. Enhanced neural differentiation was observed when *hh* and *shiva* were coexpressed in *shiva*^{e52} mutants (Table 3). Curiously, it was coexpression by the *ey*-promoter and not the *pGMR*-promoter that provided enhanced rescue, confirming that *shiva* is required anterior to the MF in aiding MF progression (Figure 23H, Table 3). This is further supported by the *in situ* results in which *shiva* was found to be expressed primarily anterior to the MF

(Figure 20G, H). Thus, *shiva* is required in the anterior for coordinating MF progression.

(1) MF morphology

Cells in the MF are marked by an indentation, which is readily discernable with propidium iodide (Fig. 21C, right). However *shiva*^{e52} mutants lack any clear indentation in the nuclei of their MF, and the MF can only be detected with BrdU incorporation (Fig. 21D, E). During the overexpression studies, discs were also examined for improvements in the morphology. Improvements in MF morphology were observed with *hh* overexpression and with both *hh* and *shiva* overexpression. In contrast, no discernable correction in MF morphology was observed in *shiva* overexpression studies. Discs expressing *pGMR-GAL4,UAS-hh-1* had corrected MF's with an average of 9 rows of cells in width (n=8), while for discs with *ey-GAL4,UAS-hh-1* the MF's had an average of 7 rows of cells (n=12). The MF's of discs with *pGMR-GAL4,UAS-hh-1,UAS-shiva* expression contained on average 8 cell rows in width (n=6); and the MF of *ey-GAL4,UAS-hh-1,UAS-shiva* contained on average 10 cell rows in width (n=6). Thus, *hh* not *shiva* is sufficient to rescue MF morphology in *shiva*^{e52} mutant eye discs, although both molecules are simultaneously required to rescue MF progression.

Discussion

The identification of the *shiva*^{e52} mutant led to the study of a role for *shiva* during eye development. The *shiva*^{e52} mutants contain bar eyes with no ommatidia. Developmental studies of these mutants found a failure in neural differentiation which resulted in cell death and morphologically small discs. The bar-eye phenotype was reminiscient to the *hh* mutant, *hh-1*, which was previously shown to have a failure in MF progression due to an absence of *dpp* expression (Heberlein et al., 1995). As *shiva*^{e52} resembled *hh-1*, I looked at the expression pattern of *dpp* in the mutants. The *shiva*^{e52} mutant discs lacked *dpp* expression. The effect of *shiva* on *dpp* expression in the eye was further studied by clonal analysis. Cells of clones null for *shiva* deregulated *dpp* expression only when positioned adjacent to the anterior edge of the MF. These clones are in proximity to endogenous Hh, and the ectopic *dpp* in clones could have been induced by Hh. As *dpp* is a marker for the MF, *shiva* mutant clones adjacent to the MF had the effect of accelerating the rate of MF progression, which was supported by precocious neural differentiation surrounding *shiva*$^{-}$ clones.

The possibility that *shiva* may act to regulate MF progression was intriguing. Following up on the clonal analysis, I characterized the MF in my *shiva*^{e52} mutants. Despite the lack of *dpp* in the discs, these mutants did have a MF which continued to progress. However, although the anterior margin progressed, the posterior remained stationary resulting in a widening MF. This is the first example that the anterior and posterior margins of the MF can be uncoupled. These results together with the clonal analysis and *shiva* expression studies, suggest that *shiva* may act in the anterior to coordinate movement of the MF.

Arrest of the posterior margin of the MF in *shiva*^{e52} mutant discs immediately begged the question, what about *hh*? Hh in the posterior is secreted by photoreceptor cells and has been shown to 'push' the MF by serial induction of *dpp* expression (Heberlein et al., 1995; Ma et al., 1993). No *hh* expression was found in *shiva*^{e52} discs, thereby explaining the lack of *dpp* expression, and arrest of neural differentiation in the mutants. If *hh* was responsible for MF 'pushing', then reintroduction of *hh* expression in these mutants should restore neural differentiation. Overexpression studies demonstrated that *hh* could partially rescue neural differentiation and the MF morphology. Curiously, over-expression of both *hh* and *shiva* in *shiva*^{e52} mutants significantly enhanced the neural differentiation.

The dual requirement for *hh* and *shiva* in restoring photoreceptor cell differentation in *shiva*^{e52} mutants suggests that the two molecules coordinate progression of the MF (Fig. 24). Although overexpression of *shiva* or *hh* can partially rescue photoreceptor cell numbers in *shiva*^{e52} mutants, the coexpression of both molecules has an enhanced effect. I propose the "push-push" model in which both *shiva* and *hh* are required to coordinate MF progression. Such a model implies that *shiva* and *hh* must cross-talk in order to act coordinately. This cross talk would assume a requirement for Hh activity in the anterior, and SHIVA in the posterior.

The data support a role for Hh anterior to the MF. The over-expression of *hh* both posterior to the MF and throughout the disc rescued MF morphology. Thus, *hh* expression posterior to the MF can rescue the morphology of cells anterior to the MF, suggesting that Hh can diffuse and signal to anterior cells.

Several lines of evidence also support a role for *shiva* in the posterior. First, expression of *shiva* posterior to the MF can partially rescue neural differentiation (Table 3). *in situ* expression studies have demonstrated a thin band of *shiva* transcript just at the posterior margin of the MF (Fig. 20H). The $shiva^{e52}$ allele is deficient in *hh* expression, suggesting that expression of *hh* in the posterior is dependent on a signal for *shiva*. The $shiva^{e52}$ discs are also decoupled in the movement of the anterior and posterior margins of the MF, implicating loss of some coordinated action for their movement. Finally, null clones for *shiva* adjacent to the anterior edge of the MF appear to enter an MF fate earlier than surrounding wild type cells, suggesting an aberration in controlling MF progression. Taken together this data supports a model for MF progression in which Hh in the posterior pushes the MF forwards and coordinates its action with *shiva* in the anterior.

Figure 20. The *shiva*^{e52} mutant has a bar eye phenotype. Eyes are positioned anterior to left. SEM of eyes dissected from pupae cases of (A) wild type and (B) e52 mutant animals of the same age. (C-H) For all subsequent panels, eye imaginal discs are positioned posterior to left and dorsal up. (C) A wild type third instar disc stained with the neural specific antibody Elav, illustrating the clusters of differentiating photoreceptor cells posterior to the MF (arrowhead). (D) Elav-staining of an e52 mutant third instar disc. *shiva*^{e52} mutant discs display on average 21 Elav-positive single cells per disc (n=18), none of which are clustered. MF not indicated because it is morphologically difficult to visualize in mutants (see Fig. 2D and E). TUNEL staining was used to detect cell death in wild type (E) compared to e52 (F) eye discs. (G-H) *In situ* of a wild type eye disc using a DIG-labeled DNA probe containing the full-length *shiva* transcript taken from Fig. 11. (H) High magnification of the region boxed in (G). Note that the transcript is expressed anterior not posterior to the MF. *shiva* is expressed in two stripes (arrows) marking the anterior and posterior margins of the MF (bar).

A
B
C
D
G

Figure 21. *dpp* expression and MF progression in *shiva*^{e52} mutants. In all panels, posterior is positioned to the left. (A and B) Expression pattern of the *H1-1dpp-lacZ* reporter gene in wild type and *shiva*^{e52} homozygous eye discs. (A) *dpp* is normally expressed as a stripe in the MF. (B) *dpp-lacZ* is present only at the lateral margins in *shiva*^{e52} eye discs. (C-E) Discs double-stained for BrdU incorporation (green) and propidium iodide (red). (C, left) In a wild type disc, G1 arrested cells of the MF are identified by the absence of BrdU-incorporation (bracket). Double-staining of BrdU with propidium iodide allows one to count the number of cells that comprise the width of a furrow. (C, right) In a wild type MF, 8-9 rows of cells become arrested in G1 (bracket). (D, left) A second instar *shiva*^{e52} eye disc has a stripe of non-BrdU-incorporated cells arrested in G1. (D, right) Second instar *shiva*^{e52} discs contain on average 7 rows of cells in the MF (n=4) (bracket). (E, left) A third instar *shiva*^{e52} eye disc also contains a band of G1-arrested cells with 19 rows of cells (E, right (bracket)). The MF of *shiva*^{e52} third instar discs on average contain 15 rows of cells in width (n=8).

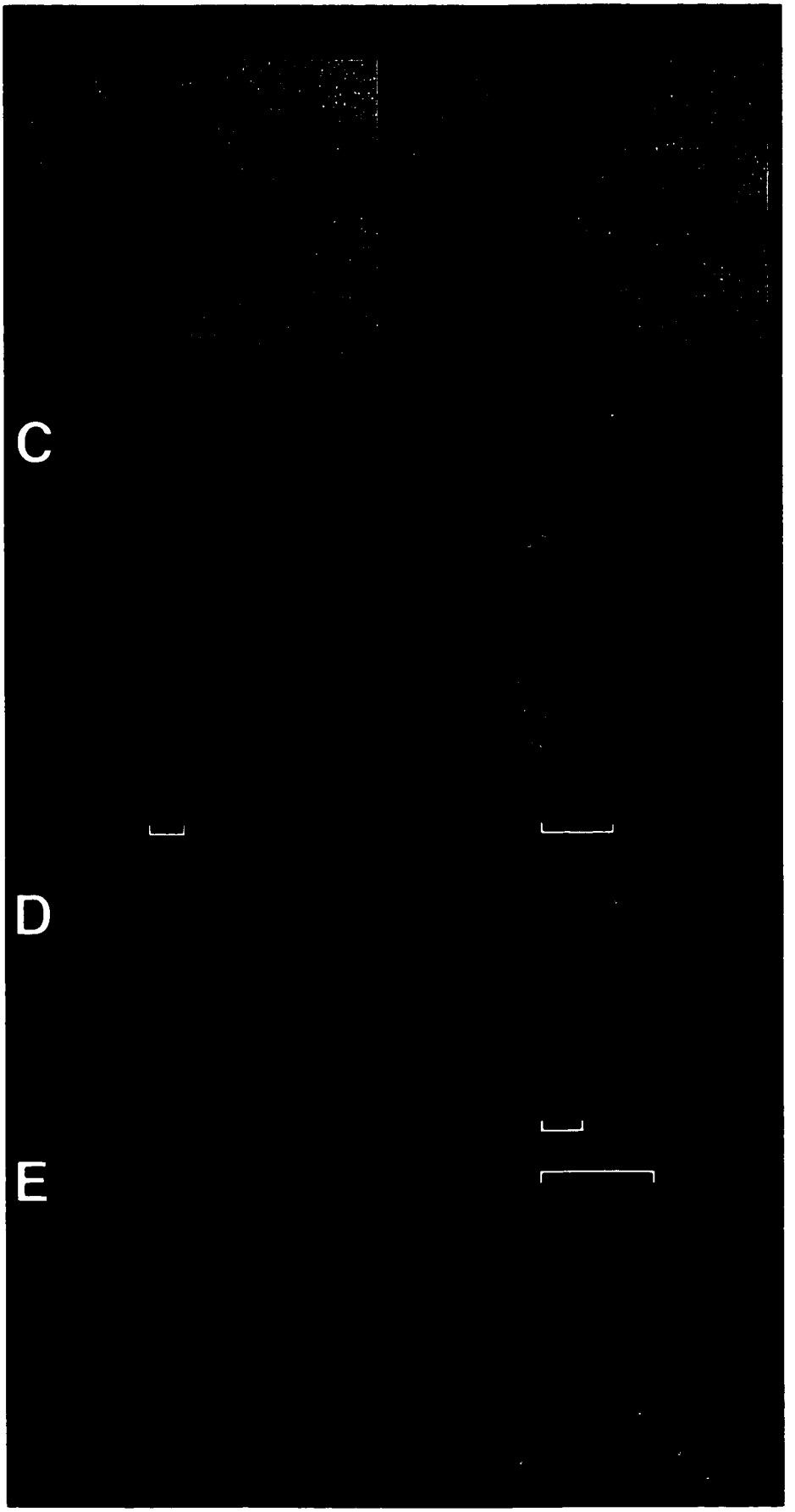
C
D
E

Figure 22. *shiva* mosaic phenotype in the developing eye. Eye discs containing clones of *shiva*$^{e4\text{-}1}$ (*shiva* null) mutant cells. All discs are positioned posterior to the left. *shiva*$^{e4\text{-}1}$ clones are identified by the lack of N-myc cell marker. (A) Disc with multiple clones positioned in and adjacent to the MF, (*), and on the anterior disc edge (arrows). (B) Same disc and focal plane as in (A) with *dpp-lacZ* marking the MF. Yellow dashed-line follows the posterior edge of the MF. Note the slight anterior bulge in the stripe of *dpp* expression. (C) Merged image of (A) and (B) demonstrating that clones within and anterior to the MF ectopically express dpp (*) while clones located at the anterior edge of the disc do not (arrows). (D) Disc containing a small *shiva*$^{e4\text{-}1}$ clone (arrow). (E) Same disc as in (D) stained with the neural-specific Elav antibody. (F) The merged image of (D) and (E) shows that the cluster of photoreceptor cells anterior to the clone is more differentiated (i.e., contains more photoreceptor cells) than other clusters in the same row (compare arrowheads).

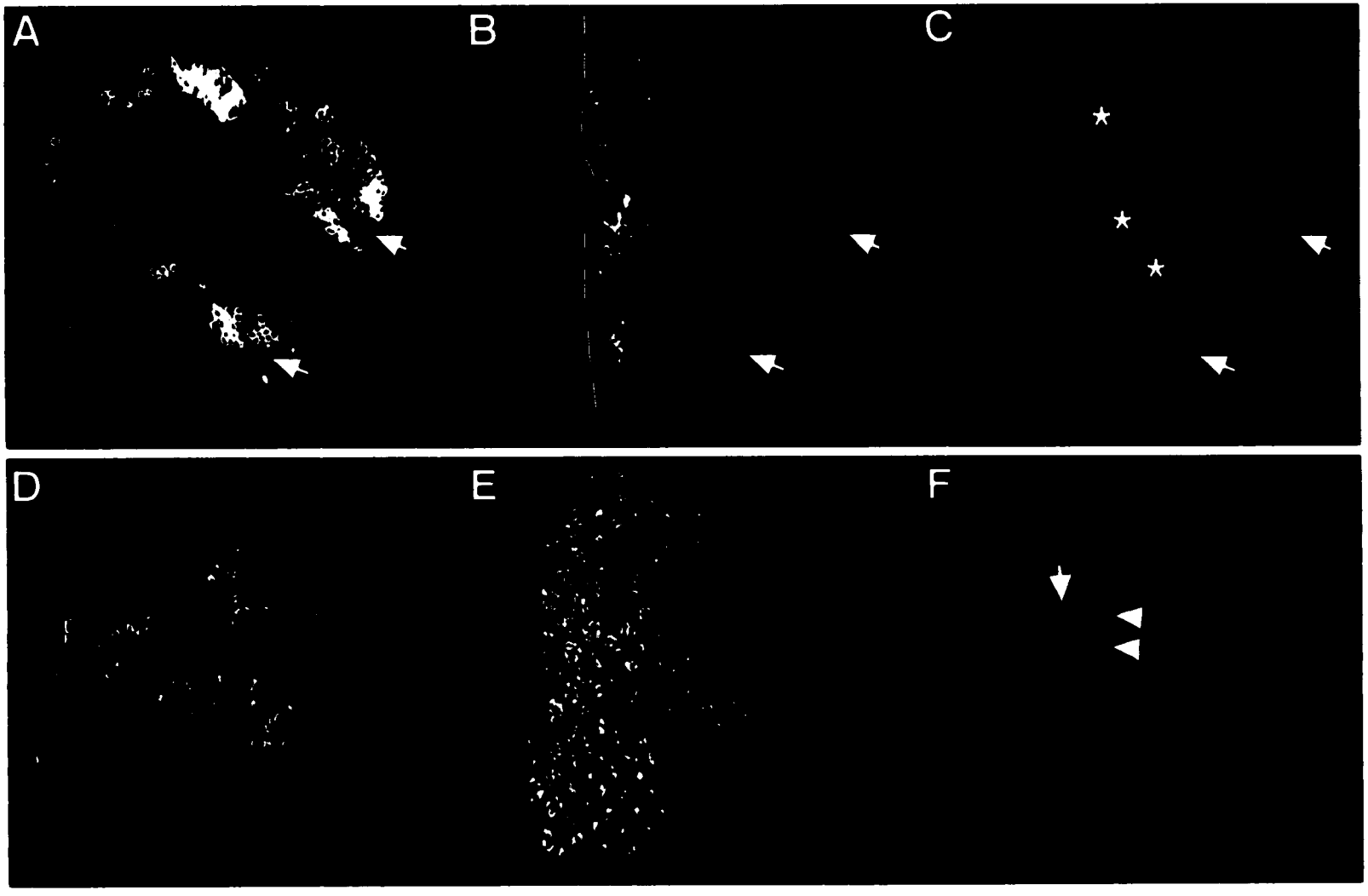
A
B
C
D
E
F

Figure 23. *hh* and *shiva* overexpression restores differentiation in *shiva*^{e52} mutants. All discs are positioned posterior to the left. (A and B) Expression pattern of the *P30,hh-lacZ* reporter gene in wild type and *shiva*^{e52} homozygous eye discs. (A) *hh* is made and secreted by photoreceptor cells posterior to the MF. (B) Note the absence of *hh-lacZ* in *shiva*^{e52} discs. (C-D) Discs stained for Elav. (C) The *hh-1* mutant disc contains eight rows of photoreceptor cell clusters. (D) *shiva*^{e52}, *hh-1* double mutant disc contains on average 12 single Elav-positive cells (n=19). (E-H) Discs double-stained for Elav (green) and propidium iodide (red). (E) *pGMR-GAL4,UAS.-hh-1* expression in a *shiva*^{e52} mutant disc. Elav expression illustrates partial rescue of neural differentiation (average of 53 Elav+ cells per disc; n=8). The MF morphology in these discs is also rescued (arrowhead). (F) *pGMR-GAL4,UAS.-hh-1,UAS-shiva* expression in a *shiva*^{e52} mutant background only partially rescues differentiation (average of 33 Elav+ cells per disc; n=9). (G) *ey-GAL4,UAS-hh-1* expression in a *shiva*^{e52} mutant background is able to partially rescue neural differentiation (average of 66 Elav+ cells per disc; n=11). (H) Expression of *ey-GAL4,UAS-hh-1,UAS-shiva* in the *shiva*^{e52} mutant background has the most dramatic rescue (average of 109 Elav+ cells per disc; n=8). Discs of this genotype have a morphologically rescued MF containing on average 10 rows of cells (arrowhead). Photoreceptor cells also display some clustering in threes. *shiva*^{e52} discs themselves contain no clustering, only single photoreceptor cells.

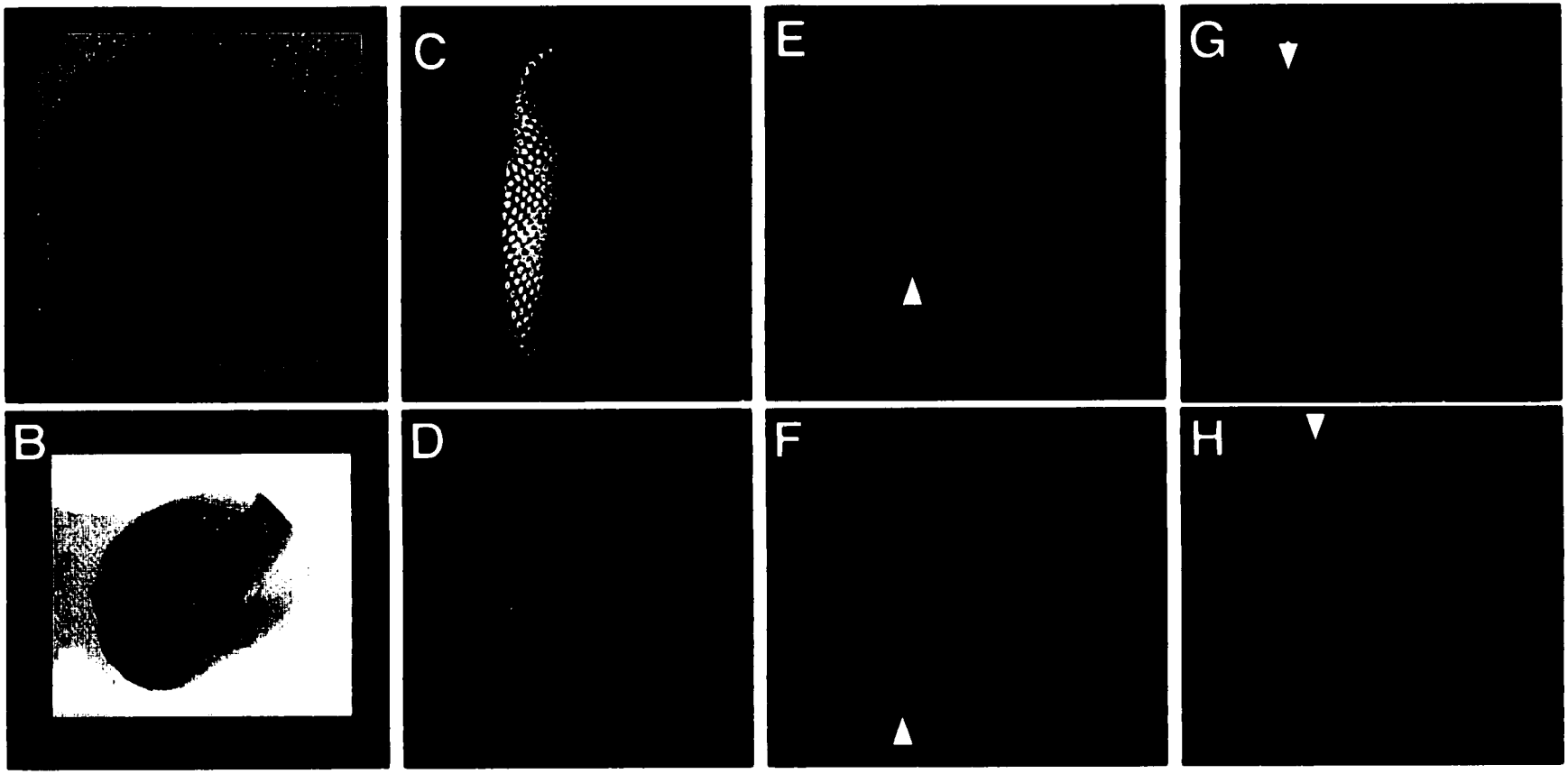
B
C
D
E
F
G
H

Table 3. *hh* and *shiva* overexpression studies in *shiva*^{e52} mutants. Indicated are the genotypes of discs observed in a *shiva*^{e52} mutant background, and the average number of Elav+ cells they contained. The numbers of discs characterized per genotype are shown.

Genotype	average number of elav+ cells
e52	21 n=18
pGMR-GAL4, UAS-shiva	40 n=7
pGMR-GAL4, UAS-hh-1	53 n=8
pGMR-GAL4, UAS-shiva, UAS-hh-1	33 n=9
ey-GAL4, UAS-shiva	20 n=8
ey-GAL4, UAS-hh-1	66 n=11
ey-GAL4, UAS-shiva UAS-hh-1	109 n=8

Figure 24. The "push-push" model controlling MF progression. In this model, *hh* and *shiva* act together to coordinate MF progression. Hh in the posterior cross-talks to *shiva* in the anterior as part of this coordination.

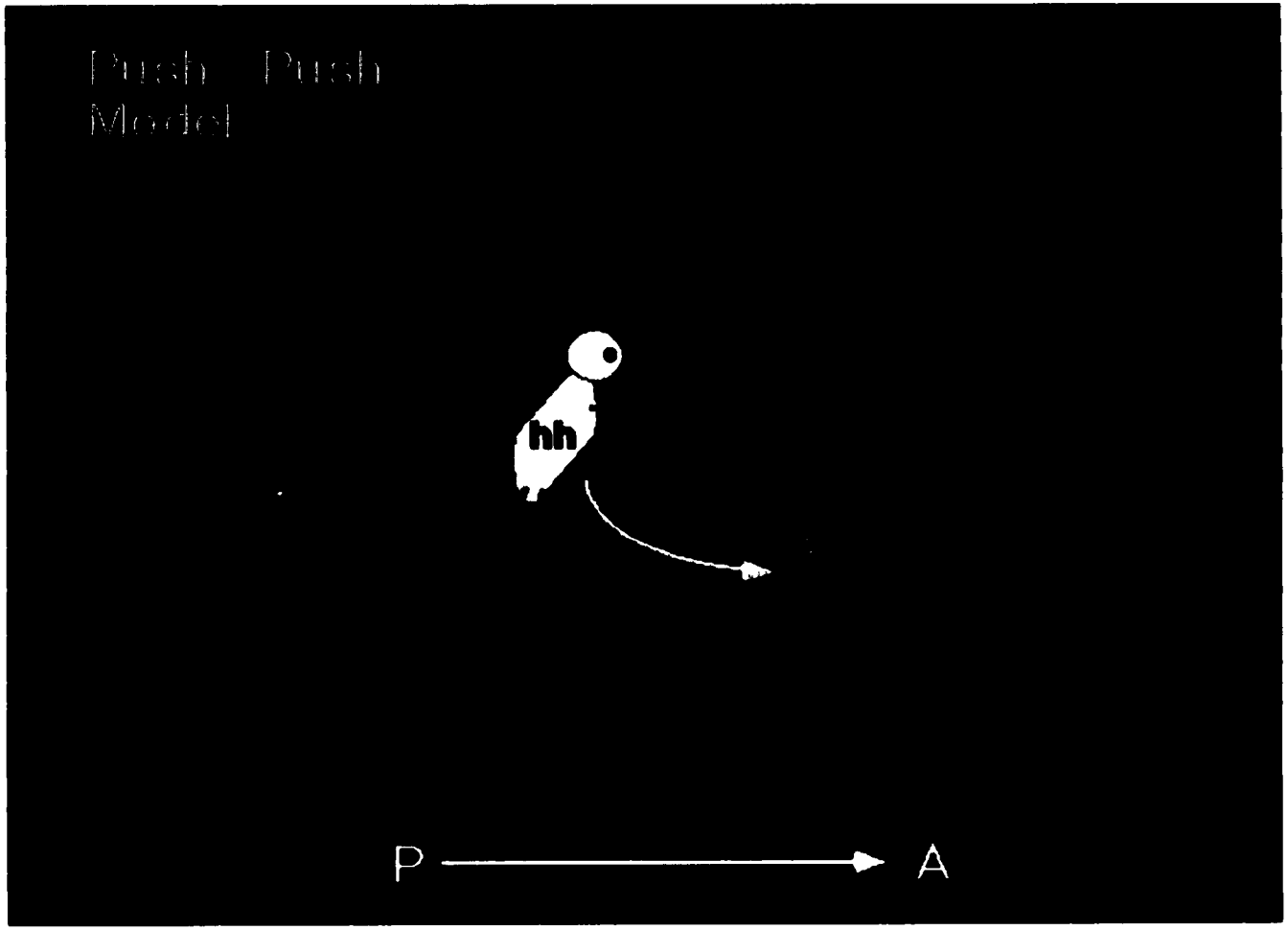
Push Push
Model
hh
P
A

Chapter VII. Experimental Procedures

Fly Strains and Crosses

The details of *Drosophila melanogaster* strains and crosses performed are given in relevant chapters. Genes, genetic markers and strains not fully described can be found in Lindsley and Zimm (Lindsey and Zimm, 1992). Stocks were maintained and crosses were performed on standard cornmeal-molasses-yeast-agar medium containing 0.2% propionic acid or Tegosept as mold inhibitors. Stocks were maintained at 18°C and crosses were performed at 25°C unless otherwise specified. A list of all relevant *shiva* stocks can be found in the "shiva genetics" notebook.

Plasmid rescue of P-element inserts

Rapid Small Scale Isolation of *Drosophila* DNA

200-400 frozen flies were placed in an eppendorf tube with 800 ul homogenization buffer (1% DEPC, 1% SDS, 0.1 M EDTA, 0.1 M TrisCl pH9) and homogenized. The mixture was incubated 30 minutes at 70°C. 112 ul 8 M KAc (14 ul per 100 ul homogenate) was added, followed by incubation on ice for 30 minutes. The homogenate was centrifuged 15 minutes at 4°C and the supernatant transferred to a new eppendorf. DNA was percipitated with 0.5 volumes of isopropanol (RT) and centrifuged 5 minutes at RT. The pellet was

washed with 70% ethanol, centrifuged briefly, dried, and resuspended in 100 ul TE.

5 ul of each prep was digested with either *Eco*RI or *Xba*I, and each digest was run on a gel to visualize a smear of DNA.

Cut, Paste and Rescue of the Plasmid

40 µl fly DNA was digested with either *Xba*I or *Eco*RI, followed by phenol, phenol/chloroform, and chloroform extraction. 17 µl 3M NaOAc was added and the DNA precipitated with 428 µl 100% ethanol, followed by resuspension in 40 µl TE. The DNA was ligated at 16°C overnight in the following reaction: 20 µl DNA, 20 µl 10X ligase buffer, 20 µl 10mM ATP, 2 µl T4 ligase, 138 µl ddH_2O. After the overnight reaction, 20 µl 3M NaOAc was added and the DNA precipitated with 550 µl 100% ethanol, then resuspended in 10 µl TE. 5 µl of each ligation was electroporated into 50 µl competent *E. coli* cells using 2.5 kV pulse, followed by the immediate addition of 1 ml cold Xa media. Cells were incubated 1 hr at 37°C, then 200 µl were plated on each of four plates of the appropriate selective media. Colonies were picked into sterile Xa media for preparation of plasmid DNA by standard methods.

Electrophoresis and transfer of nucleic acids

Horizontal gel electrophoresis of double-stranded DNA was performed in 40 mM Tris-acetate and 2 mM EDTA agarose gels as described in Sambrook et al. (Sambrook et al., 1989). Southern blot transfer to nitrocellulose membranes was

using 20X SSC as transfer buffer. Hybridization to DNA on nitrocellulose was at 65°C in the following solution: 3X SSC, 0.5% SDS, 5X Denhardt's solution, 5mg/ml single-stranded salmon sperm DNA. Filters were washed at 65°C in 1X SSC and 0.1% SDS.

Radioactive labeling of nucleic acids

Double-stranded plasmid and cosmid DNA was labeled with Klenow-incorporated α-^{32}P-cCTP using random-primer labeling kits from Gibco BRL or Boehringer Mannheim Biochemica.

Preparation of subclones for sequencing

Restriction fragments of *shiva* cDNA clones and genomic DNA were isolated on low-melting agarose gels. These fragments were subcloned into the pBluescript KS- (Stratagene) vector. Recombinant DNA was transformed into TG2 or DH10β *E. coli* host cells. Bacterial stocks containing recombinant DNA were frozen in 7% DMSO and stored at –80°C. A list of all subcloned stocks can be found in notebook "shiva", section "constructs". For information of the location of these stocks in the –80°C freezer, see notebook "shiva" under section "–80°C freezer".

In order to obtain overlapping clones for sequencing the 3.5kb fragment of cDNA6, the standard random deletion protocol using DNaseI was used as described in Frischaul et al. (Frischauf et al., 1980).

Computer analysis

The MacVector and Lasergene programs analyzed the *shiva* nucleotide sequences and predicted amino acid sequence. Homology to known genes was found using BLASTP and BLASTN algorithms (Altschul et al., 1990) to search Genbank and other databases. Alignment of SHIVA and its homologs was performed using the MegAlign feature of Lasergene.

Inducing clones for analysis in adult tissues

Crosses were set up using the *y* and *Sb* markers for labeling cells in adult cuticle (Theodosiou and Xu, 1998). Eggs were collected every 12 hours by transfer and cultured at 25°C. To induce clones in imaginal discs, late first instar larvae were heat shocked for 60 minutes in a 38°C water bath. Progeny were cultured at 25°C until they hatched as adults. *shiva* mutant clones were identified by the presence of the y^- cuticle marker and the Sb^+ bristle marker in mosaic flies.

Mounting adult legs and wings

Legs and wings were pulled from anaesthetized flies using forceps, then dipped in 100% ethanol and then in dH_2O before being placed in a drop of Permount on a glass coverslip. A second coverslip was placed on top and

weighted with several coins overnight while the Permount dried and set. Coverslips were used in lieu of slides to allow all sides of the limbs to be imaged.

Inducing clones for analysis in developing tissues

Crosses were set up using the appropriate marker for labeling cells in imaginal tissues (Theodosiou and Xu, 1998). Eggs were collected every 12 hours by transfer and cultured at 25°C. To induce clones in imaginal discs, late first instar larvae were heat shocked for 60 minutes in a 38°C water bath. After several days, wandering third instar larvae were picked to a new vial and heat shocked again for 60 to 90 minutes to induce the expression of the πM or NM cell markers. Vials were incubated again at 25°C for 60 minutes prior to dissecting.

Immunocytochemistry of *Drosophila* imaginal discs: Protocol I

Imaginal discs were dissected from third instar larvae in cold 0.1M PO_4 buffer, and fixed for 40 minutes on ice in PLP (2% paraformaldehyde, 0.01M $Na_3H_2IO_6$, 0.075M lysine, 0.037M sodium phosphate, pH 7.2). Tissues were washed by transferring into fresh PSN (0.1M phosphate pH 7.2, 1% goat serum, 0.1% Saponin) on ice four times for 10 minutes to remove any fix agent. Tissues were then incubated overnight at 4°C with a 1:50 dilution (1μg/ml) of anti-MYC (MAb MYC 1-9E10.2; American Type Culture Collection), in PSN. When used in combination with reporter genes, a 1:200 dilution of anti-βgal (rabbit polyclonal) was added to the incubation reaction. After incubation, discs were washed at

least four times with PSN and incubated with secondary antibodies for 2 to 4 hours at room temperature or overnight at 4°C (1:200 dilution of Goat anti-Mouse, Jackson Laboratories). Discs were again washed in PSN four times to remove any excess secondary antibodies, and mounted in 90% glycerol, 1XPBS, 0.5% *n*-propyl gallate for fluorescence staining.

Immunocytochemistry of *Drosophila* imaginal discs: Protocol II

While the preceding protocol was used in my clonal analysis of discs, I used the following protocol for my eye imaginal disc staining experiments. Discs were dissected in cold PBS and fixed for 30 minutes at room temperature in 4% paraformaldehyde in PBS (aliquots of fix solution can be stored in frozen aliquots). After washing several times in PBT, discs were pre-incubated in 3% NGS in PBT for 1 hour. The appropriate primary antibody was directly added to the reaction and incubated overnight at 4°C, or for 2 hours at RT. After primary incubation, discs were washed twice quickly in PBT, and twice for 20 minutes in PBT. Secondary antibody was added in PBT with 1% NGS, and tissues incubated for at least 2 hours at room temperature. Discs were washed well (sometimes overnight), dissected and mounted onto slides.

BrdU Incorporation and Propidium Iodide Staining

The protocol described above is readily modified for BrdU incorporation and PI staining. Dissect larvae in M3 medium at room temperature and immediately transfer tissues into M3 containing 0.3 mg/ml BrdU for 1 hour.

Wash several times over 30 minutes in PBS on ice, and fix in 4% paraformaldehyde in PBS. Proceed with standard conditions as in Protocol II. For primary antibody staining, incubate in mouse-anti-BrdU (1:50) with 3% NGS in PBT. In addition add RNase into the reaction and incubate overnight at 4°C. Following incubation, wash twice in PBT, and incubate in 15 µl of PI (0.5 mg/ml) per 500 ul for 5 minutes. Continue as described above. As PI staining is short-lived when exposed to light, take caution when proceeding with protocol, and collecting images on the confocal microscope.

Antibodies

anti-BrdU: Becton Dickinson

anti-Elav: Xu lab stock

anti-myc: Oncogene Science

anti-βgal: Xu lab stock

secondary antibodies: Jackson Labs

Confocal Microscopy

Confocal analysis was performed using the Biorad MRC 1024 system controlling a Zeiss Axiovert S100 TV inverted compound microscope. Images were captured to files and imported into Adobe Photoshop for analysis and for making figures.

Scanning Electron Microscopy

Pupae dissected from pupal cases and whole flies were dehydrated in serial dilutions from 100% ddH2O to 100% ethanol to 100% hexamethyldisilazane, and were dried by desiccation. Flies were coated with gold-palladium and viewed with an ISISS-40 scanning electron microscope.

***in situ* Hybridization of Imaginal Tissues (modified from Tom Serano)**

DNA probes were made using the digoxigenin-labeling kit (Boehringer Mannheim Biochemica). A gel-isolated DNA fragment of choice was denatured and incubated with 1X hexanucleotide mix, 1X dNTP mix and 1U/µl Klenow overnight at 16°C. Unincorporated nucleotides were removed by gel-filtration, and the probe was concentrated by lyophilizing and redissolving in 50 µl of hybridization solution (50% formamide, 5X SSC, 0.5 mg/ml tRNA, 1X Denhardts and 0.1% Tween). Probes can be stored in –20°C and reused.

Discs were prepared by dissecting in 1X PBS, and placed in PP (1X PBS, 4% paraformaldehyde, 0.1% Tween) on ice. Discs were transferred to RNase-free 1.7 ml tubes, fixed in PP for 30 minutes, and washed five times in PBT. Tissues were Proteinase K treated by incubating in 50 µg/ml Proteinase K in PBT for 3.5 minutes. The time of Proteinase K treatment is critical; too short and the probe doesn't penetrate the tissue, too long and the tissue morphology is destroyed. Proteinase K treatment was stopped by washing twice with 2 mg/ml glycine in

PBT and consequently washing twice with PBT. Tissues were post-fixed in PP for 20 minutes, and washing was resumed.

Discs are pre-hybridized in a series of dilutions of PBT in hybridization solution. The final pre-hybridization is in 100 µl of hybridization solution for 1 hour at 45-47°C. Just before pre-hybridization is over, the probe is denatured for 10 minutes, and placed on ice. As much hybridization solution from pre-hybridization is removed as possible, and probe is added to a volume of 100 µl and hybridized overnight at 45-47°C for a minimum of about 12 hours.

Following hybridization, discs are washed in a series of dilutions of hybridization solution in PBT at 45°C over the span of 1 hour. Tissues are then washed several times over 45 minutes in PBT, and pre-hybridized with 1% NGS for 1 hour at RT. To detect the probe, tissues are incubated with 1:2000 dilution anti-digoxigenin-AP conjugate in PBT for 2 hours at RT (or overnight at 4°C), and washed several times in PBT over 1 hour, followed by two washes in Showtime solution (100 mM Tris pH9.5, 100 mM NaCL, 50 mM MgCl2, 0.1% Tween). The staining reactions includes 4.5 µl of NBT and 4 µl X-phosphate per 1 ml Showtime solution, and is added to samples. Staining is monitored by placing samples in a dish, avoiding excessive exposure to light as reagents are light sensitive. Transferring discs into PBS as they become developed stops reactions. Mount in 80% glycerol in PBS. I have found that storing discs in glycerol for a few days at 4°C enhances the signal by cutting back on background staining, and turns the staining from brown to blue.

Appendix A: Excision Lines

Excision Lines Generated from *shiva*^{00295} P-element

Line # 00295-	Description
1-1	< 3rd instar larval lethal
2-2	"
4-1	"
5-1	pharate adult lethal
6-2	< 3rd instar larval lethal
7-1	"
8-1	"
9	"
11-1	" ; all long larvae
12	"
13	"
16	"
17-2	"
18	"
19	viable
20	viable
21	< 3rd instar larval lethal
24	"
26	< 3rd instar larval lethal

28	pharate adult lethal; brown spots on abdomen, no tail
29	< 3rd instar larval lethal
30	"
31	RT extra-long larvae and pupae; a few adult homozygous escapers
32	viable
33	< 3rd instar larval lethal
34	viable
35	< 3rd instar larval lethal
36	"
37-1	viable
38-2	< 3rd instar larval lethal
41-2	"
43-2	viable
45-1	viable
52	late pupal lethal; at 18°C very small half-bar eyes, small legs and wings, enlarged abdomen, bristles fork-like
55-1	< 3rd instar larval lethal
58-1	"
59-1	"
61-1	viable
62-2	< 3rd instar larval lethal
64-1	viable

Excision Lines Generated from *shiva*^{05415} P-element

Line # 05415-	Description
1-2	early-mid pupal lethal, very few escapers at RT
2-1	< 3rd instar larval lethal
3-1	viable
4-1	embryonic or early larval lethal
5-1	viable
5-2	"
6-1	"
8-1	"
10-1	< 3rd instar larval lethal
14-2	"
15-1	"
15-2	< 3rd instar larval lethal
17-1	"
18-1	"
18-2	< 3rd instar larval lethal
19-2	"

References

Alcedo, J., Ayzenzon, M., Ohlen, T. v., Noll, M., and Hooper, J. E. (1996). The Drosophila smoothened gene encodes a seven-pass membrane protein, a putative receptor for the Hedgehog signal. Cell *86*, 221-232.

Altschul, S. F., Gish, W., Miller, W., Myers, E. W., and Lipman, D. J. (1990). Basic local alignment search tool. Journal of Molecular Biology *215*, 403-410.

Aristotle. (350 BC). The History of Animals, D. A. W. Thompson, ed.

Aristotle. (350 BC). On Parts of Animals, W. Ogle, ed.

Bai, C., Sen, P., Hofmann, K., Ma, L., Goebl, M., Harper, J. W., and Elledge, S. J. (1996). SKP1 connects cell cycle regulators to the ubiquitin proteolysis machinery through a novel motif, the F-box. Cell *86*, 263-274.

Basler, K., and Struhl, G. (1994). Compartment boundaries and the controlof Drosophila limb pattern by hedgehog protein. Nature *368*, 208-214.

Blackman, R., Sanicola, M., Raftery, L., Gillevet, T., and Gelbart, W. (1991). An extensive 3' cis-regulatory region directs the imaginal disk expression of *decapentaplegic*, a member of the TGF-beta family in *Drosophila*. Development *111*, 657-66.

Brook, W. J., and Cohen, S. M. (1996). Antagonistic interactions between *wingless* and *decapentaplegic* responsible for dorsal-ventral pattern in the *Drosophila* leg. Science *273*, 1373-1377.

Campbell, G., and Tomlinson, A. (1995). Initiation of the proximal axis in insect legs. Development *121*, 619-628.

Campbell, G., Weaver, T., and Tomlinson, A. (1993). Axis specification in the developing Drosophila appendage: the role of wg, dpp and the homeobox gene al. Cell *74*, 1113-1123.

Campuzano, S., and Modolell, J. (1992). Patterning of the Drosophila nervous system: the achaete-scute gene complex. Trends in Genetics *8*, 202-208.

Capdevila, J., Estrada, M., Sanchez-Herrero, E., and Guerrero, I. (1994). The Drosophila segment polarity gene patched interacts with decapentaplegic in wing development. EMBO Journal *13*, 71-82.

Capdevila, J., and Guerrero, I. (1994). Targeted expression of the signaling molecule decapentaplegic induces pattern duplications and growth alterations in Drosophila wings. EMBO Journal *13*, 4459-68.

Chen, Y., and Struhl, G. (1996). Dual roles for Patched in seuqestering and transducing Hedgehog. Cell *87*, 553-563.

Chen, Y., and Struhl, G. (1998). In vivo evidence that Patched and Smoothened constitute distinct binding and transducing components of a Hedgehog receptor complex. Development *125*, 4943-4948.

Diaz-Benjumea, F. J., Cohen, B., and Cohen, S. M. (1994). Cell interaction between compartments establishes the proximal-distal axis of *Drosophila* legs. Nature *372*, 175-179.

Feldman, R. M. R., Correll, C. C., Kaplan, K. B., and Deshaies, R. J. (1997). A complex of Cdc4p, Skp1p, and Cdc53p/Cullin catalyzes ubiquitination of the phosphorylated CDK inhibitor Sic1p. Cell *91*, 221-230.

Felsenfeld, A. L., and Kennison, J. A. (1995). Positional signaling by hedgehog in Drosophila imaginal disc development. Development *121*, 1-10.

Ferguson, E., and Anderson, K. (1992). Localized enhancement and repression of the activity of the TGF-beta family member, decapentaplegic, is necessary for dorsal-ventral pattern formation in the Drosophila embryo. Development *114*, 583-97.

Frischauf, A.-M., Garoff, H., and Lehrach, H. (1980). A subcloing strategy for DNA sequence analysis. Nucleic Acids Research *8*, 5541-5549.

Goebl, M. G., Yochem, J., Jentsch, S., McGrath, J. P., Varshavsky, A., and Byers, B. (1988). The yeast cell cycle gene CDC34 encodes a ubiquitin-conjugating enzyme. Science *241*, 1331-1335.

Guillen, I., Mullor, J. L., Capdevila, J., Sanchez-Herrero, E., Morata, G., and Guerrero, I. (1995). The function of engrailed and the specification of Drosophila wing pattern. Development *121*, 3447-3456.

Heberlein, U., Singh, C. M., Luk, A. Y., and Donohoe, T. J. (1995). Growth and differentiation in the Drosophila eye coordinated by hedgehog [see comments]. Nature *373*, 709-11.

Heberlein, U., Wolff, T., and Rubin, G. M. (1993). The TGF beta homolog dpp and the segment polarity gene hedgehog are required for propagation of a morphogenetic wave in the Drosophila retina. Cell *75*, 913-26.

Heuvel, M. v. d., and Ingham, P. W. (1996). *smoothened* encodes a receptor-like serpentine protein required for *hedgehog* signaling. Nature *382*, 547-551.

Horsfield, J., Penton, A., Secombe, J., Hoffman, F. M., and Richardson, H. (1998). decapentaplegic is required for arrest in G1 phase during Drosophila eye development. Development *125*, 5069-78.

Ingham, P., Taylor, A., and Nakano, Y. (1991). Role of the Drosophila pātched gene in positional signalling. Nature *353*, 184-7.

Irish, V. F., and Gelbart, W. M. (1987). The decapentaplegic gene is required for dorsal-ventral patterning of the Drosophila embryo. Genes and Development *1*, 868-879.

Jiang, J., and Struhl, G. (1996). Complementary and mutually exclusive activities of *decapentaplegic* and *wingless* organize axial patterning during *Drosophila* leg development. Cell *80*, 563-572.

Jiang, J., and Struhl, G. (1995). Protein kinase A and Hedgehog signaling in *Drosophila* limb development. Cell *80*, 563-572.

Jiang, J., and Struhl, G. (1998). Regulation of the Hedgehog and Wingless signaling pathways by the F-box/WD40-repeat protein Slimb. Nature *391*, 493-496.

Kassis, J., Noll, E., VanSickle, E., Odenwald, W., and Perrimon, N. (1992). Altering the insertional specificity of a Drosophila transposable element. PNAS USA *89*, 1919-23.

Laney, J. D., and Hochstrasser, M. (1999). Substrate Targeting in the Ubiquitin System. Cell *97*, 427-430.

Lawrence, P. A., and Morata, G. (1976). Compartments in the wing of Drosophila: a study of the engrailed gene. Developmental Biology *50*, 321-337.

Lebovitz, R. M., and Ready, D. F. (1986). Ommatidial development in Drosophila eye disc fragments. Developmental Biology *117*, 663-671.

Lecuit, T., and Cohen, S. M. (1997). Proximal-distal axis formation in the Drosophila leg. Nature *388*, 139-145.

Lee, J. J., Kessler, D. P. v., Parks, S., and Beachy, P. A. (1992). Secretion and localized transcription suggest a role in positional signaling for products of the segmentation gene *hedgehog*. Cell *71*, 33-50.

Lepage, T., Cohen, S., Diaz-Benjumea, F., and Parkhurst, S. (1995). Signal transduction by cAMP-dependent protein kinase A in Drosophila limb patterning. Nature *373*, 711-5.

Li, W., Ohlmeyer, J. T., Lane, M., and Kalderon, D. (1995). Function of protein kinase A in hedgehog signal transduction and *Drosophila* imaginal disc development. Cell *80*, 553-562.

Lindsey, D. L., and Zimm, G. G. (1992). The genome of Drosophila melanogaster.: Academic Press).

Ma, C., and Moses, K. (1995). Wingless and patched are negative regulators of the morphogenetic furrow and can affect tissue polarity in the developing Drosophila compound eye. Development *121*, 2279-89.

Ma, C., Zhou, Y., Beachy, P. A., and Moses, K. (1993). The segment polarity gene hedgehog is required for progression of the morphogenetic furrow in the developing Drosophila eye. Cell *75*, 927-38.

Maniatis, T. (1999). A ubiquitin ligase complex essential for the NF-kappaB, Wnt/Wingless, and Hedgehog signaling pathways. Genes and Development *13*, 505-510.

Marigo, V., Davey, R. A., Zou, Y., Cunningham, J. M., and Tabin, C. J. (1996). Biochemical evidence that Patched is the Hedgehog receptor. Nature *384*, 176-179.

Neer, E. A., Schmidt, C. J., Nambudripad, R., and Smith, T. F. (1994). The ancient regulatory-protein family of WD-repeat proteins. Nature *371*, 297-300.

Nusslein-Volhard, C., and Wieschaus, E. (1980). Mutations affecting segment number and polarity in Drosophila. Nature *287*, 795-801.

Pan, D., and Rubin, G. M. (1995). cAMP-dependent protein kinase and hedgeog act antagonistically in regulating *decapentaplegic* transcription in *Drosophila* imaginal discs. Cell *80*, 543-552.

Penton, A., and Hoffman, F. M. (1996). Decapentaplegic restricts the domain of wingless during Drosophila limb patterning. Nature *382*, 162-165.

Penton, A., Selleck, S. B., and Hoffmann, F. M. (1997). Regulation of cell cycle synchronization by decapentaplegic during Drosophila eye development. Science *275*, 203-6.

Phillips, R., Roberts, I., Ingham, P., and Whittle, J. (1990). The Drosophila segment polarity gene patched is involved in a position-signalling mechanism in imaginal discs. Development *110*, 105-114.

Pignoni, F., and Zipursky, S. L. (1997). Induction of Drosophila eye development by dpp. Development *124*, 271-278.

Ready, D., Hanson, T. E., and Benzer, S. (1976). Development of the Drosophila retina, a neurocrystalline lattice. Developmental Biology *53*, 217-240.

Sambrook, J., Fritsch, E. F., and Maniatis, T. (1989). Molecular cloning: A laboratory manual: Cold Spring Harbor Laboratory Press).

Skowyra, D., Craig, K. L., Tyers, M., Elledge, S. J., and Harper, J. W. (1997). F-box proteins are receptors that recruit phosphorylated substrates to the SCF ubiquitin-ligase complex. Cell *91*, 209-219.

Spencer, E., Jiang, J., and Chen, Z. J. (1999). Signal-induced ubiquitination of IkappaBalpha by the F-box protein Slimb/beta-TrCP. Genes Dev *13*, 284-94.

Spevak, W., Keiper, B. D., Stratowa, C., and Castanon, M. J. (1993). *S. cerevisiae cdc15* mutants arrested at a late stage in anaphase are rescued by *Xenopus* cDNAs encoding N-*ras* or a protein with ß-transducin repeats. Molecular and Cellular Biology *13*, 4953-4966.

Stone, D. M., Hynes, M., Armanini, M., Swanson, T. A., Gu, Q., Johnson, R. L., Scott, M. P., Pennica, D., Goddard, A., Phillips, H., Noll, M., Hooper, J. E., deSauvage, F., and Rosenthal, A. (1996). The tumor-suppressor gene patched encodes a candidate receptor for Sonic hedgehog. Nature *384*, 129-134.

Struhl, G., and Basler, K. (1993). Organizing activity of *wingless* protein in *Drosophila*. Cell *72*, 527-540.

Strutt, D. I., and Mlodzik, M. (1997). Hedgehog is an indirect regulator of morphogenetic furrow progression in the Drosophila eye disc. Development *124*, 3233-40.

Strutt, D. I., Wiersdorff, V., and Mlodzik, M. (1995). Regulation of furrow progression in the Drosophila eye by cAMP- dependent protein kinase A [see comments]. Nature *373*, 705-9.

Tabata, T., Eaton, S., and Kornberg, T. B. (1992). The Drosophila hedgehog gene is expressed specifically in posterior compartment cells and is a target of engrailed regulation. Genes and Development *6*, 2635-2645.

Tabata, T., and Kornberg, T. B. (1994). Hedgehog is a signaling protein with a key role in patterning *Drosophila* imaginal discs. Cell *76*, 89-102.

Tabata, T., Schwartz, C., Gustavson, E., Ali, Z., and Kornberg, T. B. (1995). Creating a Drosophila wing de novo, the role of engrailed and the compartment border hypothesis. Development *121*, 3359-3369.

Theisen, H., Haerry, T. E., O'Connor, M. B., and March, J. L. (1996). Developmental territories created by mutual antagonism between Wingless and Decapentaplegic. Development *122*, 3939-3948.

Theodosiou, N. A., and Xu, T. (1998). Use of FLP/FRT system to study Drosophila development. Methods *14*, 355-65.

Theodosiou, N. A., Zhang, S., Wang, W. Y., and Xu, T. (1998). slimb coordinates wg and dpp expression in the dorsal-ventral and anterior-posterior axes during limb development. Development *125*, 3411-6.

Treisman, J. E., and Rubin, G. M. (1995). wingless inhibits morphogenetic furrow movement in the Drosophila eye disc. Development *121*, 3519-27.

Wilder, E. L., and Perrimon, N. (1995). Dual functions of *wingless* in the *Drosophila* leg imaginal disc. Development *121*, 477-488.

Willems, A., Lanke, S., Patton, E., Craig, K., Nason, T., Mathias, N., Kobayashi, R., Wittenberg, C., and Tyers, M. (1996). Cdc53 targets phosphorylated G1 cyclins for degradation by the ubiquitin proteolytic pathway. Cell *86*, 453-63.

Winston, J. T., Strack, P., Beer-Romero, P., Chu, C. Y., Elledge, S. J., and Harper, J. W. (1999). The SCFbeta-TRCP-ubiquitin ligase complex associates specifically with phosphorylated destruction motifs in IkappaBalpha and beta-catenin and stimulates IkappaBalpha ubiquitination in vitro. Genes Dev *13*, 270-83.

Xu, T., and Rubin, G. M. (1993). Analysis of genetic mosaics in developing and adult *Drosophila* tissues. Development *117*, 1223-1237.

Xu, T., Wang, W. Y., Stewart, R. A., and Yu, W. (1995). Identifying tumor suppressors in genetic mosaics: the Drosophila lats gene encodes a putative protein kinase. Development *121*, 1053-1063.

Yaron, A., Hatzubai, A., Davis, M., Lavon, I., Amit, S., Manning, A. M., Andersen, J. S., Mann, M., Mercurio, F., and Ben-Neriah, Y. (1998). Identification of the receptor component of the IkappaBalpha-ubiquitin ligase. Nature *396*, 590-594.

Yochem, J., and Byers, B. (1987). Structural comparison of the yeast cell division cycle gene CDC4 and a related pseudogene. Journal of Molecular Biology *195*, 233-45.